PRINCE WILLIAM SOUND RCAC

LONG-TERM ENVIRONMENTAL MONITORING PROGRAM

2002-2003 LTEMP Monitoring Report

PWSRCAC Contract 951.03.1

James R. Payne, Ph.D.

William B. Driskell

Jeffery W. Short
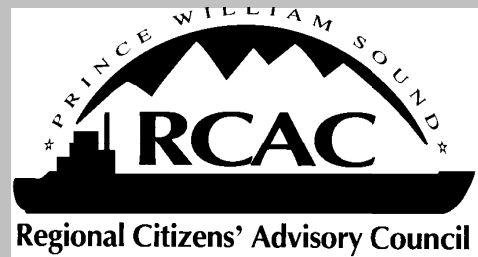
November 6, 2003

PRINCE WILLIAM SOUND RCAC
LONG-TERM ENVIRONMENTAL MONITORING PROGRAM

2002-2003 LTEMP Monitoring Report

PWSRCAC Contract 951.03.1

James R. Payne, Ph.D.
Payne Environmental Consultants, Inc.
1991 Village Park Way, Suite 206 B
Encinitas, CA 92024
760-942-1015
jamesrpayne@compuserve.com

William B. Driskell
6536 20th Avenue NE
Seattle, WA 98115
206-522-5930
bdriskell@comcast.net

Jeffery W. Short
NOAA/NMFS Auke Bay Laboratory
11305 Glacier Highway
Juneau, AK 99801
907-789-6065
jeff.short@noaa.gov

Prepared for
Lisa Ka'aihue
Project Manager
Prince William Sound Regional Citizens' Advisory Council
3709 Spenard
Anchorage, Alaska   99503
907/277-7222 or 273-6225
kaaihue@pwsrcac.org

TABLE OF CONTENTS

LIST OF FIGURES

LIST OF TABLES

LIST OF APPENDICES

List of Abbreviations

Stations:

AMT	Alyeska Marine Terminal, Port Valdez
AIB	Aialik Bay, west of Seward
DII	Disk Island, Knight Island Group, western PWS
GOC	Gold Creek, Port Valdez
KNH	Knowles Head, eastern PWS
SHB	Sheep Bay, eastern PWS
SHH	Shuyak Harbor, Kodiak
SLB	Sleepy Bay, LaTouche Island, western PWS
WIB	Windy Bay, Outer Kenai Peninsula
ZAB	Zaikof Bay, Montague Island, central PWS

ABL	NOAA/NMFS Auke Bay Laboratory, Juneau AK
AHC	aliphatic hydrocarbons
ANS	Alaskan North Slope
BWTF	Alyeska Terminal's Ballast Water Treatment Facility
CPI	carbon preference index
CRUDE	crude oil index
EVOS	*Exxon Valdez* oil spill
FFPI	fossil fuel pollution index
GC/FID	gas chromatography/flame ionization detector
GC/MS	gas chromatography/mass spectrometry
GERG	Geochemical and Environmental Research Group, Texas A&M
KLI	Kinnetic Laboratories, Inc., Anchorage AK
MDL	analytic method detection limit
MPI	Mytilus pollution index
MSD	mass selective detector
NIST	National Institute of Standards and Technology
NMFS	National Marine Fisheries Service
NOAA	National Oceanographic and Atmospheric Administration
PAH	polycyclic (or polynuclear) aromatic hydrocarbons
PDR	particulate/dissolved ratio
PECI	Payne Environmental Consultants, Inc., Encinitas, CA
PGS	particle grain size
PWS	Prince William Sound
SIM	selected ion monitoring
SRM	NIST standard reference material
TAHC	total AHC
TALK	total n-alkanes
TC	total carbon
TIC	total inorganic carbon
TOC	total organic carbon
TPAH	total PAH
UCM	unresolved complex mixture

1   Executive Summary

After reviewing the LTEMP 2002-2003 results, we have concluded that the intertidal sites monitored by the LTEMP program are currently extremely clean.   With the exception of the Alyeska Marine Terminal (AMT) site and, to a lesser extent, the Gold Creek (GOC) site in Port Valdez, the regional sites do not show elevated concentrations of hydrocarbons from either Alyeska Marine Terminal operations and discharges, or oil transportation activities within Prince William Sound (PWS). Even at AMT and GOC, where PAH and AHC contaminants from the AMT Ballast Water Treatment Facility (BWTF) are detected, the measured concentrations are probably not environmentally significant.

A large part of this report covers two main topics: 1) reevaluating historic trends and analytic issues and 2) the inter-calibration of laboratory analyses (since the program has now changed from GERG to Auke Bay Lab (ABL) for chemical analyses).

In order to interpret the current year's results in a historic context, we meticulously reviewed the chemistry results for individual samples from the preceding years of the program. During the review, we immediately identified several data-quality issues, some of which were mentioned in our 1998 LTEMP data synthesis report (Payne et al. 1998), and others more recently discussed in our 2001 evaluation of whether or not there were potential toxicity concerns reflected in the LTEMP data specific to Port Valdez (Payne et al. 2001).   Investigation of these data quality issues led to successively deeper examinations of the historic data. For some samples, the data integrity appears partially compromised, most likely from lipid interference with the laboratory instruments used for analyses of both aliphatic hydrocarbon (AHC) and (less frequently) polynuclear aromatic hydrocarbon (PAH) analytes. Based on the available data and known signatures and trends, we have attempted to discriminate between real data and obvious artifacts. Through these analyses, we have concluded that although there are some time periods when we have concerns, the overall data-quality picture is not quite so grim, and much of the data still tells a story even if some analytes were erratic.

In general, the LTEMP data suggest that when actual spills or other episodic hydrocarbon inputs occurred, the mussel tissue and sediment results detected the event, for example, after the 1994 *T/V Eastern Lion* spill, the 1997 BWTF sheening event, and the 1994 mussel-bed cleaning activities on Disk Island (and possibly Sleepy Bay). In the other routine surveys, the background levels were extremely low and generally near or below the laboratory method detection limits (MDL). When the signal levels are so low, it is easy to pick up spurious noise (real or artifacts) from the clean samples. In the 1997-1998 data set, however, there is an unusual trend of elevated hydrocarbon concentrations across all stations throughout the study region (Figure 35). Some sites peak in 1997 and then decline; in 1998, others do the same. The fact that the peaks occur across the entire study area suggests a region-wide event (Valdez to Kodiak) and yet, oddly, other parts of the same region peak in the next year. Because that would be an unlikely scenario for any contaminant behavior, we find a more likely explanation in a systematic change or

bias introduced by either collection or analytical chemistry procedures. In 1997, GERG changed instruments and data-integration procedures, upgrading to a newer more sensitive GC/MS and automating the integration of alkylated PAH homologues, an analytic task previously done manually by the GC/MS operator. We suspect the coincidence of trends may be related but lack conclusive evidence without additional laboratory data that were unavailable at this time.

Laboratory inter-calibration then becomes a pertinent issue when there are data-quality issues to resolve. In fact, it became even more important because there were significant differences in the lower levels of contaminants reported this year versus the previous years' results. By comparing split samples and National Institutes of Standards and Technology (NIST) standard reference materials analyzed by both GERG and ABL, it was determined that the labs are actually fairly close on most analytes, but GERG does get elevated results for some analytes, quite possibly due to lipid interference.

The inter-comparison anomalies thus corroborate the approach in this report of correcting the trend analyses for the known spurious peaks in selected analytes. This approach is acknowledged to be subjective but appears to be properly directed. To be less subjective the task would requires more detailed data to be less subjective. Still, even with the corrections, the overall conclusions reached would be nearly the same except perhaps with a better resolution/understanding of the apparent 1997-98 peaks in hydrocarbon concentrations.

In summary, because the typical hydrocarbon contaminant concentrations measured in mussel tissues outside Port Valdez are so low (often at or below method detection limits), detailed trend analyses are confounded by background levels, spurious events, and historic data-quality issues. Nevertheless, portions of the historic dataset are internally consistent with known pollution events, observed seasonal changes, and plausible transitions to the current low oiling levels.

With the possible exception of the 1997-1998 timeframe, the LTEMP program appears to be on-track with high-quality, high-sensitivity data with a good record of detected events. These are the hallmarks of a good monitoring program. The LTEMP data have also proven invaluable as a corroborating data set in acquiring a much more in-depth perspective of the trends and behavior of oil contaminants in the region.

2   LTEMP Oil Primer

Prior to the usual introductory portion of the report, this section is included as background material for those readers unfamiliar with oil chemistry or the oil contaminants found in Prince William Sound and central Alaskan coastal regions.

2.1 Regional Sources

In the LTEMP regional environment, oil hydrocarbons arrive from numerous and varied sources. Topping the list would be Alaskan North Slope (ANS) crude including lingering residues from the *Exxon Valdez* oil spill (EVOS); oil products from the Alyeska Marine Terminal (not necessarily ANS); coal, peat and organic-rich shales from vast local and regional deposits; Cook Inlet crude; and refined petroleum products that have made their way into the marine environment.

Of primary interest to LTEMP is, of course, ANS crude. This crude actually consists of a blend of petroleum from the production fields on the Alaskan North Slope, including Prudhoe Bay, Kuparuk, Endicott, and Lisburne, that together exhibit a chemical fingerprint that is quite distinct from that of oil found in other geographic areas. The EVOS of March 1989 consisted of ANS crude, which over time has weathered to produce a significantly different fingerprint than that of fresh ANS crude. Petroleum that originates from organic-rich shales (or hydrocarbon "source rock") and coal deposits in the Gulf of Alaska also contribute significantly to the natural (or "background") hydrocarbons in the study area, and these also exhibit a distinctly different fingerprint. Recent work shows the source rock signature to be particularly widespread in the deep sediments of PWS, but fortunately, animals exposed to these sediments do not seem to accumulate hydrocarbons because these contaminants are not bioavailable. Natural terrestrial oil seeps have also been invoked as hydrocarbon sources, but recent work indicates inputs from these seeps is insignificant compared with the other sources.

Other petroleum products that may have been introduced into the marine environment in Prince William Sound (PWS) include oil products from source locations other than Alaska. For example, the Great Alaskan Earthquake of 1964 and the resultant tsunamis washed fuel oil and asphalt made from California source oils into Port Valdez, and subsequently into PWS (Kvenvolden et al. 1995). These authors noted that tarballs from these California-sourced products have been found throughout the northern and western parts of PWS.

2.2 Oil Chemistry, Source Allocations, and Weathering Behavior

Chemically, oil is a complex mixture of decayed ancient organic matter broken down and modified under geologic heat and pressure. Each deposit is a unique blend but there are commonalities. Hydrocarbons are by far the most abundant compounds in crude oil, accounting for 50-98% of the volume. And in various proportions, all crude blends contain "lighter fractions" of hydrocarbons (similar to gasoline), "intermediate fractions"

like diesel or fuel oil, heavier tars and wax-like hydrocarbons, and ultimately residual materials like asphalt. For purposes of the LTEMP program, crude oil is identified by its signature blend of just two compositional hydrocarbon groups, the polynuclear aromatic hydrocarbons (PAH) and the aliphatic hydrocarbons (AHC), also referred to as n-alkanes. These two compositional groups encompass the intermediate, heavier tars, and wax-like fractions. As shown by the histogram plots in Figure 1, we work with approximately 40 PAH compounds and 26 AHC components to identify a hydrocarbon source. (Names and abbreviations of the individual analytes shown in this and all following figures are presented in Table 2 in Section 4.2 - Analytical Methods.) These PAH typically account for 2% - 5% of petroleum by weight (and about 3% of ANS crude).

For source identifications, it is useful to distinguish between five main families of PAH components. In order from light to heavy (left to right in the histogram plots), they are: naphthalenes (N), fluorenes (F), phenanthrenes/anthracenes (P/A), dibenzothiophenes (D), and chrysenes (C).

The naphthalenes are two-ring aromatics (i.e., two 6-carbon loops linked together) and are less persistent in the environment compared to the other higher-molecular-weight groups. They typically disappear from bulk, spilled oil by evaporation and dissolution weathering and as such, they may or may not be present in the histogram plots of oil residues or oil-contaminated sediments obtained from the environment. Because they readily dissolve in water, they can also be detected moving directly from the water column into exposed organisms. The fluorenes, anthracenes, and phenanthrenes (which are all three-ring aromatics) are each more persistent in the environment, and as such, they can act as markers to help differentiate among different sources. The dibenzothiophenes (another three-ring compound that also contains sulfur) are important, because they are characteristic of Alaskan North Slope crude oil, but not Cook Inlet or Katalla crude oil. Finally, the heavier four- and five-ring aromatics (including, the chrysenes (C) through benzo(g,h,i)perylene) (BP) are important because: 1) they can help distinguish between crude oils and refined products (such as diesel oil) that may have been produced from a particular crude oil; and 2) they are also representative of combustion by-products.

Chemists have developed a nomenclature to distinguish the various members of each family. The simple parent compounds in each of the five PAH families are referred to as "C_0" (e.g., C_0-naphthalene, here abbreviated as "N"). Their other family members, known to chemists as alkyl-substituted homologues, are adorned with an alkyl molecule in a discriminating position around the margin of the PAH ring. These homologues thus become known by their sequence name, e.g., C1-naphthalene (abbreviated as N1), C2-naphthalene (N2), and so on (N3 and N4) (see Figure 1).
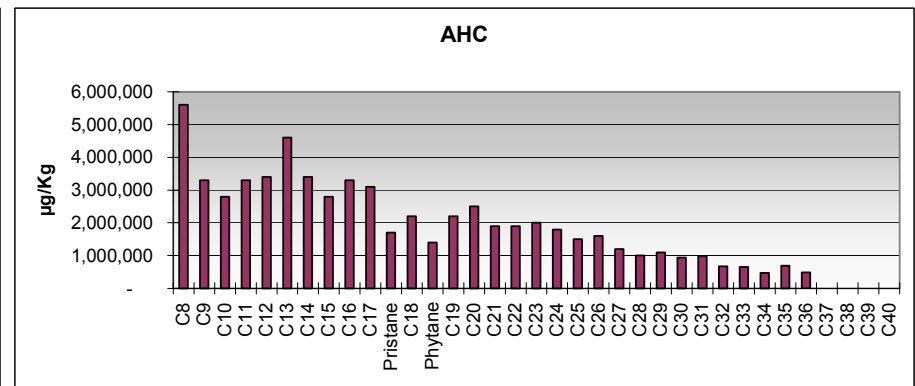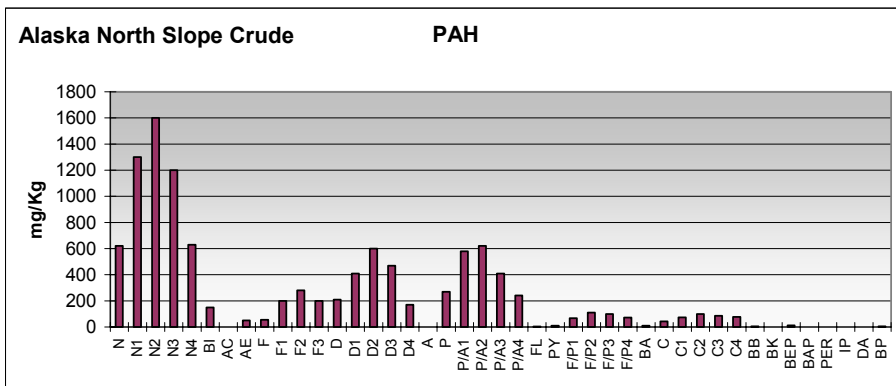
Figure 1 Example histograms of ANS PAH and AHC components.

Regarding the family structure, it is important to note that petrogenic (petroleum-derived) PAHs have a characteristic fingerprint whereby the parent compounds in each of the five PAH families (e.g., C_0-naphthalene abbreviated N) are usually at lower concentrations than their other family members (see Figure 1). With evaporation/dissolution weathering, these lower-molecular-weight components are further eliminated, generating a characteristic "water-washed profile" with the levels of $C_0<C_1<C_2<C_3$ within each PAH group. Eventually, with continued weathering, only the most persistent alkylated phenanthrenes/anthracenes, dibenzothiophenes, and chrysenes are seen and typically at very characteristic and source-specific ratios in the remaining oil residues (Figure 2).

Likewise, in the AHC fraction, the n-alkanes also show the effects of evaporation weathering with losses of all components with molecular weights below n-C_{14} clearly apparent after several weeks (Figure 2). With continued microbial degradation, the remaining n-alkanes will be selectively removed leaving only the branched compounds, pristane and phytane, which are also slowly removed but at a much slower rate over time. Incidentally, phytoplankton make C15 and C17, and mussels can accumulate it by filter feeding on the phytoplankton. Substantial concentrations of pristane are naturally present in some zooplankton; they biosynthesize it from chlorophyll ingested with the phytoplankton they eat. Therefore, all three compounds can show up in mussel and sediment samples as a result of biogenic input. In a spring plankton bloom, these natural n-alkanes can easily dominate the AHC fraction. Phytane, on the other hand, is almost exclusively associated with oil, so its presence in samples can also be used as another indicator of petroleum contamination.

Pyrogenic PAHs come from combustion sources including atmospheric fallout and surface runoff from the burning of fossil fuels (diesel, heating oil, gasoline, etc.) and from other pyrogenic sources such as forest fires and camp fires. Creosote, which is used to preserve wood pilings, is also usually included in this category. Pyrogenic PAHs are characterized by high molecular weight PAHs, greater than C_3-dibenzothiophene (D3), and by high concentrations of the parent compounds compared to their alkyl homologues. A typical pattern for pyrogenic PAHs is decreasing concentration with increasing molecular weight within a group, i.e., $C_0>C_1>C_2>C_3>C_4$, opposite the trend seen in crude oil.

For the aliphatic hydrocarbons, the nomenclature strategy changes. The abbreviation for the aliphatic compound, n-C_{10}, now refers to 10 carbon atoms linked in a straight chain (no cyclic rings). In contrast to the PAHs, aliphatic hydrocarbons can account for more than 70 percent of petroleum by weight. Also, as noted above, aliphatic hydrocarbons can be synthesized by organisms (both planktonic and terrestrial), and they can be present as degradation products in some bacteria. As shown in Figure 1, crude petroleum contains a homologous series of n-alkanes ranging from one to more than 30 carbons with odd- and even-numbered n-alkanes present in nearly equal amounts. In contrast, biogenic hydrocarbons (produced by living organisms) preferentially contain specific suites of normal alkanes with mainly odd-numbered carbons between n-C_{15} and n-C_{33}. In addition to the example of n-C_{15}, n-C_{17}, and pristane from marine plankton cited above,
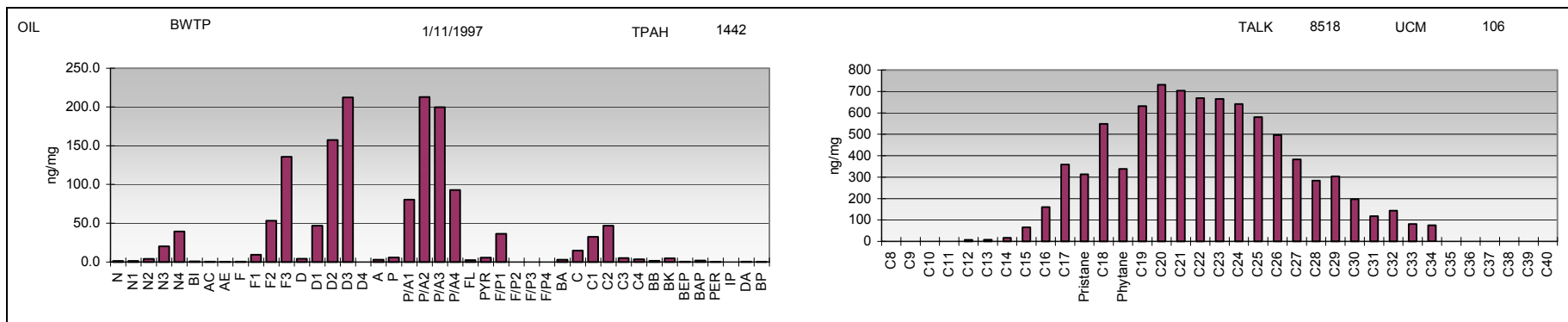
Figure 2 Histogram of weathered ANS from LTEMP 11/97.

terrestrial plants contribute a predominant odd-numbered carbon pattern including n-C_{25}, n-C_{27}, n-C_{29}, n-C_{31}, and n-C_{33}. These so-called "plant waxes" are commonly observed in marine sediments in depositional areas receiving significant amounts of terrestrial runoff.

Petroleum also contains a complex mixture of branched and cyclic compounds generally not found in organisms. This complex mixture can include oxygenated compounds that produce an "unresolved complex mixture" of compounds (the UCM) on the gas chromatographic chart. The UCM appears proportionally more prominent in analyses as additional oxygenated compounds are introduced to oil by bacterial and photochemical processes, and the presence and amount of the UCM can be a diagnostic indicator of heavily-weathered petroleum contamination.

Once in water, a crude oil signature can be modified by several processes including evaporation and dissolution weathering, and microbial degradation. We've recently identified another twist in tracking an oil source, the dissolved versus particulate fractions. As a droplet of oil enters water, the more readily dissolvable components, particularly the naphthalenes, are removed from the droplet thus leaving behind a particulate fraction with the "water-washed pattern" mentioned above. The receiving water then has the dissolved components signature. In essence, one source produces two signatures in water. This process is readily apparent in the discharge into Port Valdez from the Ballast Water Treatment Facility (BWTF) at the Alyeska Marine Terminal.

Figure 3 presents histograms of the PAH and AHC associated with this discharge (Payne et al. 2001; Salazar et al. 2002). In this case, the PAH pattern associated with the colloidal/particulate (oil-droplet) phase shows the depletion of naphthalene (N) and methyl-naphthalene (N1) compared to higher alkylated homologues (N2, N3, and N4), and, to a lesser extent, this same "water-washed pattern" is observed for the fluorenes (Fs), dibenzothiophenes (Ds), and phenanthrenes/anthracenes (P/As). The AHC (n-alkane) distribution from the BWTF discharge still shows the presence of minute oil droplets (they are not water soluble and hence do not dissolve), and in addition to evaporation weathering, there is evidence of microbial degradation from the biological treatment tanks at the BWTF as shown by the depleted concentrations of the n-alkanes compared to pristane and phytane (compare the AHC patterns in Figures 1 and 3).

Average BWTP Water Sample

Average BWTP Water Sample
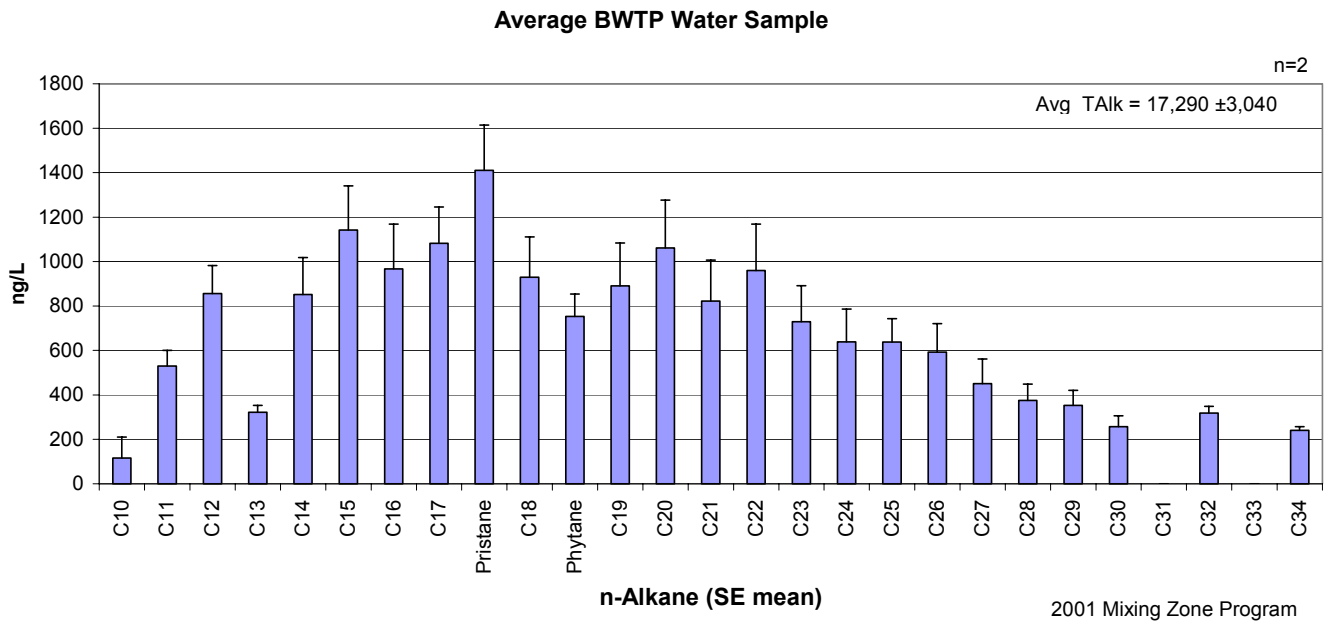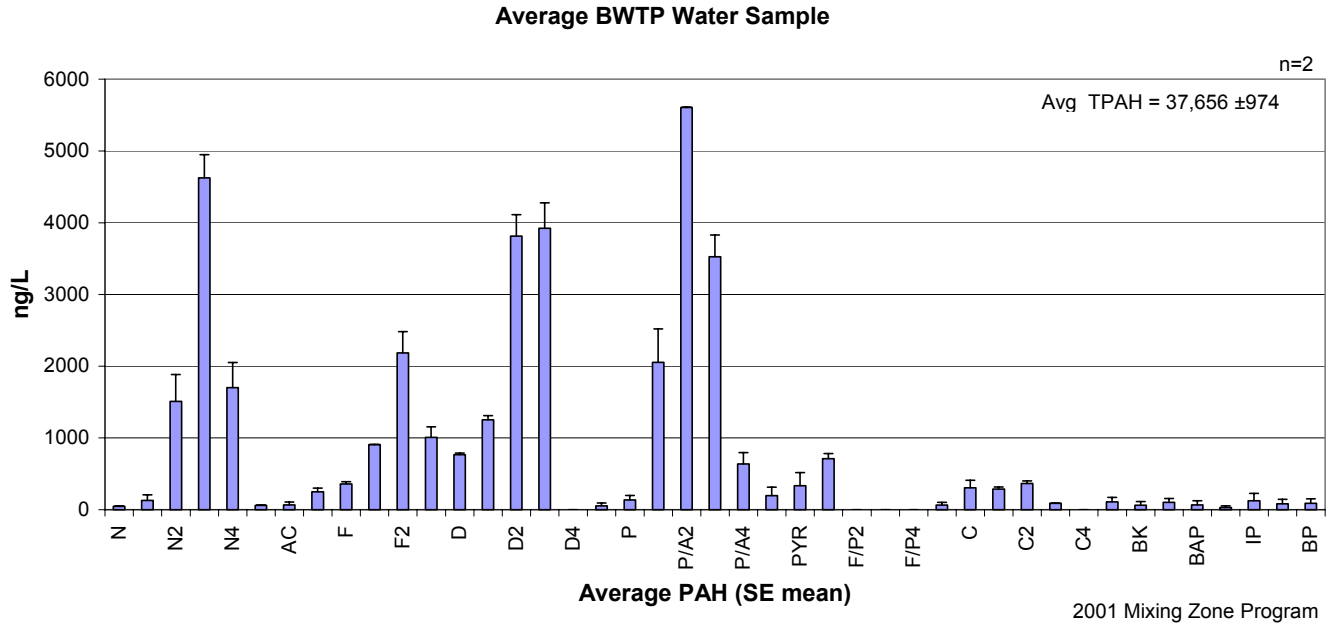
Figure 3 PAH and AHC histograms of effluent from the Alyeska Marine Terminal BWTF (from Salazar et al. 2001).

2.3 Mussels as Indicator Organisms

When analyzing the mussel samples collected as part of LTEMP, it is important to recognize that as filter feeders, mussels can accumulate oil from both the dissolved and particulate/oil-droplet phases. Figure 4 (from Payne et al. 2001) presents examples of mussels collected from oiled areas of Cabin Bay, Naked Island in Prince William Sound in May 1989 immediately after the *Exxon Valdez* oil spill and again in May/June in 1990 and 1991. In 1989, the mussels clearly accumulated PAH and aliphatic hydrocarbons from both the dissolved and particulate phases to which they were exposed; however, the particulate (dispersed oil droplet phase) was the predominant source for the accumulated higher-molecular-weight PAH (C_2-dibenzothiophenes (D2) through higher alkylated homologues of the phenanthrenes/anthracenes and chrysenes) and the aliphatics (phytane plus the even distribution of n-alkanes from n-C_{19} through n-C_{34}). As noted above, these higher-molecular-weight components have only limited water solubilities and have long been associated with the whole oil (droplet) phase. By 1990 and 1991, the mussels were accumulating primarily dissolved-phase PAH (at significantly reduced overall concentrations) from the more water-soluble hydrocarbons still leaching from the intertidal zone. This is manifest in the histogram plots at the bottom of Figure 4 by the predominant naphthalene and alkyl-substituted naphthalene homologues in greater relative abundance compared to the other PAH. Likewise, the AHC profile for the mussel samples in 1990-1991 is characterized primarily by lower molecular weight biogenic components (n-C_{15}, n-C_{17}, and pristane) with little or no contribution of higher molecular weight n-alkanes from dispersed oil droplets.

This series of histogram plots are presented as examples of what should be considered in the report that follows and specifically kept in mind when reviewing the data generated during the past 10 years of the LTEMP. The histogram profiles in Figure 4 are particularly important, because they also illustrate typical patterns of oil contamination (from both particulate and dissolved phases) in the absence of other confounding factors, such as lipid interference.
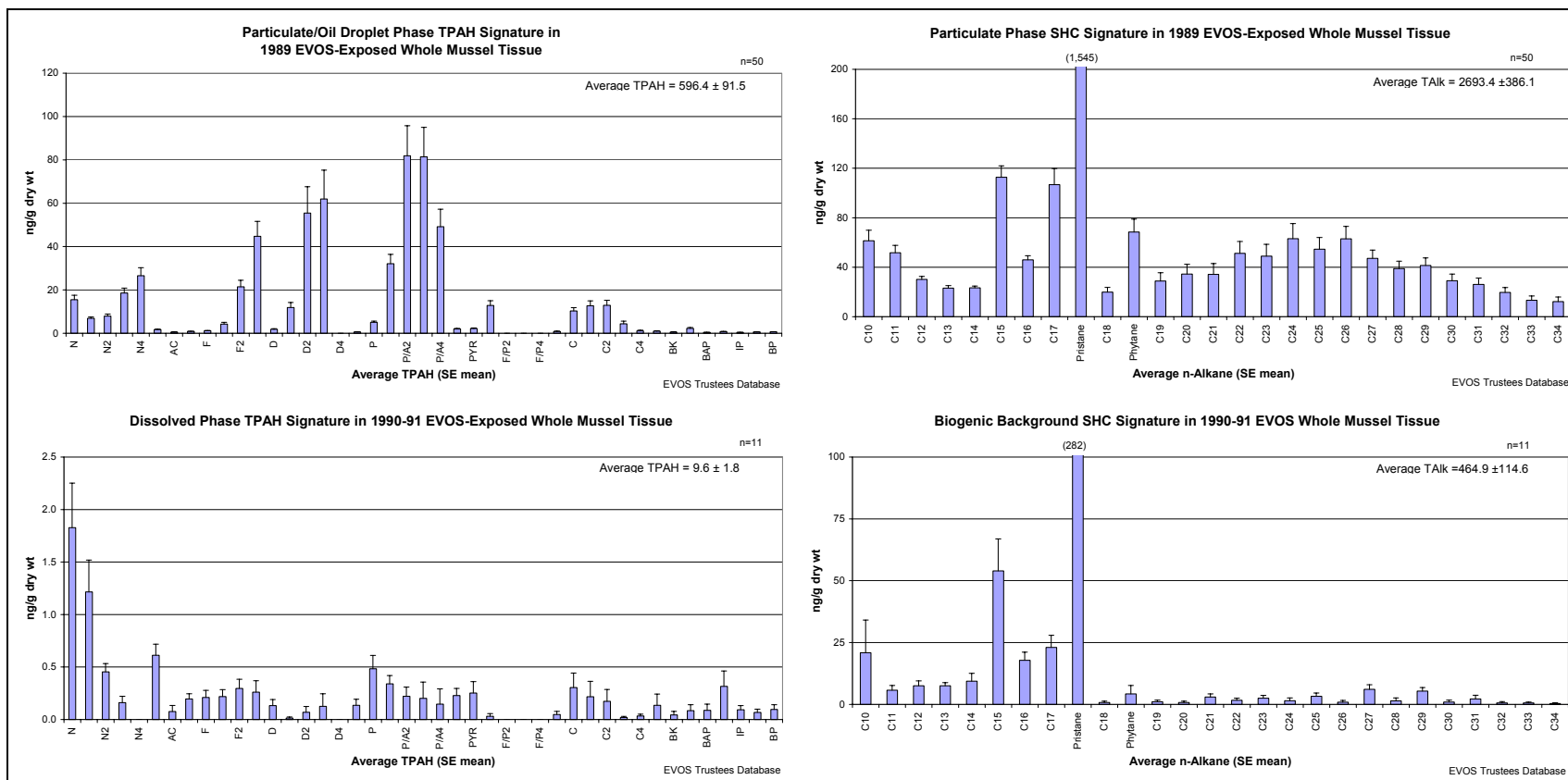
Figure 4 Average PAH and AHC histograms of whole mussel extracts from samples collected from oiled areas of Cabin Bay, Naked Island in Prince William Sound in May 1989 after the Exxon Valdez oil spill (EVOS) and again in May/June 1990 and 1991. The number of samples contributing to each composite is denoted by "n." (From Payne et al. 2001; data from NOAA EVTHD database).

3 Introduction

The primary objective of the ongoing Long-Term Environmental Monitoring Program (LTEMP) is to collect "…standardized measurements of hydrocarbon background in the EVOS region as long as oil flows through the pipeline." Currently measured variables include polycyclic (or polynuclear) aromatic and aliphatic hydrocarbon levels (PAH and AHC) in mussel (*Mytilus trossulus*) tissues from ten stations between Valdez and Kodiak and sediments from two stations in Port Valdez. The Port Valdez sediment samples are also analyzed for particle grain size and total organic carbon content. Sampling and analytical methods are patterned after the protocols developed by the National Oceanic and Atmospheric Administration (NOAA) Status and Trends Mussel Watch Program as fully detailed in the annual Monitoring Reports prepared by Kinnetic Laboratories, Inc. (KLI) and the Geochemical and Environmental Research Group (GERG).

Since the program's inception in 1993, LTEMP samples have been collected by KLI and analyzed by GERG. In July 2002, Payne Environmental Consultants, Inc (PECI) and the NOAA/NMFS Auke Bay Laboratory (ABL) began conducting the program. The LTEMP results were last reviewed in a synthesis paper (Payne et al. 1998) covering the 1993-97 results. At that time, background oil levels were higher, hot spots were identified, large and small spill events were visible in the data set, and identification of weathered sources was important. The authors recommended several changes to the existing program at that time, including:

- adjusting the sampling plan to include more sites,
- modifying the statistical criteria,
- adding intertidal sediment samples,
- rectifying MDL problems in the laboratory analyses,
- paying closer attention to field and procedural blank contamination problems,
- reinstating aliphatic hydrocarbon analyses in mussel tissue samples,
- tightening field sample procedures regarding sampling depth and mussel size,
- dropping mussel lipid corrections, seasonal sampling, and unnecessary shell measurements, and
- sampling and analyzing potential background sources with common laboratory methods.

The RCAC subsequently made several changes reducing the scope of the program and resulting in the current biannual sampling program of regional mussel tissues and Port Valdez sediments. In recent years, in addition to the early spring and mid-summer samplings, another set of mussel samples, taken in the fall just in Port Valdez (Alyeska Marine Terminal – AMT and Gold Creek – GOC), was added to the sample design. Analysis of aliphatic hydrocarbons in mussel tissues, dropped from the original program in 1995 due to results confounded from lipid interference, was reinstated in 1998.

In 2001, another data evaluation and synthesis review was completed on just the LTEMP results from the Port Valdez sites (Payne et al. 2001). Review of the data from AMT and the GOC control site suggests Alaska North Slope (ANS) crude oil residues from the terminal's ballast water treatment facility (BWTF) have accumulated in the intertidal mussels within the port. As noted above, PAH and AHC levels measured in sediments and mussel tissues (and the estimated water-column levels) continue to be low and unlikely to cause deleterious effects. From the signature of analytes, however, we were able to discriminate between particulate- (oil droplet) and dissolved-phase signals in the water column and then correlate those signals with seasonal uptake of hydrocarbons in mussels and with absorption in herring eggs (from other studies). These findings give new insight into the transport and exposure pathways in Port Valdez. The results also suggest a surface microlayer mechanism may be responsible for seasonal transport of ANS weathered oil residues from the BWTF diffuser to intertidal zones to the north and west of the terminal. Payne et al. (2001) concluded that the possibility of concentrated contaminants in a surface microlayer combined with the potential for photo-enhanced toxicity should be considered in future investigations of potential impacts in Port Valdez.

This report examines the current and historic results of 634 tissue and 108 sediment samples collected from within Prince William Sound and the surrounding region (Figure 5) in addition to the laboratory quality control results. Other sampling depths or locations in the original sample design that are no longer occupied are not included in this review.

4　Methods

4.1 Sampling Design

For both the tissue and sediment collections, the current sample design followed the previous years' efforts (KLI 2002) with slight modifications. As noted above, mussel tissues are sampled at ten sites and sediments from two sites in Port Valdez on a biannual basis (March-April and July-August). Mussel tissues are also collected from the two Port Valdez sites in October.

For tissues, three replicates were taken from random locations along the transect at each site but forgoing the proscribed randomization, detailed documentation, and beach-freezing procedures used by KLI. In a more streamlined procedure, a replicate of 25-30 mussels was collected by hand using Nitrile gloves, wrapped in aluminum foil, Ziplock® bagged, labeled, double-bagged and kept chilled until reaching the nearest freezer. The collection site was photographed and GPS coordinates recorded for chain-of-custody documentation. The entire trip collection was eventually air-freighted frozen to the NOAA/NMFS Auke Bay Laboratory in Juneau.
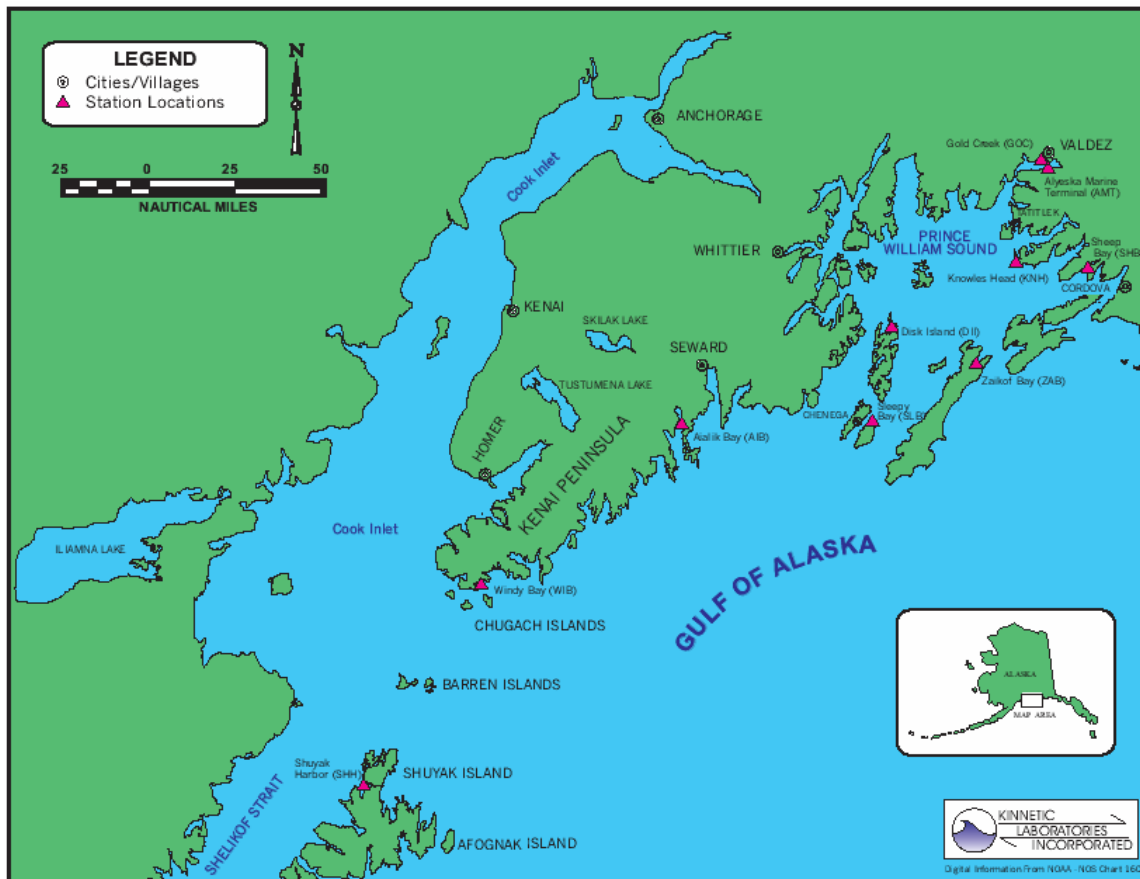
Figure 5 Map of LTEMP sites (from KLI, 2002).

Sediments were collected using the general techniques instituted by KLI but again some procedures varied. For example, a standard Van Veen grab was used rather than KLI's modified Van Veen; the standard version lacks a stabilization frame that encircles the grab. A comparison trial of the two sampler versions was conducted in July 2003; results are pending. Another significant change was replacing KLI's multi-solvent decontamination procedure with a simple seawater hose rinse. In low-oil-level environments such as PWS, a non-solvent rinse is less prone to picking up secondary contamination (e.g., from ship's oils and lubricants or airborne diesel particulates and combustion products).

Both LTEMP contractors have used a combination of vessel and float plane to access the sampling sites. Typically, the PECI field trips used the *M/V Auklet* for the Port Valdez stations and a float plane to sample all other sites.

Table 1 LTEMP Stations 2002-2003

Station Location	Station Code	Sample Type	Sampling Date	Average Station Depth	Global Positioning System (GPS) Coordinates Latitude (N)	Longitude (W)
Aialik Bay	AIB-B		7/13/2002		59° 52' 43.98"	149° 39' 5.82"

		Intertidal Mussel	3/21/2003		59° 52' 44.04"	149° 39' 5.76"
Alyeska Marine Terminal	AMT-B	Intertidal Mussel	7/9/2002 10/8/2002 3/18/2003		61° 5' 25.62" 61° 5' 25.62" 61° 5' 24.48"	146° 24' 8.78" 146° 24' 8.78" 146° 24' 0.12"
	AMT-S	Subtidal Sediment	7/10/2002 3/18/2003	66m 73m	61° 5' 24.70" 61° 5' 23.58"	146° 23' 34.78" 146° 23' 1.16"
Disk Island	DII-B	Intertidal Mussel	7/20/2002 3/20/2003		60° 29' 54.22" 60° 29' 54.6"	147° 39' 9.65" 147° 39' 39.3"
Gold Creek	GOC-B	Intertidal Mussel	7/10/2002 10/8/2002 3/18/2003		61° 7' 28.44" 61° 7' 28.44" 61° 7' 26.46"	146° 29' 7.32" 146° 29' 7.32" 146° 29' 6.74"
	GOC-S	Subtidal Sediment	7/10/2002 3/18/2003	35m 31m	61° 7' 28.62" 61° 7' 27.18"	146° 29' 26.00" 146° 29' 6.18"
Knowles Head	KNH-B	Intertidal Mussel	7/20/2002 3/20/2003		60° 41' 26.07" 60° 41' 26.94"	146° 35' 8.29" 146° 35' 8.46"
Sheep Bay	SHB-B	Intertidal Mussel	7/21/2002 3/20/2003		60° 38' 45.92" 60° 38' 45.84"	145° 59' 0.96" 145° 59' 1.12"
Shuyak Harbor	SHH-B	Intertidal Mussel	7/17/2002 3/23/2003		58° 30' 4.74" 58° 30' 4.56"	152° 37' 9.57" 152° 37' 9.42"
Sleepy Bay	SLB-B	Intertidal Mussel	7/25/2002 3/20/2003		60° 4' 2.15" 60° 4' 3.06"	147° 50' 0.08" 147° 49'59.58"
Windy Bay	WIB-B	Intertidal Mussel	7/9/2002 3/23/2003		59° 13' 5.65" 59° 13' 5.58"	151° 31' 3.01" 151° 31' 2.96"
Zaikof Bay	ZAB-B	Intertidal Mussel	7/25/2002 3/20/2003		60° 15' 54.72" 60° 15' 54.66"	147° 5' 7.13" 147° 5' 7.26"

4.2 Analytic Methods

Sediment samples (50 g wet weight) or mussel samples (10 g wet weight) were spiked with a suite of 5 aliphatic and 6 aromatic perdeuterated hydrocarbon surrogate standards (identified in Table 2) and then extracted with dichloromethane at 100 °C and 2000 psi for 10 min in a Dionex ASE 200 accelerated solvent extractor. The dichloromethane solutions were exchanged with hexane over steam, and separated into aliphatic and aromatic fractions by column chromatography (10 g 2%-deactivated alumina over 20 g 5%-deactivated silica gel; columns for sediments also contained 20 g granular elemental copper and 8 g anhydrous sodium sulfate for removal of sulfur and water, respectively). Aliphatics eluting with 50 mL pentane were analyzed by gas chromatography with a flame ionization detector (GC/FID) following concentration to ~ 1 mL hexane over steam

Table 2 Polycyclic aromatic hydrocarbon (PAH) and aliphatic hydrocarbon analytes measured in this study, along with analyte abbreviations, internal and surrogate standards.

4.2.1.1.1.1 Analytes	Abbreviation	Internal Standard	Surrogate Standard
PAH			
Naphthalene	N	A	1
C1-Naphthalene	N1	A	1
C2-Naphthalene	N2	A	2
C3-Naphthalene	N3	A	2
C4-Naphthalene	N4	A	2
Biphenyl	BI	A	2
Acenaphthylene	AC	A	2
Acenaphthene	AE	A	2
Fluorene	F	A	2
C1-Fluorenes	F1	A	2
C2-Fluorenes	F2	A	2
C3-Fluorenes	F3	A	2
Dibenzothiophene	D	A	3
C1-Dibenzothiophene	D1	A	3
C2-Dibenzothiophene	D2	A	3
C3-Dibenzothiophene	D3	A	3
C4-Dibenzothiophene	D4	A	3
Anthracene	A	A	3
Phenanthrene	P	A	3
C1-Phenanthrene/Anthracene	P/A1	A	3
C2-Phenanthrene/Anthracene	P/A2	A	3
C3-Phenanthrene/Anthracene	P/A3	A	3
C4-Phenanthrene/Anthracene	P/A4	A	3
Fluoranthene	FL	A	3
Pyrene	PYR	A	3
C1-Fluoranthene/Pyrene	F/P1	A	3
C2-Fluoranthene/Pyrene	F/P2	A	3
C3-Fluoranthene/Pyrene	F/P3	A	3
C4-Fluoranthene/Pyrene	F/P4	A	3
Benzo(a)Anthracene	BA	A	4
Chrysene	C	A	4
C1-Chrysenes	C1	A	4
C2-Chrysenes	C2	A	4
C3-Chrysenes	C3	A	4
C4-Chrysenes	C4	A	4
Benzo(b)fluoranthene	BB	A	5
Benzo(k)fluoranthene	BK	A	5
Benzo(e)pyrene	BEP	A	5

Benzo(a)pyrene	BAP	A	5
Perylene	PER	A	6
Indeno(1,2,3-cd)pyrene	IP	A	5
Dibenzo(a,h)anthracene	DA	A	5
Benzo(g,h,i)perylene	BP	A	5
Total PAH	TPAH		5
n-Alkanes			
n-Decane	C10	B	7
n-Undecane	C11	B	7
n-Dodecane	C12	B	7
n-Tridecane	C13	B	7
n-Tetradecane	C14	B	8
n-Pentadecane	C15	B	8
n-Hexadecane	C16	B	8
n-Heptadecane	C17	B	8
Pristane	Pristane	B	8
n-Octadecane	C18	B	9
Phytane	Phytane	B	9
n-Nonadecane	C19	B	9
n-Eicosane	C20	B	9
n-Heneicosane	C21	B	9
n-Docosane	C22	B	10
n-Tricosane	C23	B	10
n-Tetracosane	C24	B	10
n-Pentacosane	C25	B	10
n-Hexacosane	C26	B	10
n-Heptacosane	C27	B	10
n-Octacosane	C28	B	10
n-Nonacosane	C29	B	11
n-Triacontane	C30	B	11
n-Hentriacontane	C31	B	11
n-Dotriacontane	C32	B	11
n-Tritriacontane	C33	B	11
n-Tetratriacontane	C34	B	11
Total n-Alkanes	TALK		

Calibrated analytes are identified by boldface. Internal standards: A = hexamethyl benzene; B = dodecylcyclohexane. Surrogate standards: 1 = naphthalene-d8, 2 = acenaphthene-d10, 3 = phenanthrene-d10, 4 = chrysene-d12, 5 = benzo[a]pyrene-d12, 6 = perylene-d12, 7 = dodecane-d26, 8 = hexadecane-d34, 9 = eicosane-d42, 10 = tetracosane-d50, and 11 = triacontane-d62.

and addition of dodecylcyclohexane as an internal standard to evaluate recoveries of the surrogate standards. PAH constituents from the sample extracts were further purified by gel-permeation high performance liquid chromatography (HPLC). The injection volume was 0.5 mL into dichloromethane flowing at 7 mL/min through two size-exclusion gel columns (Phenomenex, phenogel, 22.5 mm x 250 mm, 100 Å pore size) connected sequentially. The initial 110 mL eluate was discarded, and the following 50 mL was concentrated over a 60 - 70 C water bath and exchanged with hexane to a final volume of ca. 1 mL, then spiked with hexamethylbenzene as an internal standard for estimating recoveries of the initially added perdeuterated aromatic hydrocarbon surrogate standards.

PAHs in extracts were separated and analyzed with a Hewlett-Packard 6890 gas chromatograph equipped with a 5973 mass selective detector (MSD). The injection volume was 1 µL into a splitless injection port at 300°C. The initial oven temperature was 60°C, increasing at 10°C per minute immediately following injection to a final temperature of 300°C, then held for 12 min. The chromatographic column was a 25 m fused silica capillary (0.20 mm ID) coated with 5% phenyl methyl silicone. The helium carrier gas was maintained at 70 kPa inlet pressure.

The gas chromatographic column eluted into the 70 eV electron impact MSD through a 240°C transfer line. The ionizer temperature and pressure were 240°C and 10^{-5} torr, respectively. The MSD was operated in the selected-ion-monitoring (SIM) mode. The MSD was tuned with mass 69, 102, and 512 fragments of perfluorotributylamine before each batch of samples was analyzed.

Calibrated PAHs were identified based on retention time and ratio of two mass fragment ions characteristic of each hydrocarbon. Calibrated PAHs are identified in Table 2, and include dibenzothiophene and the aromatic hydrocarbons in Standard Reference Material (SRM) supplied by the National Institute of Standards and Technology (NIST). Chromatographic peaks were identified as a calibrated aromatic hydrocarbon if both ions were co-detected at retention times within ±0.15 minutes (9 seconds) of the mean retention time of the hydrocarbon in the calibration standards, and if the ratio of the confirmation ion to the quantification ion was within ±30% of the expected ratio.

Uncalibrated PAHs include the alkyl-substituted isomers of naphthalene (except the methyl-substituted homologues), fluorene, dibenzothiophene, phenanthrene/anthracene, fluoranthene/pyrene, and chrysene listed in Table 2. Uncalibrated PAHs were identified by the presence, within a relatively wide retention time window, of a single mass fragment ion that is characteristic of the uncalibrated PAH sought. Wider retention time windows were necessary for the uncalibrated PAH because of the range of retention times of the various isomers that comprise an uncalibrated PAH homologue grouping (e.g. C3-phenanthrene).

Concentrations of calibrated PAHs in extracts were estimated by a method employing multiple internal standards and a five-point calibration curve for each calibrated PAH. The deuterated surrogate standards that were initially spiked into each sample are treated as internal standards, where each surrogate compound is associated with one or more

calibrated PAHs (see Table 2). A calibration curve for each calibrated PAH and batch of samples analyzed was based on five different hexane dilutions of dibenzothiophene and NIST SRM 1491. Each calibration curve was derived from linear regression of (1) the ratio of MSD/SIM quantification ion response of the calibrated PAH and the associated deuterated surrogate standard and (2) the ratio of the amount of calibrated PAH and the amount of deuterated surrogate in the calibration standards.

Concentrations of uncalibrated PAHs in extracts were determined with calibration curves and procedures for the most similar calibrated PAH. The MSD/SIM response to the quantification ion of each uncalibrated PAH homologue isomer were summed; this sum was used in place of the calibrated PAH response in the procedure described above for calculating concentrations of calibrated PAHs. For example, the fluorene calibration curve and procedure was used for all the alkyl-substituted fluorenes identified, but 2,6-dimethylnaphthalene, 2,3,5-trimethylnaphthalene and 1-methylphenanthrene calibration curves were used for C2-naphthalenes, C3-naphthalenes and for all the alkyl-substituted phenanthrenes, respectively.

Alkanes in extracts were separated and analyzed with a Hewlett-Packard 5890 gas chromatograph equipped with a flame ionization detector (FID). The injection volume was 1 µL into a splitless injection port at 300°C. The 60°C initial oven temperature was maintained for 1 minute, then increased at 6°C per minute to a final temperature of 300°C, then held for 25 min. The detector temperature was 320°C. The chromatographic column was the same as that used for PAH analysis (see above). The helium carrier gas flow rate was 0.80 - 2.0 mL per minute, and the column effluent was combined with 34 mL per minute nitrogen make-up gas before entering the FID. The FID was operated with hydrogen- and air-flow rates of approximately 33 and 360-410 mL per minute, respectively. Alkane hydrocarbons were identified based on their retention times. Any peak detected above the integrator threshold within ±0.25% of the mean retention time of an alkane in the calibration standards was identified and quantified as that alkane.

Concentrations of calibrated alkanes (listed in Table 2) were determined by an internal-standard method employing a five-point calibration curve for each alkane. The deuterated surrogate standards that were initially spiked into each sample were treated as internal standards, where each surrogate compound was associated with a group of calibrated alkanes (see Table 2). A calibration curve for each calibrated alkane and batch of samples analyzed was based on five different hexane dilutions of the alkane standards. Each calibration curve was derived from linear regression of (1) the ratio of FID response of the alkane and the associated deuterated surrogate standard, and (2) the ratio of the amount of calibrated alkane and the amount of deuterated surrogate in the calibration standards.

Amounts of uncalibrated alkane hydrocarbons and the cumulative amount of hydrocarbons in the unresolved complex mixture (UCM) were calculated with respective detector responses and the calibration curve for hexadecane. Flame ionization detector response due to the UCM was determined as the difference of the total FID response and the response due to distinguishable peaks using valley-to-valley baseline integrations.

4.3 Quality Assurance

Quality control samples were analyzed with each batch of 12 samples to assess the accuracy and precision of the analysis, and to verify the absence of laboratory contaminants introduced during analysis. Two quality control samples for accuracy assessment were prepared from hydrocarbon standards prepared by NIST (for PAH) or by ABL (for aliphatics), and run with each batch. Precision was assessed by analysis of two NIST standard reference material (SRM) samples analyzed with each batch: SRM 1974a for mussels and SRM 1944 for sediments. The mussel reference is especially appropriate for these analyses because the PAH concentrations are quite low, with many of the PAH analytes present at concentrations near the method detection limits (MDLs). Absence of laboratory contaminants was verified by analysis of one method blank sample with each batch.

Method detection limits were estimated for each calibrated alkane and PAH analyte following the procedure described in Appendix B, 40 Code of Federal Regulations, Part 136.   Method detection limits for uncalibrated PAHs were not experimentally determined. Consequently, detection limits for these analytes were arbitrarily assumed as the MDL of the most closely related calibrated PAH analyte.

4.4 Inter-laboratory Comparison

The comparability of hydrocarbon analysis results between ABL and GERG was assessed through analysis of two kinds of inter-comparison samples. First, two mussel samples and one sediment sample from each of the two Port Valdez stations (AMT and GOC) during the July 2002 sampling event were split and analyzed at both laboratories. These samples were each homogenized at ABL prior to splitting, then aliquots of the homogenates were frozen and submitted to each facility for analysis. Second, the same NIST SRM (1974) was analyzed with the duplicate mussel samples within the batch containing the mussel duplicate samples at each laboratory, providing a comparison of a sample of known composition. Unfortunately, the laboratories each use a different SRM for sediments, so comparisons of the sediment standards was not possible.

4.5 Determination of Moisture Content

Weighed aliquots of wet mussel homogenates or of sediments were dried at 100°C for 24 h and re-weighed to determine the moisture content, and the ratio of these wet and dry weights was used to convert PAH and AHC concentrations to a dry weight basis.

4.6 Particle Grain Size Determination

Determination of the distribution of particle grain sizes in the sediment samples was determined by a combination of sieving and pipette methods as described in GERG SOP 8908.

4.7 Determination of Total Organic and Total Carbon

Analytical measurements of total organic and total carbon are determined on oven dried and pulverized sediment samples using a Dohrmann DC-85A TOC catalytic combustion (oxygen @ 200 ml/min and cobalt oxide on alumina) furnace. The carbon dioxide produced is passed through an acidified liquid sparger (scrubs out entrained water vapor and corrosive species), two scrubbers (copper and tin) and linerarized non-dispersive infrared detection, by comparison with results from a calibration curve based on potassium acid phthalate. Total organic carbon (TOC) and total carbon (TC) are determined on samples treated with and without 10% HCl in methanol. Total inorganic carbon is calculated as the difference between TC and TOC.

4.8 Data Analysis

The LTEMP program was designed to determine baseline conditions and help identify potential future impacts of oil transportation in the study area. In the conception of this project, the sample design was configured to facilitate inferential testing of null hypotheses. For example, the number of replicates was assessed to ensure that the desired power would be obtained in testing three primary hypotheses. Following the project review in 1998 (Payne et al. 1998), this emphasis was relegated to lesser priority. It was realized at that time that there was more information available in the individual samples than in simply looking at trends of averaged indices. A more cogent story could be told by subjectively assessing the chemical composition and levels of the analytes than could be garnered from evaluating the trends in means and variances. Over the past five years, we have also developed new analytic tools and insights into the behavior and fate of oil in the regional environment (Payne et al. 2001). For this report, it was decided that a complete review of all the tissue and sediment data would be required to place the current samplings in context and to attempt to understand the events in the region.

Several indices have been developed and used in prior LTEMP studies. KLI has diligently reported these values during recent years. For the current report, we utilize a number of these and introduce several more. The goal here is not to just be clever about making up new indices but rather to quantify as much as possible, the subjective task of source identification and to provide supporting evidence for suppositional trends and scenarios, including the identification of laboratory artifacts. Should they be required, these ratios may also be useful in developing testable null hypotheses.

The indices used for this report are presented in Table 3; their function and composition have been explained in earlier KLI reports. New to this program are the PDR, Upper Aliphatic Hump, Plant Wax, and Marine Biogenic indices. The PDR (particulate/dissolved ratio) arose from the observation that hydrocarbon residues in Mytilus tissues in Port Valdez tend to change seasonally from particulate (primarily oil droplet) to the dissolved fractions (Payne et al. 2001). This shift is basically due to seasonal changes in the stability of the water column; oil droplets from the BWTF diffuser reach the surface during winter and early spring months when winds keep the

water column unstratified. Mussels then ingest the tiny droplets, albeit at low levels. Empirically, the PDR quantifies the identity of the fraction: below a value of 1, the fraction is dissolved, above 2, the fraction is particulate, values between 1 and 2 represent a blend of these two physical states.

Table 3 Hydrocarbon Parameters Used in the LTEMP Data Analysis (adapted partially from KLI, 1997).

Parameter	Relevance
TPAH (mussel tissue and sediments)	Total PAH as determined by high resolution GC/MS with quantification by selected ion monitoring; defined as the sum of 2 to 5-ring polycyclic aromatic hydrocarbons: Naphthalene + fluorene + dibenzothiophene + phenanthrene/anthracene + chrysene, and their alkyl homologues + other PAHs (excluding perylene); useful for determining TPAH contamination and the relative contribution of petrogenic, pyrogenic, and diagenic sources
FFPI (sediments)	The Fossil Fuel Pollution Index is the ratio of fossil-derived PAHs to TPAH and is defined as follows: $$FFPI = (N + F + P + D)/TPAH \times 100$$ where: N (Naphthalene Series) = C_0-N + C_1-N + C_2-N + C_3-N + C_4-N F (Fluorene series) = C_0-F + C_1-F + C_2-F + C_3-F P (Phenanthrene/Anthracene series) = C_0-A +C_0-P + C_1-P + C_2-P + C_3-P + C_4-P D (Dibenzothiophene Series) = C_0-D + C_1-D + C_2-D + C_3-D FFPI is near 100 for petrogenic PAH; FFPI for pyrogenic PAH is near 0 (Boehm and Farrington 1984)
TAHC (sediments)	Total Aliphatic Hydrocarbons quantifies the total n-alkanes (n-C_{10} to n-C_{34}) + pristane and phytane; represents the total resolved hydrocarbons as determined by high resolution gas chromatography with flame ionization detection (GC/FID); includes both petrogenic and biogenic sources
UCM (sediments)	Petroleum compounds represented by the total resolved plus unresolved area minus the total area of all peaks that have been integrated; a characteristic of some fresh oils and most weathered oils

CPI (sediments)	The Carbon Preference Index represents the relative amounts of odd and even chain alkanes within a specific boiling range and is defined as follows: $$CPI = 2(C_{27} + C_{29})/(C_{26} + 2C_{28} + C_{30})$$ Odd and even numbered n-alkanes are equally abundant in petroleum but have an odd numbered preference in biological material; a CPI close to 1 is an indication of petroleum and higher values indicate biogenic input (Farrington and Tripp 1977)
CRUDE Index (sediments)	A summation of TPAH, TAHC and UCM weighted to assess the petrogenic fractions $$CRUDE = (TPAH \times FFPI/100) + (TAHC/CPI^2) + UCM/1000$$
MPI (mussel tissues)	The Mytilus Petrogenic Index isolates the FFPI fraction of TPAH $$MPI = TPAH \times FFPI/100$$
PDR (mussel tissues and sediments)	The Particulate/Dissolved Ratio identifies a sample as containing the dissolved or particulate (oil droplet) PAH fractions of oil. $$PDR = (Phenanthrenes\_Anthracenes + Dibenzothiophenes + Chrysenes)/Naphthalenes$$ Samples having PDR values less than 1.0 are dissolved oil fractions, greater than 2.0 are particulate/oil droplet fractions, between 1 and 2 are blends of the fractions.
Upper Aliphatic Hump (mussel tissues)	The modal group of analytes termed the Upper Aliphatic Hump is thought to be a laboratory artifact of lipid or other interference that over-reports these values. This index is used in screening for AHC data quality. $$\text{Upper Aliphatic Hump} = \text{Sum of } C_{22} \text{ to } C_{32}/TAHC$$
Plant Wax Index (sediments)	The Plant Wax Index is the sum of aliphatic hydrocarbons typical of naturally-occurring terrestrial plant wax compounds $$\text{Plant Wax Index} = (C_{25} + C_{27} + C_{29} + C_{31})/TAHC$$
Marine Biogenic Index (mussel tissues)	Mussels and copepods accumulate selected aliphatic hydrocarbons from their phytoplankton diets. $$\text{Marine Biogenic index} = (C_{15} + C_{17} + pristine)/TAHC$$

The Upper Aliphatic Hump is a relative quantification of the C_{22} to C_{32} mode in the aliphatic compounds. This modal group is thought to possibly be an artifact of lipid interference in measuring the AHC. This cluster was ubiquitous in many mussel samples across all stations and seasons in the early years of the program, and it made up anywhere from 50-90% of the total AHC (TAHC) signal. Despite an appearance that was temptingly close to the homologous series of even and odd higher-molecular-weight n-alkanes characteristic of heavily weathered fuel oils, it did not correlate with individual or total PAH (TPAH) concentrations in any of the samples and therefore could not be associated with oil. In an effort to try and tease out meaningful AHC data against this background signal, the Upper Aliphatic Hump was used to plot its frequency of appearance and in various other attempts to define quantitative correlations among it and other variables. The new plant wax and the marine biogenic indices are based upon the well-known attribution of specific aliphatic hydrocarbons to these sources. These indices quantify the portion of the TAHC that come from these specific sources. Terrestrial plant waxes add to the C_{25}, C_{27}, C_{29} and C_{31} values. Sediments heavy in terrestrial deposits will spike the plant-wax constituents. From their diets of phytoplankton and detrital organic matter, mussels accumulate C_{15}, C_{17} and pristane.

For this program, we find the CRUDE index very effective for evaluating sediments and the MPI for evaluating tissues. Using the CRUDE index for tissues is limited in this program due to the missing aliphatic data and problems with lab analyses.

Data analysis for this project relied heavily on reviewing the histogram plots of each sample. To facilitate this effort, an application was developed to plot each sample from a station in replicate groups with lab method detection limits (MDLs) superimposed on the histogram and the relevant lab method blank adjacent to the group. For example, from Aialik Bay, 64 tissue PAH samples were plotted three to a row plus the lab blank for that batch. Another application would present the AHC samples in the same manner. Finally, a third graphing application would call up all analytes from two selected samples and a reference standard to be viewed in close detail with relevant indices' values.

Single graphs of various indices or groupings of indices were also useful for evaluating trends at particular sites.

4.9 Data Management

For this project, data received in spreadsheet format from ABL were combined with historic data from KLI database archives. Microsoft Excel pivot tables were used for most data compilations. Graphing and data processing routines were then custom programmed using Microsoft Visual Basic for Applications (VBA) code.

Finally, new data from ABL were incorporated into the existing Microsoft Access LTEMP archive using KLI's relational database structure (described in KLI 2002).

5   Results and Discussion

5.1 Laboratory Inter-comparison Results

5.1.1 Duplicate Field Samples

Results from ABL and GERG for analysis of the split sediment and mussel samples differed substantially, with results from GERG usually higher than those from ABL. These differences were greatest for uncalibrated PAH in mussels (Table 4 presents the split samples summary -- full data are in appendix A-3). Total PAH (TPAH) in the two split AMT mussel samples were 1,240 ng/g and 576 ng/g, and were 2,030 ng/g and 1,080 ng/g in the two split GOC samples when analyzed at GERG, compared with concentrations ranging from 75 ng/g to 126 ng/g in the duplicates analyzed at ABL.. (All data in this report are reported on a dry weight basis.) About half of the GERG TPAH was due to alkylated fluorenes, followed by alkylated phenanthrenes (Figure 6). Based on discussions with Dr. Guy Denoux at GERG (personal communication 8/7/03), the reported alkylated fluorenes are actually believed to be false positives due to lipid interference. It is not known if the elevated phenanthrenes may also be due to lipid interference. The highest PAH results in the GERG-analyzed samples were usually above MDL, but concentrations found in the ABL-analyzed samples were consistently below MDL (except for naphthalene, which was the single most abundant PAH measured in the ABL duplicates). Agreement of the calibrated PAH was usually closer, and ABL values exceeded GERG values for the 5- and 6-ring PAH in one AMT sample (Figure 6).

Table 4 Inter-laboratory Split Sample Results – Summary (ng/g dry wt.)

	ABL	GERG	ABL	GERG
Tissues				
Sample Number	**AMT-B 1A**		**AMT-B 2A**	
Total PAH	127	1240	86	576
Fluorenes	7.5	730.5	5.5	115.1
Dibenzothiophenes	8.0	49.4	3.7	18.7
Tot. Alkanes	1,845	132,133	2,363	135,516
Sample Number	**GOC-B 1A**		**GOC-B 2A**	
Total PAH	98	2032	75	1076
Fluorenes	6.1	1233.1	5.5	681.9
Dibenzothiophenes	3.6	47.3	4.2	34.3
Tot. Alkanes	2,056	34,393	2,258	84,628
Sediments				
Sample Field Number	**AMT-S 1**		**GOC-S 1**	
Total PAH	193	607	42	281
Fluorenes	10.1	39.5	4.7	53.0
Dibenzothiophenes	21.0	33.6	3.0	18.5
Tot. Alkanes	354	1,291	161	2,661
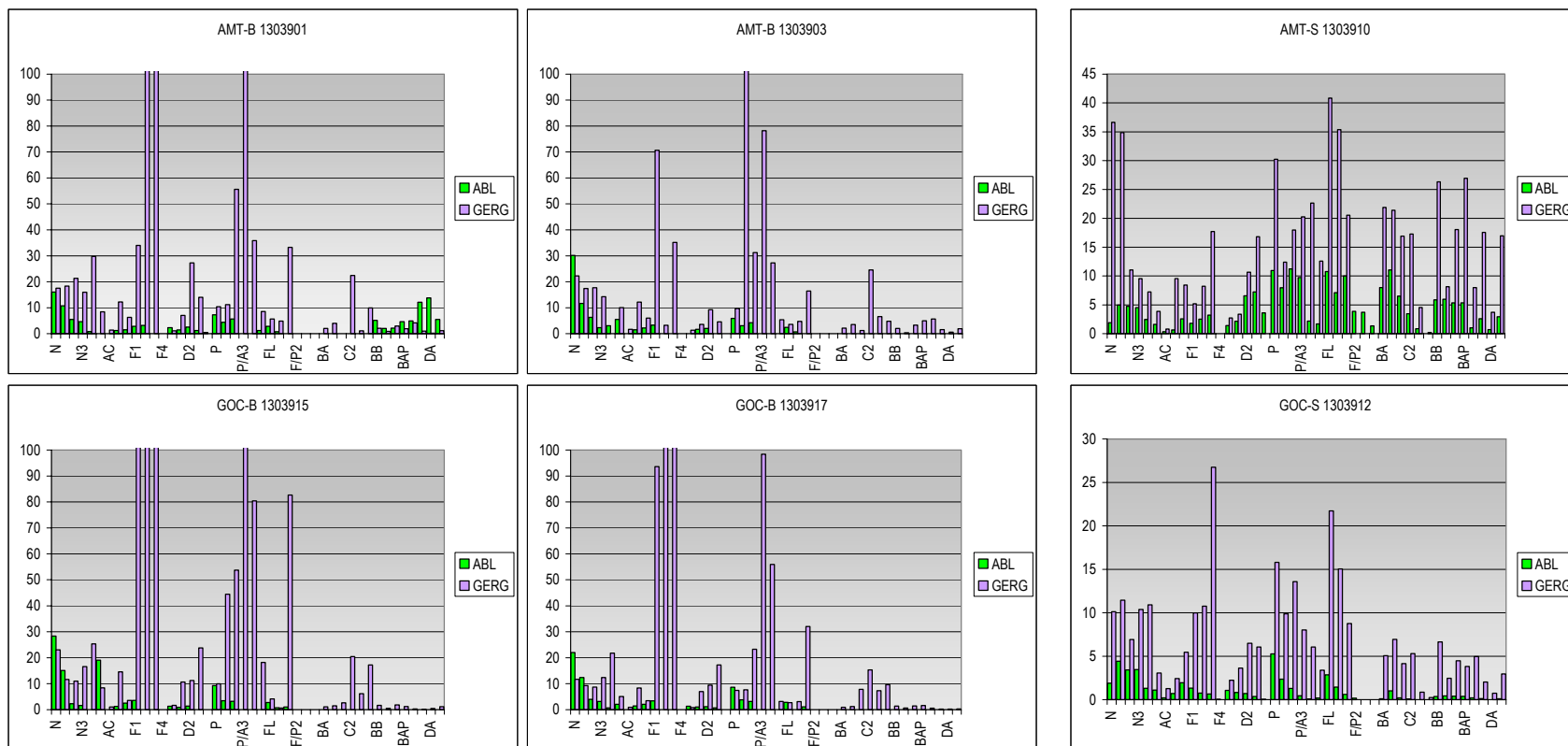
Figure 6 PAH histograms for split tissue and sediment samples analyzed in by GERG and ABL in interlaboratory comparison study.

Concentrations of aliphatic hydrocarbons reported by GERG also tended to be higher than those reported by ABL in the split mussel samples. Both laboratories detected n-alkanes in the range of n-C_{11} to n-C_{17}, as well as pristane, n-C_{25} and n-C_{27}, usually at concentrations near MDL, especially at ABL. At GERG, these detected concentrations were consistently lower than 2,800 ng/g. At GERG, n-C_{21} and n-alkanes in the range from n-C_{28} to n-C_{31} were also often detected, especially n-C_{29} and n-C_{30} at concentrations that approached 50,000-100,000 ng/g, but these were not detected at ABL (Figure 7). Based on past reports from KLI and GERG and the detailed analyses presented in the following sections, these later eluting n-alkanes are believed to be the result of lipid interferences.

Results from GERG-analyzed sediments also tended to be higher than those from ABL for corresponding sample duplicates. Total PAH in the split AMT and the split GOC sediment samples were 607 ng/g and 281 ng/g when analyzed at GERG, compared with 180 ng/g and 42 ng/g in the duplicates analyzed at ABL (Table 4). Differences for the specific PAH analytes are best evaluated graphically as shown in Figure 6. Results from both laboratories were usually above MDL for the AMT sample, and at ABL were usually above MDL for GOC sample as well because of the larger sediment sample aliquots analyzed at ABL (~25 g at ABL vs. < 3 g at GERG). Unlike the duplicate mussel samples, GERG-analyzed PAH tended to be greater than ABL for both calibrated and uncalibrated PAH, by factors of ~3 to >10 (Figure 6).

Concentrations of aliphatic hydrocarbons reported by GERG in the split sediment samples were somewhat higher than those reported by ABL, but were near or below MDL at both labs. The highest aliphatic concentrations reported were 672 ng/g and 523 ng/g for n-C_{31} and n-C_{27} reported by GERG for the GOC sediment, but otherwise were usually well below 200 ng/g. The highest aliphatic concentrations reported by ABL were 69 ng/g and 64 ng/g for n-C_{32} and n-C_{34} in the AMT sediment.

5.1.2 SRMs

The laboratory differences noted above for the split mussel samples are confirmed in the analysis of the SRM 1974a. Both laboratories agree well with the certificate values for the calibrated PAH as well as for most of the uncalibrated PAH (Figure 8). However, the alkylated fluorenes reported by GERG are substantially higher than those reported by ABL, and as noted above, the elevated fluorenes noted in the SRM are also attributed to lipid interference.

The NIST doesn't certify n-alkanes in their SRM samples, but both GERG and ABL analyzed n-alkanes in the tissue SRM samples. Figure 9 presents the results from these analyses. Fairly close agreement was obtained for the lower molecular weight n-alkanes; however, there is a significant discrepancy between the two laboratories for the higher molecular weight components (particularly C_{20}, C_{25}, C_{29} and C_{30}), and this is believed to be due to lipid interference problems at GERG.

34
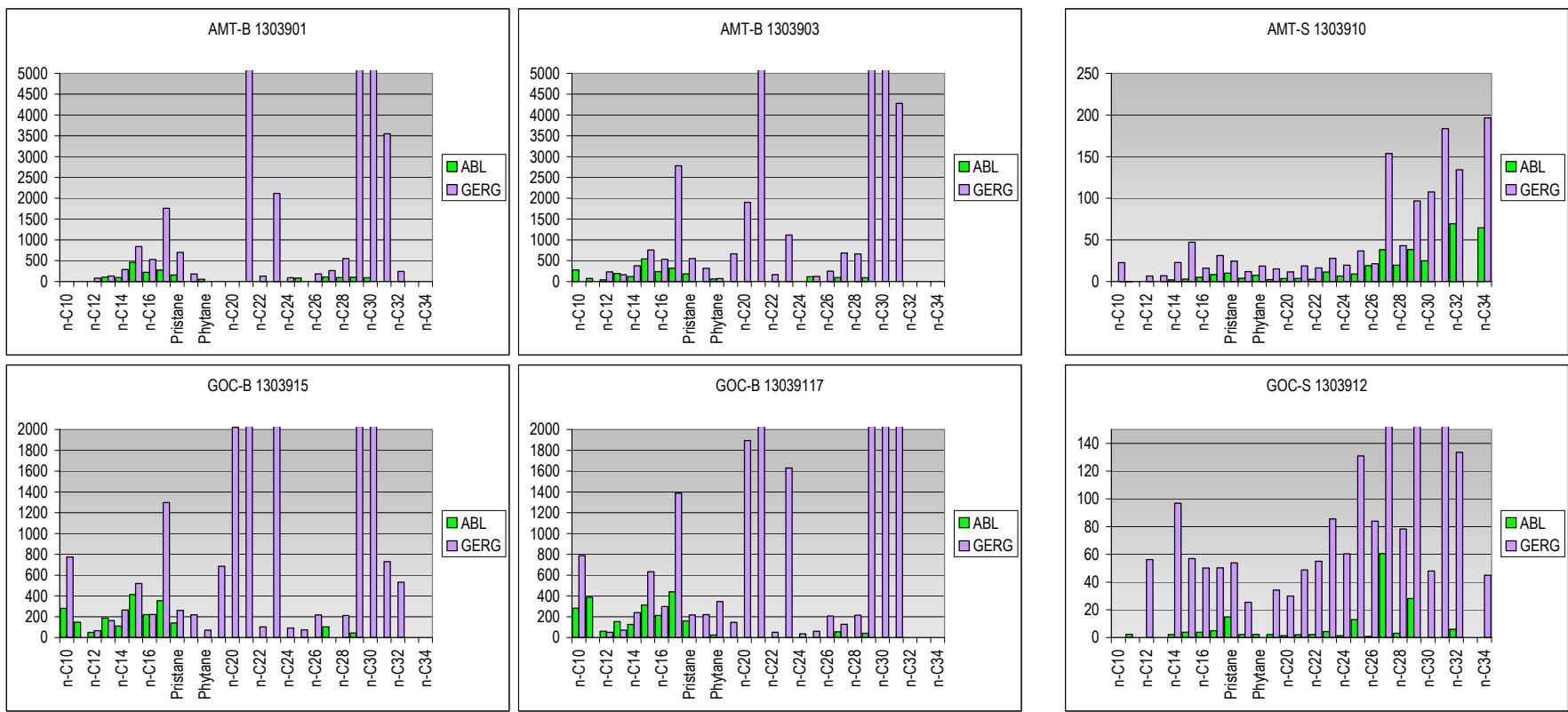
Figure 7 AHC histograms for split tissue and sediment samples analyzed in by GERG and ABL in inter-laboratory comparison study.
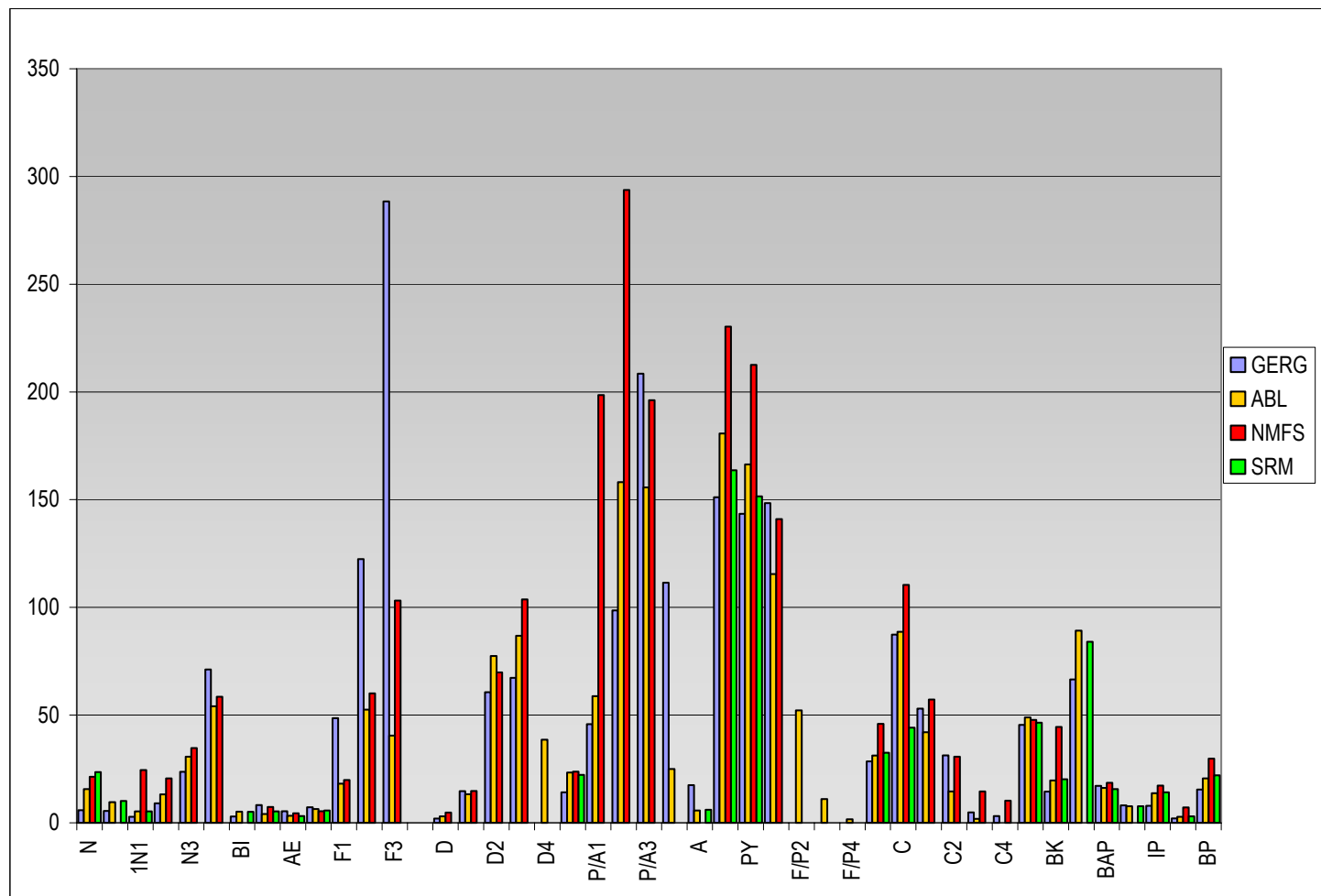
Figure 8 PAH histogram for NIST Tissue SRM 1974a analyzed by GERG, ABL, and NMFS/NOAA Montlake Laboratory compared to NIST certified values (SRM).
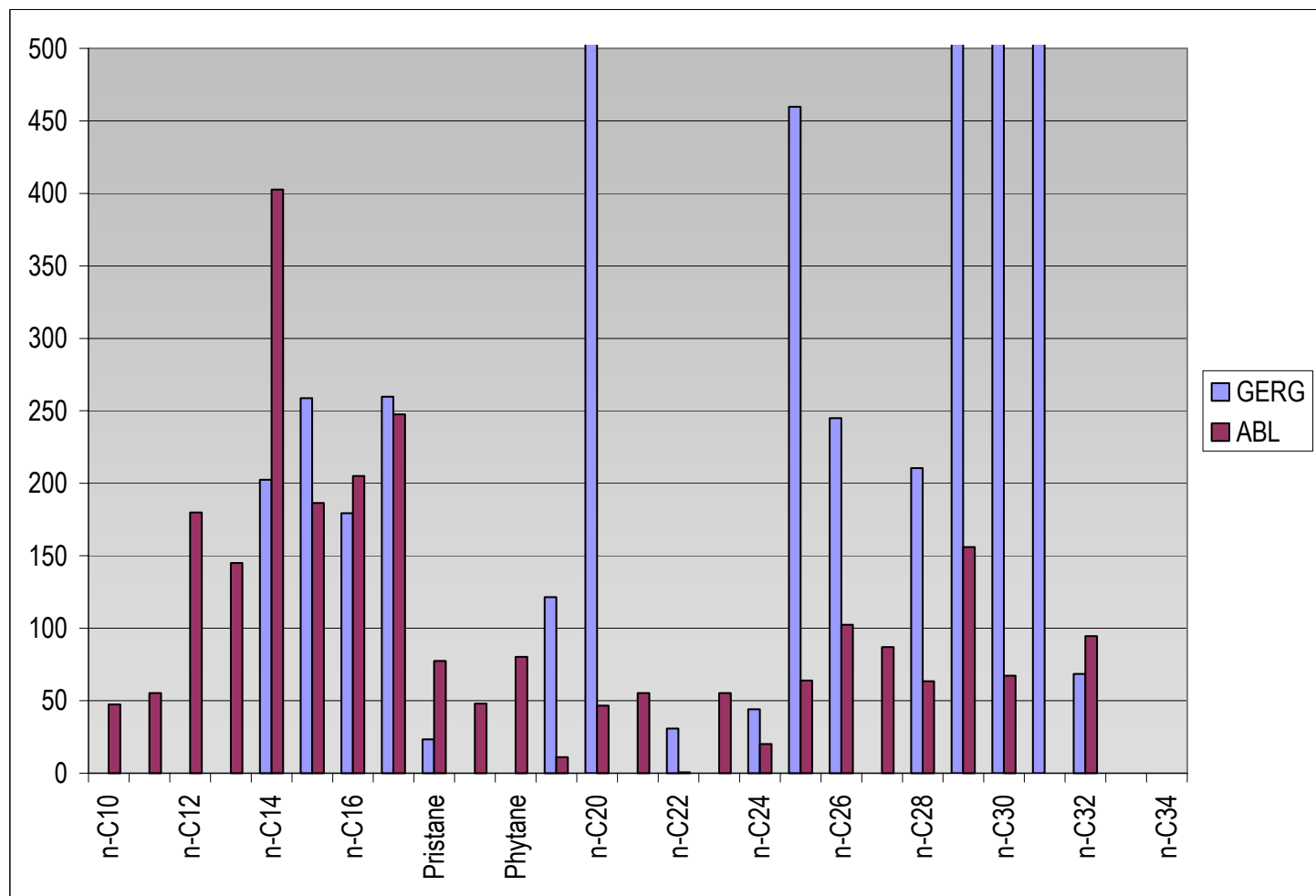
Figure 9 AHC histogram for NIST Tissue SRM 1974a analyzed by GERG and ABL. (There are no NIST certificated values for AHC).

The laboratories analyzed different SRMs along with their split sediment samples, but their agreement with the certificate values of the respective SRMs is excellent (appendix A-5).

As the results provided above indicate, there were substantial discrepancies among the split samples analyzed at GERG and ABL, with results reported by GERG generally higher than those reported by ABL. This indicates either a positive interference at GERG, or a negative interference at ABL. Analysis of the mussel SRM 1974a provides a means of resolution, but only for the calibrated PAH because only these have values certified by NIST. Comparison of results from GERG and from ABL for their respective analyses of SRM 1974a shows that both laboratories report results for the calibrated PAH with impressive accuracies. The problem is with the uncalibrated PAH and with some of the aliphatics, neither of which have certified values in this SRM, and the aliphatics are present at concentrations that are usually below the MDLs of both laboratories.

In an attempt to provide further resolution of the discrepancies for the alkyl PAH we compared results from GERG and ABL with those from the Montlake Facility, Northwest Science Center, National Marine Fisheries Service, a third laboratory that has a well-established reputation for these analyses (Figure 8). Comparison of these results shows the alkyl-fluorene results from GERG are substantially higher than the other two laboratories, whereas the alkyl-phenanthrene results from Montlake are substantially higher than those reported by either GERG or ABL. This comparison fairly illustrates the problems attending the analysis of the uncalibrated compounds at low concentrations. The analytical control available for these compounds is much less tight, mainly because their measurement inevitably depends on a greater degree of the analyst's subjectivity. Calibrated compounds are single chromatographic peaks that occur at a relatively precise retention time ($< \pm 1$ sec) on a (usually) well-defined baseline, whereas the uncalibrated compounds occur as a multiplet of peaks within a retention time window of several minutes on a more variable baseline. These uncalibrated PAH are thus inherently more vulnerable to interferences that may be positive or negative if the baseline is not well controlled, and the multiplet includes several peaks, each present at relatively low magnitude. In the present case, the comparison of results from the three laboratories suggests that alkyl-fluorenes reported by GERG may be affected by positive interferences, whereas alkyl-phenanthrenes reported by ABL may be affected by negative interferences, based on the consensus values.

The discrepancy between the split sediment samples analyzed at GERG and at ABL may also be affected by differences in sample aliquot sizes. Reported results were generally higher at GERG for both calibrated as well as uncalibrated PAH for these sediments compared with ABL. The sample aliquot analyzed at ABL was larger than that analyzed at GERG by factors of ten and forty. Low sample aliquot sizes can sometimes inflate the reported concentration because a low signal is divided by a low sample mass. Alternatively, the possibility that analyses at ABL are less sensitive at low PAH concentration compared with GERG cannot be discounted. However, results from both laboratories are usually below their respective MDLs, making quantitative comparisons more problematic. The results reported by ABL for the sediment SRM do not help

resolve this matter because the PAH concentrations in SRM 1944 (analyzed at ABL) are substantially higher than those in SRM 1941b (analyzed at GERG), so the performance at ABL on sediments containing low PAH concentrations cannot be compared. However, in general, both laboratories reported quite low PAH concentrations in the split sediment samples compared.

5.1.3 Particle Grain Size

The laboratory comparisons for grain size and sediment total organic and inorganic carbons (Figure 10 and Appendix A-2) are generally within an expected range of variability, given the inherent difficulties in homogenizing and splitting soil samples, and in the methods typically used for grain size analysis (sieving sands/silts and hydrometer analysis for silt/clay fractions). Notably, there is a 2-3% difference in sand content in the sample split analyzed by both GERG and ABL. If the samples were perfectly split, the sand results might be a bit closer for AMT. But the overview is that the sediments are a really fine-grained material with a little bit of sand size material. Per ASTM, less than or equal to 5% sand would be "with trace sand" and 5 to 15% sand would be "with sand" (D. Pischer, pers comm. August 2003). The relevancy of these differences is discussed in the PGS section below.

5.2 Analysis of Field Samples

5.2.1 ABL Quality Assurance Results

For the 2002-2003 field samples, all the hydrocarbon analytes listed on Table 2 were lower than respective MDLs by at least a factor of five in the method blanks analyzed with each batch of samples for this report, verifying the absence of positive interferences introduced at the laboratory. Analysis of the ten accuracy-check samples (i.e. SRM 1491 or the ABL aliphatic standard) indicated that accuracy for the calibrated compounds ranged from 88% to 110% of certified or expected values. The median precision of the PAH (including the uncalibrated PAH) in the eight SRM 1974a samples analyzed for the mussel batches, expressed as the coefficient of variation, was 14%. The precision ranged from 5% to 101%, and was less than 40% for all but two analytes (biphenyl and C-4 dibenzothiophenes). Precision of aliphatics was not evaluated for this SRM because aliphatics were usually below MDLs, and because certified values are not available. Precision of the PAH in sediments was not evaluated because only two reference samples were analyzed for the sediment sample batch for this project; however, the precision of PAH analyses of sediments at ABL has historically been comparable to precision for PAH in mussels.

Recoveries of surrogate standards were between 30% and 113% for 98% of the surrogate hydrocarbons monitored. Three unacceptably low recoveries (<30%) occurred in one sample (mussels from AMT-B collected in July 2002) and would ordinarily be re-analyzed. This sample is one of those split for duplicate analysis at ABL and GERG, so the re-analysis will be performed pending a decision on the best use of the remaining homogenate.
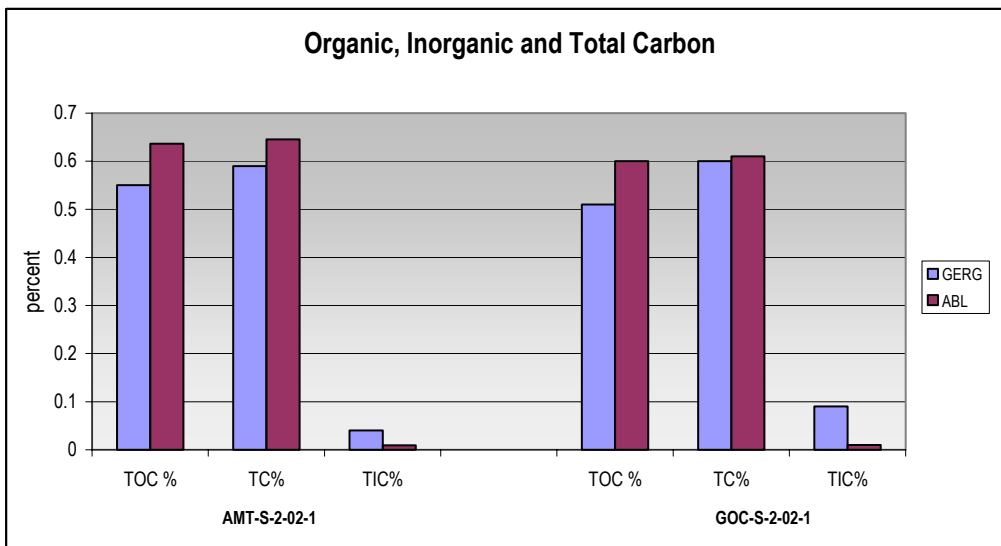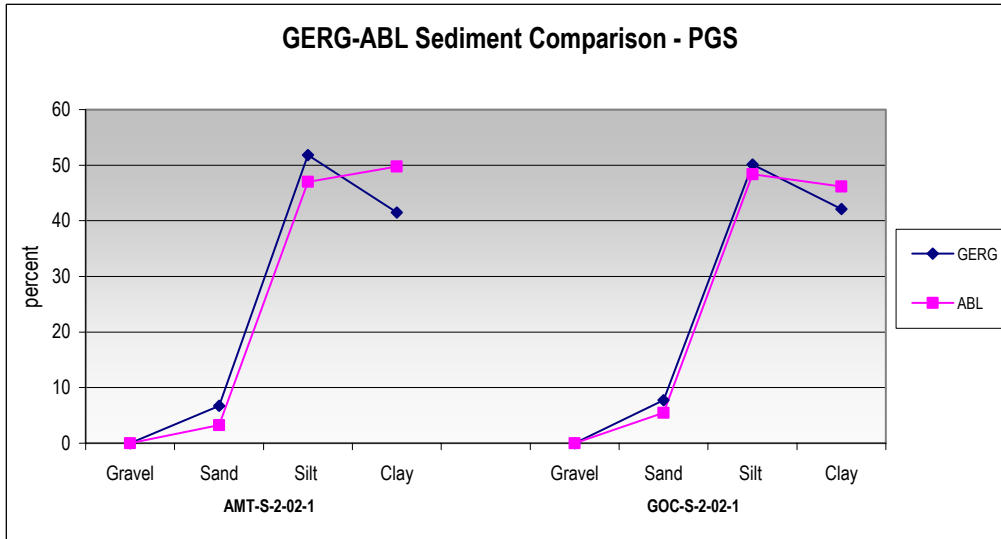
Figure 10 Comparison of split-sample analysis for sediment grain size, total carbon, total organic and inorganic carbon for inter-laboratory calibration.

5.2.2 Sediments

5.2.2.1 Particle Grain Size

Sediment grain size plots (Figure 11) show that sediment compositions from the last two samplings are within the variance of previous years. But variance there is, which suggests several possibilities: 1) the bottom is not homogeneous, 2) the vessel is unable to sample the same exact location, 3) the sample was collected by non-uniformly scrapping the surface, 4) the sample was handled or processed differently or 5) the laboratory procedure is variable. From the data and field notes, we have likely encountered all of the above to various degrees.

Firstly, the bottom of Port Valdez is not homogeneous. Shallow near-shore deposition is subject to a variety of processes including seasonal rainfall, river flows, wave energy, tidal currents, biological production and fixed-station sampling. Secondly, the ability to reoccupy a station is dependent upon the "size of the station" and the skill of the vessel operator. GPS positioning, with a 10 m error, is only partially helpful; other navigational skills are required. For example, the GOC site appears on vessel sonar as a small knoll. We sample from the top of the feature as the sides are too steep to get a good grab. Frequently, the vessel drifts until finding the spot from the depth cues, then we anchor and readjust our position trying to remain there. At the AMT site, navigation is equally challenging as the skipper maneuvers to a triangulated sighting and depth point. On the last two samplings, a containment boom encircling an actively loading tanker interfered with reaching that particular spot. We ended up sampling at a slightly-deeper-than-preferred depth immediately adjacent to the boom. At GOC in March 2003, a combination of these two factors, bottom changes and navigation issues, resulted in obtaining an individual grab sample containing 46% sand and gravel (rather than the typical 2-3%). Unbeknownst to us at the time, the sample was anomalous and should have been rejected. Fortunately, the oil signature for this sample is the same, although lower in TPAH, as that seen in the other two replicates. This "sampling error" corroborates the local oil transport mechanism involving adsorption of the minute oil droplets onto finer-grained suspended particulate matter that eventually settles to the bottom.

Another variable was the handling procedure. In March 2003, the PGS samples were inadvertently frozen rather than refrigerated. In theory, freezing a silt sample might cause the ice crystals to disassociate the agglomerated silt particles into clay particles. A small trial was run using the unfrozen July 2002 samples versus frozen splits from the same samples. The results showing the differences between the unfrozen and frozen PGS samples appear in Table 5. The results from AMT-S rep 3 seem anomalous for unknown reasons; however, in general, freezing Port Valdez sediments tends to increase clay content approximately 5%.
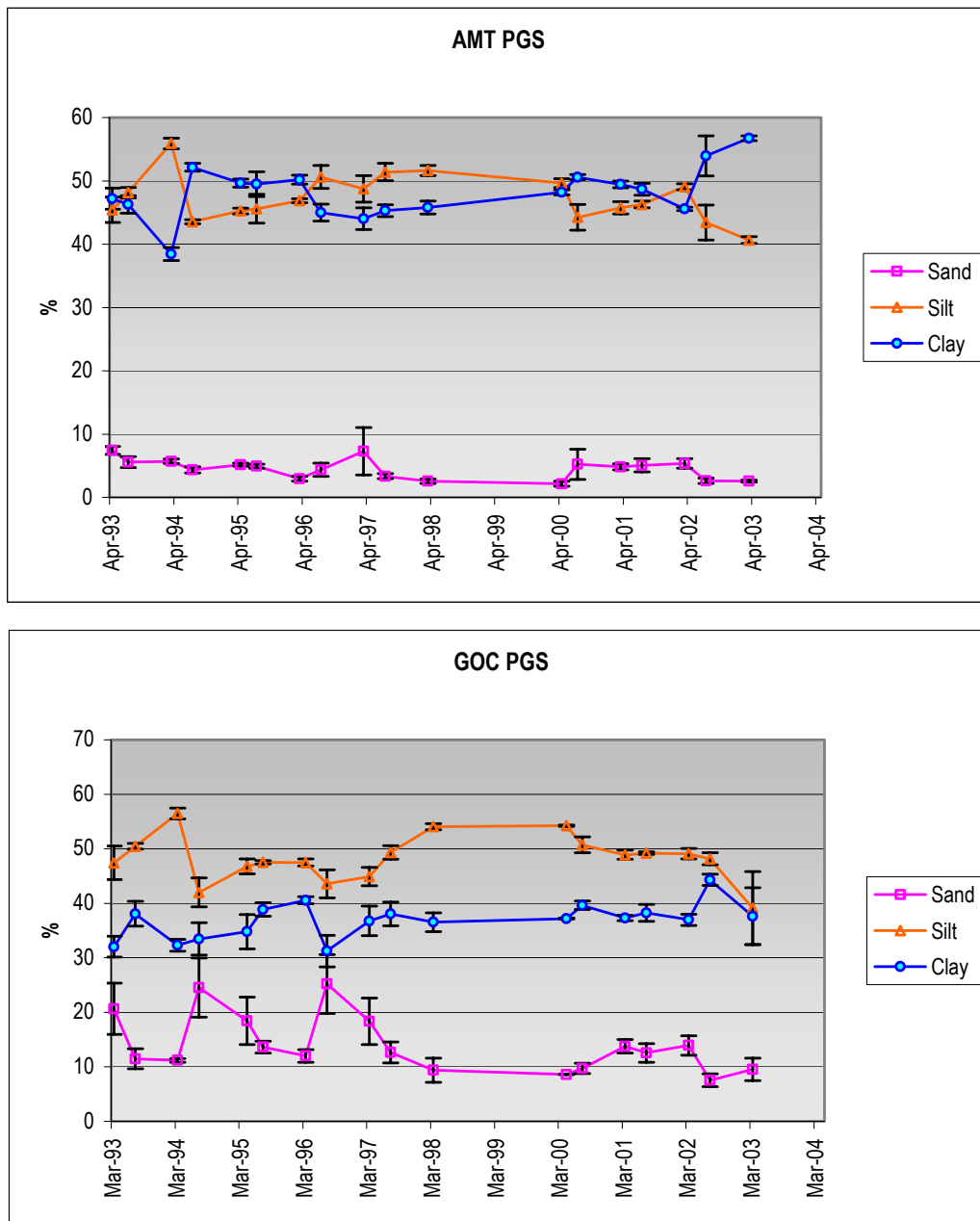
Figure 11 Grain size composition at Alyeska Marine Terminal and Gold Creek, 1993-2003.

Table 5 Comparison of frozen versus non-frozen particle-grain-size (PGS) samples.

	Non-frozen			Frozen			Difference		
	% Sand	% Silt	% Clay	% Sand	% Silt	% Clay	% Sand	% Silt	% Clay
AMT-S rep1	3.24	46.99	49.77	2.57	40.17	57.25	0.7	6.8	-7.5
AMT-S rep2	2.82	45.28	51.90	2.31	41.83	55.86	0.5	3.4	-4.0
AMT-S rep3	1.84	37.98	60.18	2.04	40.55	57.40	-0.2	-2.6	2.8
GOC-S rep1	5.48	48.36	46.16	5.02	44.74	50.25	0.5	3.6	-4.1
GOC-S rep2	7.49	49.94	42.57	7.92	44.33	47.76	-0.4	5.6	-5.2
GOC-S rep3	9.61	46.19	44.20	7.90	41.09	51.00	1.7	5.1	-6.8
						Average	.5	3.7	-4.1
						SE	0.31	1.35	1.50

Finally, the differences between frozen and non-frozen sand content and the inter-laboratory comparisons of PGS samples (above section), suggests that method inaccuracies also exist. Apparently, PGS results will never reach the precision or accuracy of the chemistry results. So, how relevant are these differences to the LTEMP program?

The PGS data serve two main purposes to the LTEMP program. First, they ensure that the monitored location has not undergone drastic changes, e.g., slope failures, dredge spoils deposits, etc. Secondly, the silt + clay value allows a rough confirmation or calibration of TPAH levels should it ever become necessary. In summary, the current inaccuracies in PGS measurements, while not desirable, do not seriously compromise LTEMP's objectives.

5.2.2.2   Chemistry Data Quality

Overall the data quality (as reflected by deuterated surrogate recoveries, the lack of significant interference by target analytes and other unknown components in procedural blanks, acceptable precision in duplicate samples and as measured by comparison to specific calibrated PAH analytes in SRMs) was reasonably good for sediment samples examined at both GERG and ABL. Surrogate recoveries for deuterated PAH ranged from 48 to 104 percent at GERG and from 50 to 98 percent at ABL. These values are within the accepted ranges published in the standard operating procedures (SOP's) of each laboratory and those recommended in NOAA Status and Trends protocols.

When target analytes were observed in the procedural blanks associated with a batch of field samples, they were generally less than 10 percent of the values observed in the field samples. Furthermore, when PAH or AHC components in the blanks exceeded those observed in the field samples, the patterns were sufficiently different to ensure that what was observed in the field replicates was representative of conditions in the field and not the result of laboratory artifacts or contamination. Figure 12 presents representative PAH and AHC histograms plots from field samples and associated blanks obtained from Alyeska Marine Terminal (AMT) and Gold Creek (GOC). Method detection limits (corrected for sample size) are shown by the blue diamonds and solid blue line in each figure. These plots illustrate that although numerous components are often at or below MDLs (particularly for GOC), that reasonable precision among the field replicates was obtained and that significantly different patterns were generated in the field samples and the associated procedural blanks.

5.2.2.3 Correlation of Aromatic and Aliphatic Fractions

As described in the primer on oil chemistry, petroleum hydrocarbons constitute a mixture of aliphatic and aromatic components. Therefore, in samples contaminated by hydrocarbon residues, one would expect reasonable correlations between the total PAH (TPAH) and total AHC (TAHC). Figure 13 presents the plots comparing TPAH and TAHC for AMT and GOC. As expected, at AMT, where the sediment hydrocarbon levels are higher because of their immediate proximity to the Alyeska Marine Terminal BWTF diffuser, there is a good correlation between TPAH and TAHC ($r^2 = 0.450$, n = 54). At Gold Creek, where the potential for a mixture of various sources (e.g., biogenic hydrocarbons such as fecal pellets from copepods, terrestrial plant waxes, diesel residues from fishing and commercial boat traffic, as well as particulate and dissolved AMT BWTF sourced components) is greater, the correlation is not as strong ($r^2 = 0.295$, n = 54).

Figure 14 presents the relationship between total PAH and particle grain size distributions at both sites. As expected, TPAH concentrations increase as the sediment particle grain size decreases in line with known mechanisms of PAH association with finer grained particles and deposition in sedentary regimes.
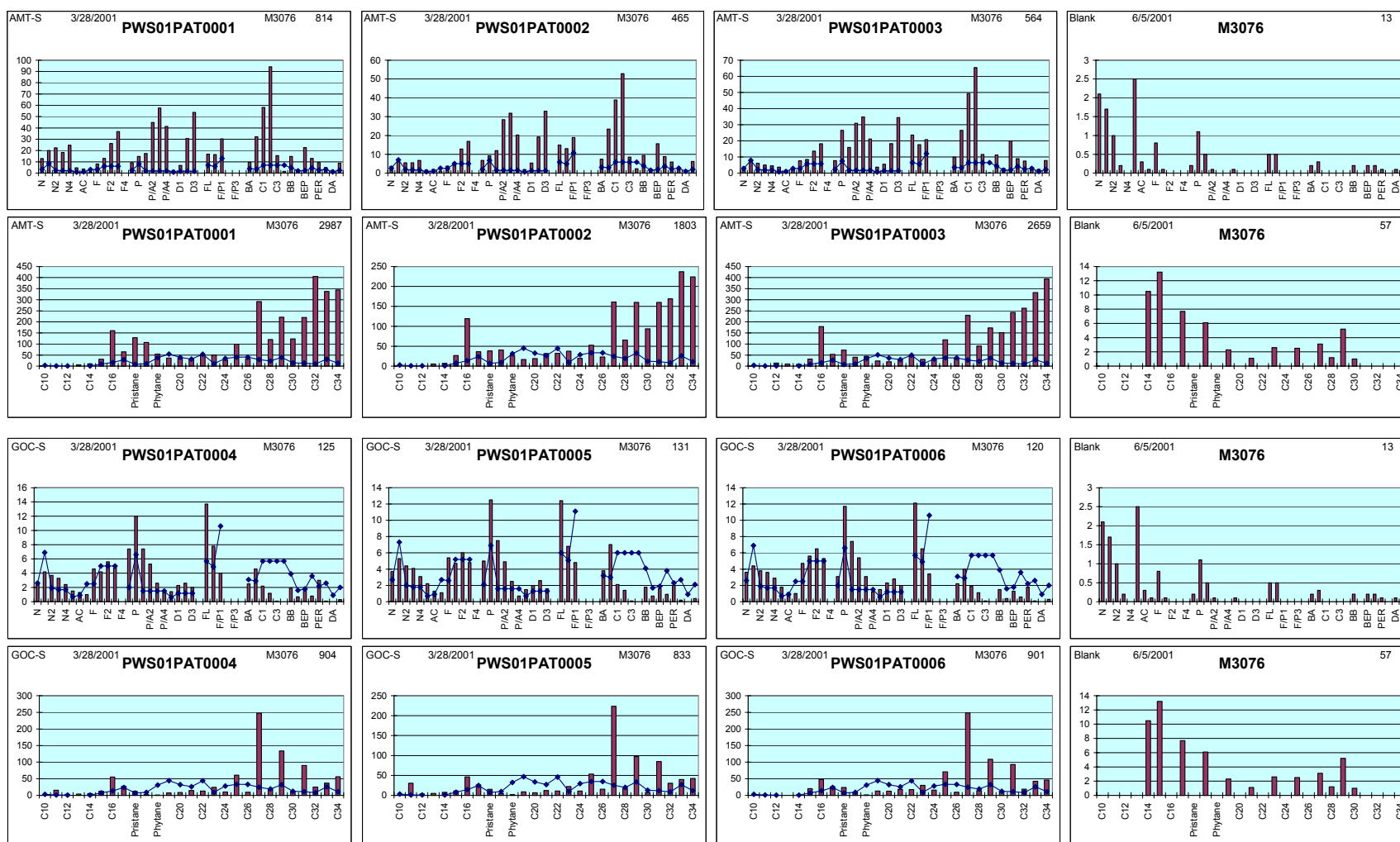
Figure 12 Example of PAH and AHC histograms from AMT and GOC (3/28/2001) showing typical low oil, combustion product, and biogenic hydrocarbon levels and the relative differences in fingerprint patterns and concentrations measured in the associated procedural blanks.

AMT-S

KLI data
$$y = 3.2069x + 657.48$$
$$R^2 = 0.5621$$

ABL only
$$y = 0.512x + 493.29$$
$$R^2 = 0.0975$$

- KLI data
- Outliers
- ABL data
- Linear (KLI data)
- Linear (ABL data)

GOC-S

KLI data
$$y = 5.9717x + 260.94$$
$$R^2 = 0.3027$$

ABL only
$$y = 5.0653x + 23.436$$
$$R^2 = 0.2209$$

- KLI data
- Outliers
- ABL data
- Linear (KLI data)
- Linear (ABL data)
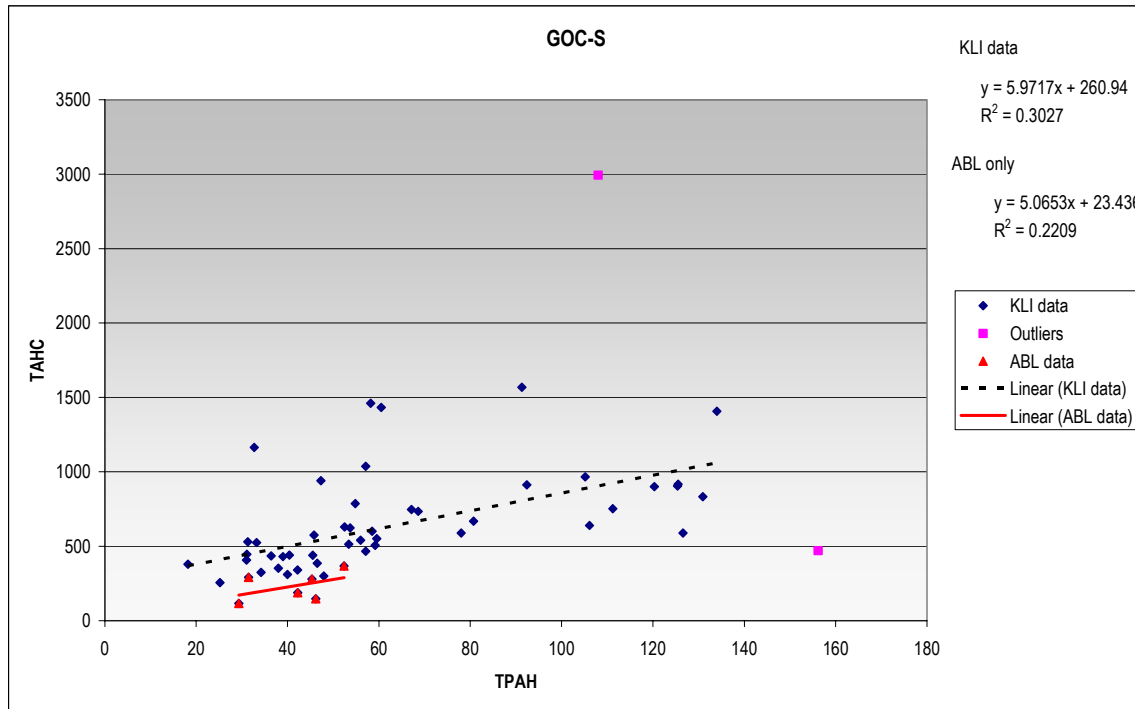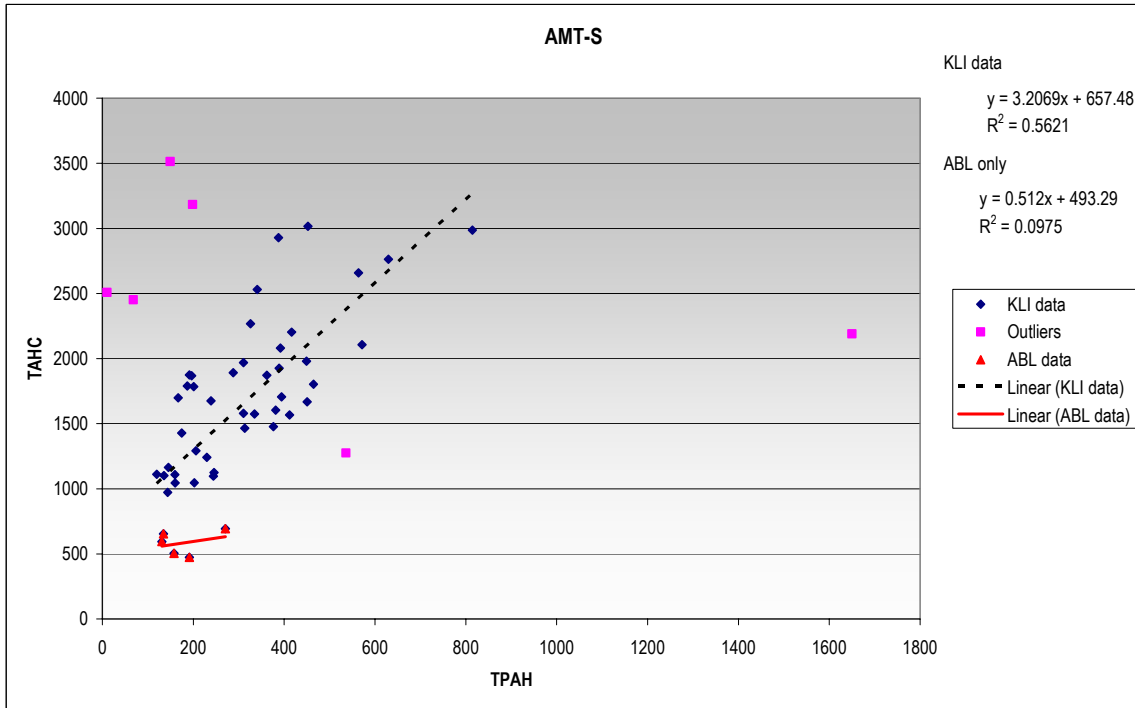
Figure 13 Correlation of TPAH vs. TAHC for AMT sediments analyzed at GERG and ABL.
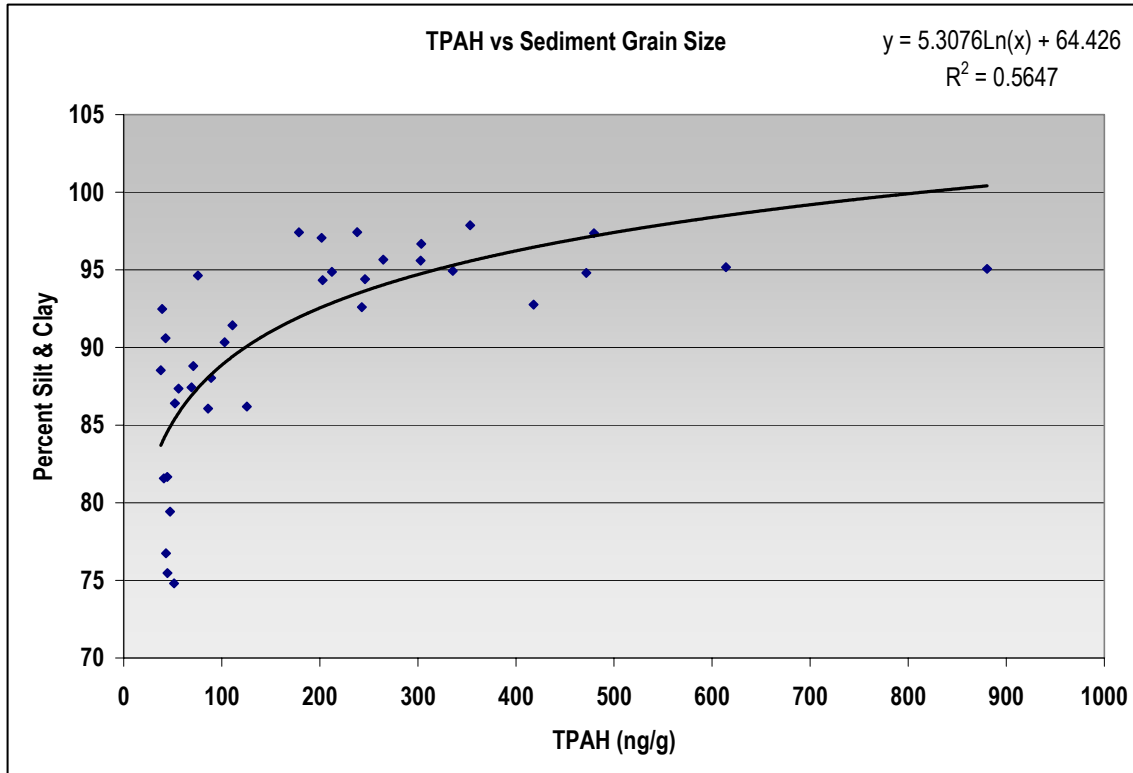
Figure 14 Relationship between PGS (% silt and clay) and TPAH measured in sediments from AMT and GOC.

5.2.2.4   Sediment Hydrocarbon Concentration Trends and Source Analyses

Appendix A-6 presents the total AHC and PAH values of individual sediment samples, seasonal averages, and the associated coefficients of variation for the replicate measurements completed between 1993 and 2003. The TPAH values in the sediments from Gold Creek are uniformly low, ranging from 25 ng/g in March 1995 to only 156 ng/g in March 1996. The sediments obtained at Alyeska Marine Terminal exhibit more variability and ranged from a low of 10 ng/g dry wt. measured in March 2002 to a high of 1,650 ng/g dry wt. observed in July 1995.

Figure 15 presents the mean TPAH concentrations (and associated standard error of the mean) measured in the sediments as a function of time. This figure illustrates the temporal variability and shows that the TPAH concentrations in the sediments at the two sites do not appear to be related. Concentrations for two intertidal samples collected in July 1998 are also shown and are clearly lower than their respective subtidal trend lines.

Figures 16 and 17 present the average sediment PAH and SHC histogram profiles for both Port Valdez stations and allows comparison between the stations by season and intertidal versus subtidal sample location. The PAH concentrations in the intertidal stations are significantly
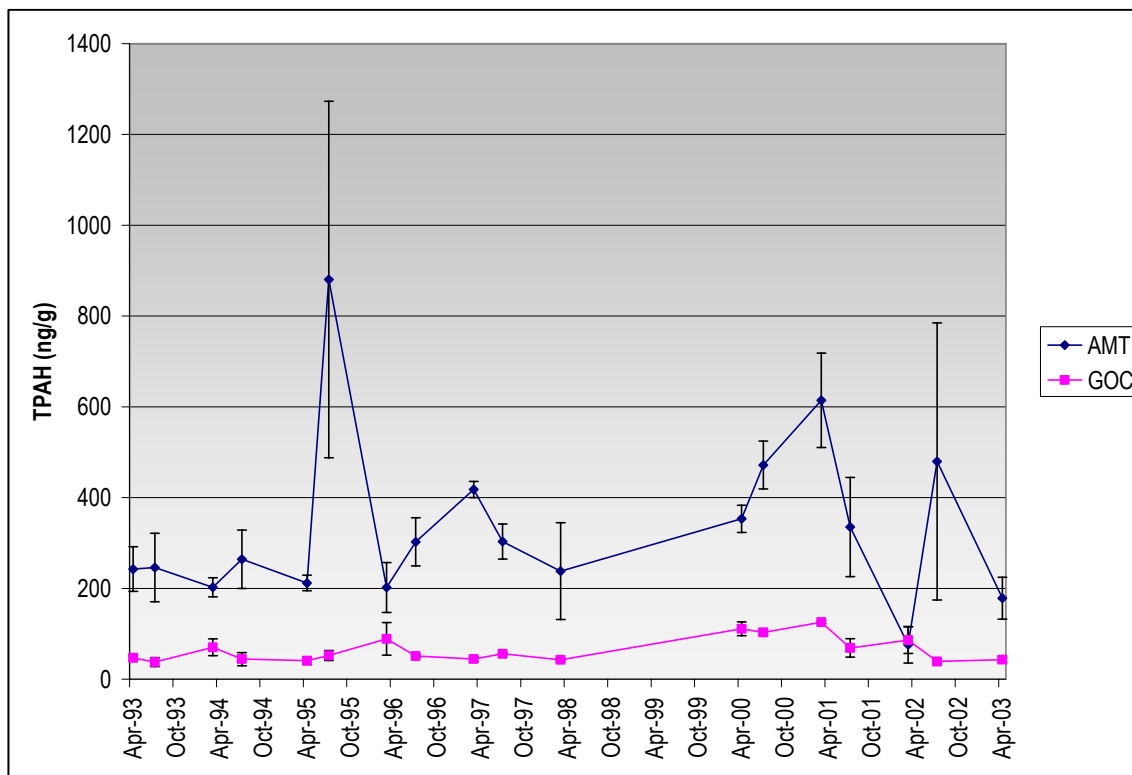
Figure 15 Time series mean sediment TPAH concentrations (and standard error of the mean) measured from March 1993 through March 2003 at AMT and GOC.

lower than the subtidal samples at both locations; however, the compositions are slightly different. The AMT intertidal site collected in July 1998 appears to have both a dissolved- and particulate-phase petroleum signal, while the GOC intertidal sample exhibits characteristics of both a petrogenic and pyrogenic signal.

There does not seem to be a seasonal PAH pattern observed in the sediments at either AMT or GOC, although the variability is higher at AMT in the summer. Likewise, the AHC profiles look very similar in both seasons, with the only major difference being increased relative concentrations of pristane (copepod related) in the summer.

Figure 18 plots the sediment CRUDE index values (Payne et al. 1998) for both stations over the ten years of the program to date. The CRUDE index combines into a single value many of the numerous individual factors and characteristic ratios that have been used for oil data analysis by chemists and environmental scientists in the past (see Table 3). With this single-value approach emphasizing the petrogenic over the pyrogenic and biogenic signals, some of the variability in the Gold Creek trend line in Figure 15 is reduced (the CRUDE Index values range from 20 –100 as opposed to the TPAH range of 25 – 156), and the importance of the petrogenic versus the pyrogenic influence at the Alyeska Marine Terminal station in the 1993 samples is emphasized.
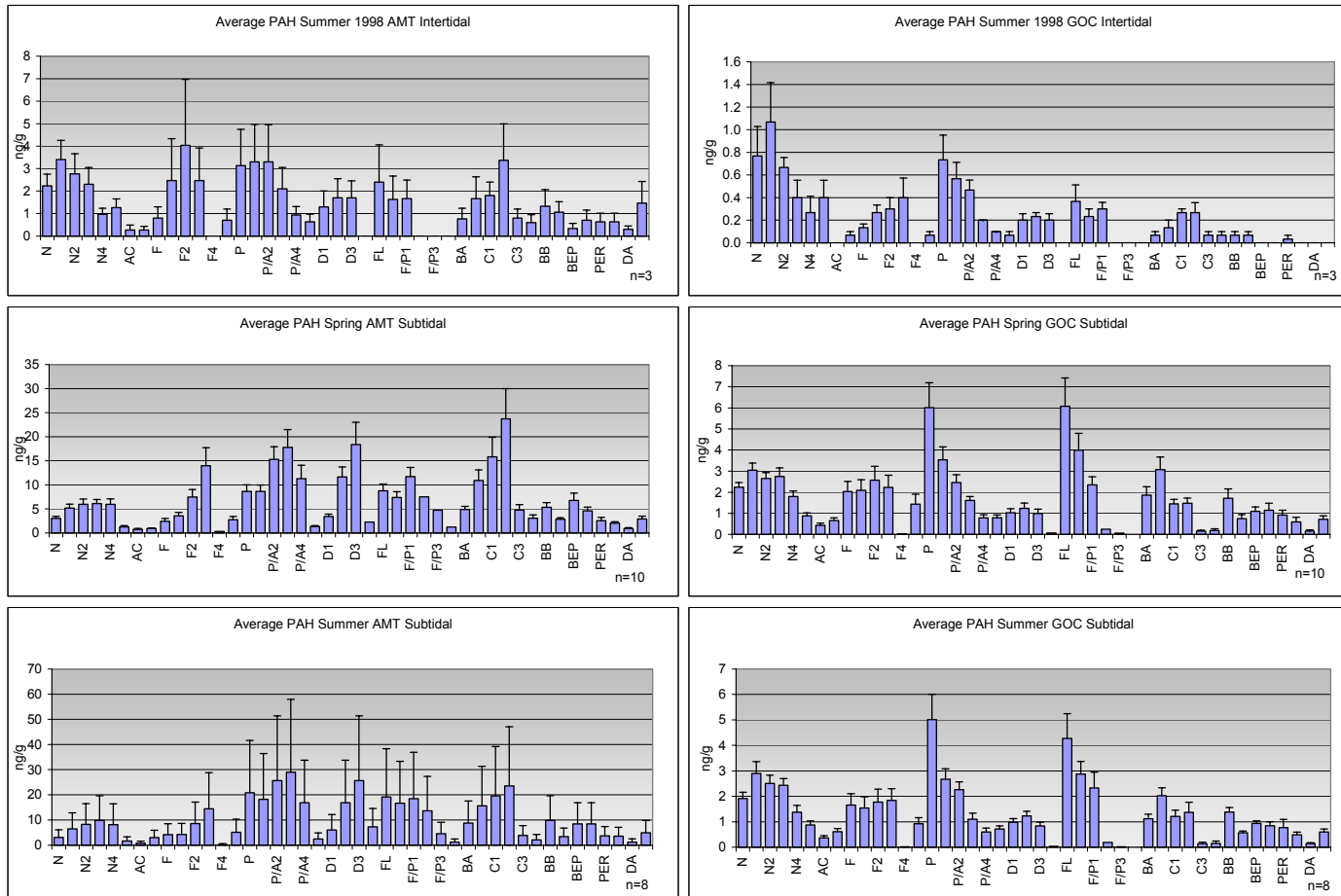
Figure 16 Average PAH histograms comparing intertidal and seasonal subtidal sediments samples from Alyeska Marine Terminal and Gold Creek stations. Error bars represent the standard error of mean; n indicates the number of samples (intertidal) or cruises (subtidal) contributing to each average.
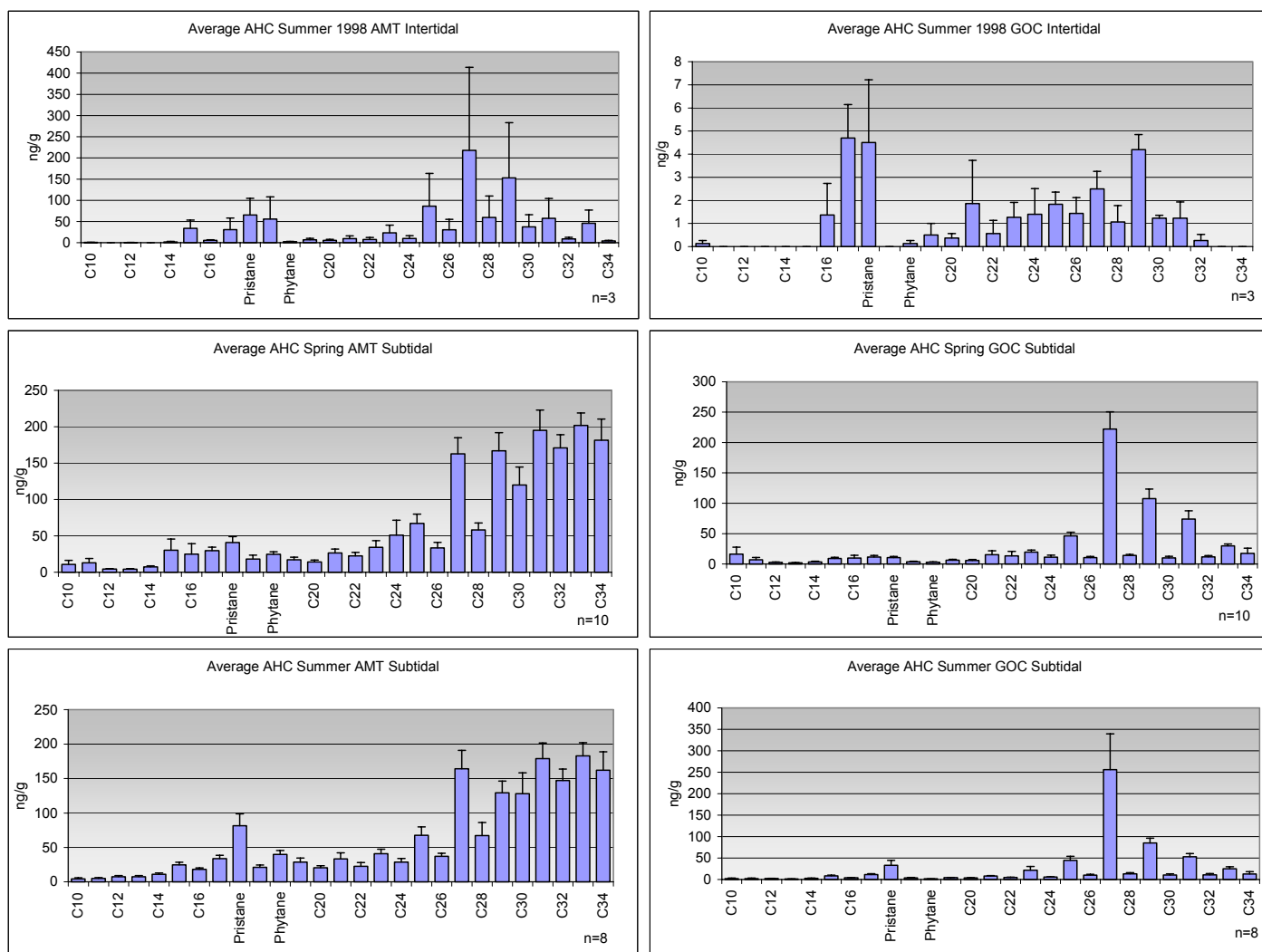
Figure 17 **Average AHC histograms comparing intertidal and seasonal subtidal sediments samples from Alyeska Marine Terminal and Gold Creek stations. Error bars represent the standard error of mean; n indicates the number of samples (intertidal) or cruises (subtidal) contributing to each average.**
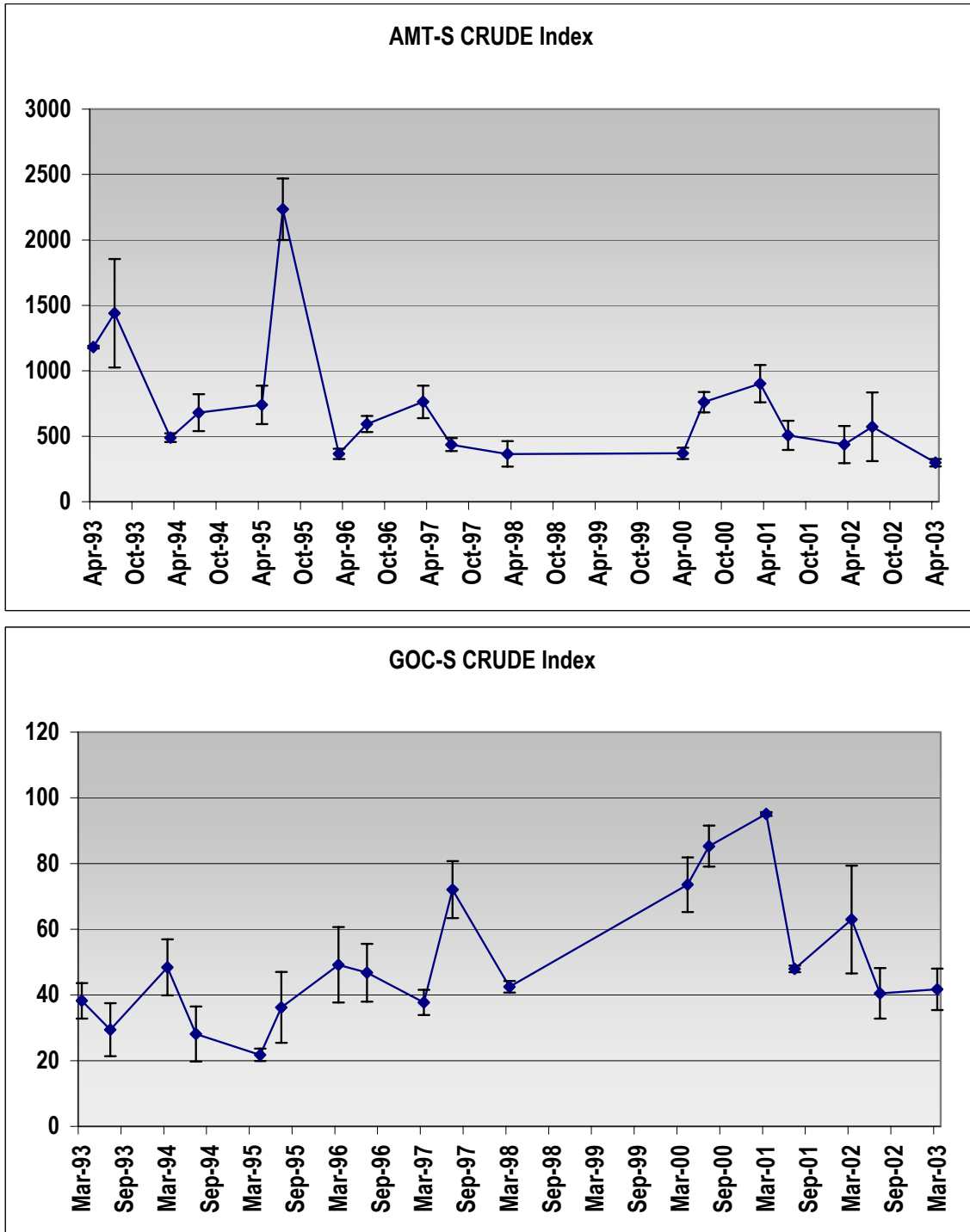
Figure 18 CRUDE Index values (Payne et al. 1998) for AMT and GOC sediments samples collected between March 1993 and March 2003. Error bars represent the standard error of the mean for all samples.

The plots demonstrate order-of-magnitude higher concentrations at AMT compared to Gold Creek. With the exception of two elevated values in the July 1993 and 1995 collections, the values at Alyeska Marine Terminal appear to be relatively constant (ranging from around 300 to 900) with low standard errors from April 1996 to present. The elevated TPAH and CRUDE Index values (and higher associated standard error) for the July 1995 samples at AMT may have been due to inclusion of a highly weathered tarball or oil droplet in the samples. The individual PAH histograms for these three samples (Figure 19) show elevated concentrations of the alkylated phenanthrenes/anthracenes, fluoranthenes and chrysenes compared to the historical averages shown in Figure 16. The AHC patterns for the July 1995 samples, however, do not appear to be significantly different from the historical averages shown in Figure 17. As noted earlier, the values at Gold Creek are uniformly low, ranging from a low of 20 in March 1995 to a high of 95 in March 2001. The increase in the GOC CRUDE Index signal culminating in March 2001 appears to coincide with another increase at AMT peaking at the same time; however, examination of the PAH profiles for the GOC samples reveals that the increase is due to an influx of combustion products (parent component > alkylated homologues) as shown in Figure 20 for March 2001, while the corresponding signal at AMT (Figure 21) at the same time is clearly from a highly weathered petrogenic source (parent component < alkylated homologues). The CRUDE index values for both sites appear to be dropping again since that sampling period.

From examination of all the PAH data from both of these sites, it is clear that the AMT subtidal sediments are primarily contaminated by a weathered ANS oil signal, which would be consistent with BWTF diffuser-sourced dispersed oil droplet/suspended particulate material (SPM) interactions and concomitant sedimentation (Payne et al. 1989; 2003). The GOC sediments, on the other hand, show PAH contamination from a low-level petrogenic source with slightly greater relative input from combustion (pyrogenic) sources. The pyrogenic signal at GOC may be slightly greater in the spring, but it is probably not statistically significant. It is not possible to tell if the low-level petroleum source in the subtidal sediments at GOC is from the BWTF and other activities at AMT or other sources (boat traffic, sewage and wastewater discharges from the City of Valdez). This source may be identified through a limited set of sterane/triterpane analyses of GOC sediments and comparisons to AMT sediments and Alyeska BWTF discharges as part of future LTEMP or other PWS RCAC research activities.

The AHC patterns presented in Figure 17 show a predominantly biogenic signal in the two intertidal samples with significant variability observed among the replicates at each site. The subtidal sediments at AMT show a combination of biogenic and very weathered ANS oil signal, again consistent with terrestrial and marine fecal-pellet sources along with significant oil droplet SPM interactions given the elevated levels of dispersed oil droplets introduced to region from the BWTF diffuser (Payne et al. 2001; Salazar et al. 2002). The AHC signals in the subtidal sediments at GOC show a combination of marine and terrestrial biogenic input, with very little weathered oil signal in keeping with the extremely low CRUDE index values observed at the site.
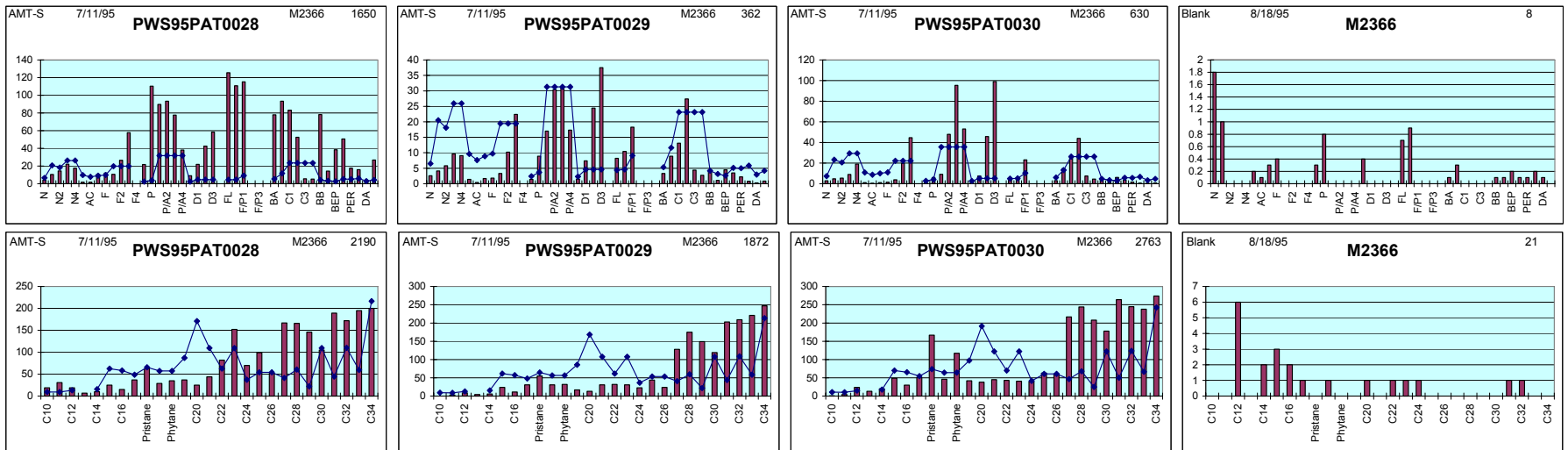
Figure 19 PAH and AHC histogram plots from the July 1995 AMT sediment samples along with their associated procedural blanks.

53
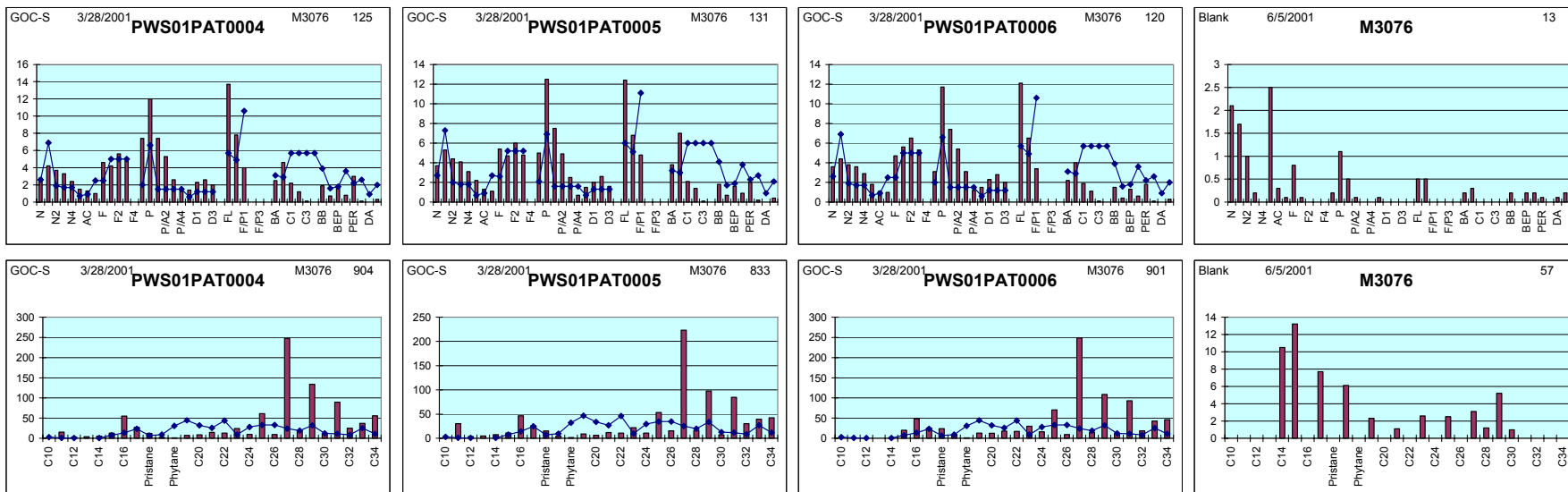
Figure 20 PAH and AHC histogram plots from the March 2001 GOC sediment samples along with their associated procedural blanks.
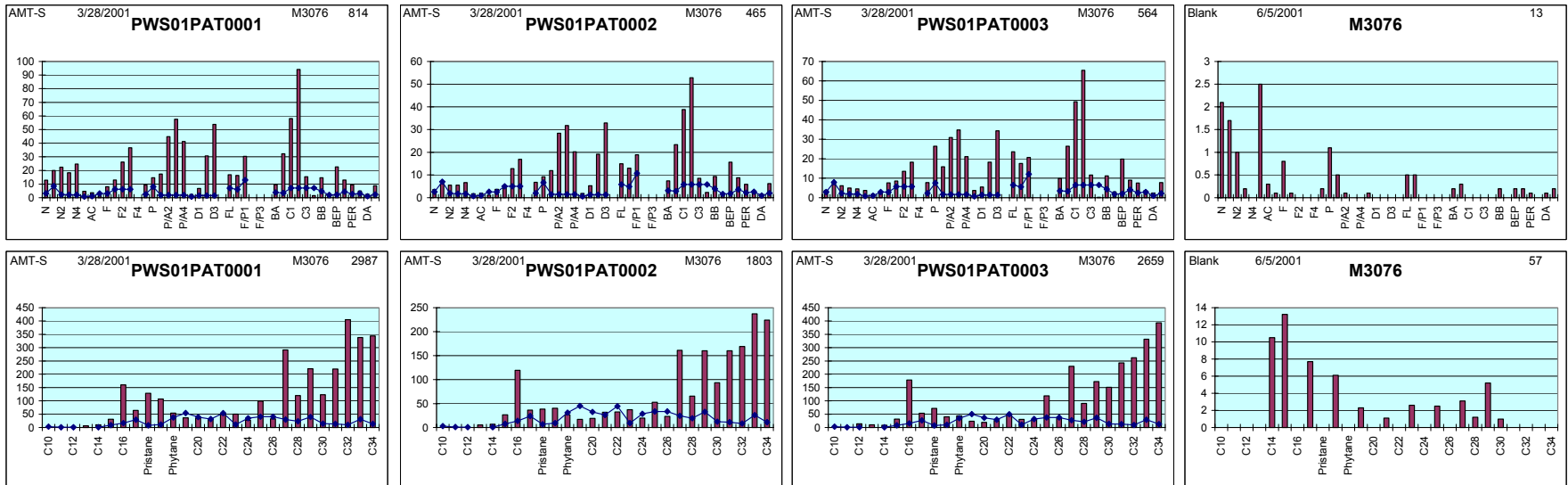
Figure 21   PAH and AHC histogram plots from the March 2001 AMT sediment samples along with their associated procedural blanks.

5.2.3 Tissues

5.2.3.1   Mytilus Availability

One issue of moderate concern is the availability of Mytilus at some of the sites. Some locations have but patchy remnants of former colonies so boldly obvious in earlier KLI photos. At most sites, there is attrition in the dominant 6-7 year old mussel age class (based on growth rings) but there appears to be a 3-4 year old class maturing to fill the space. There are also new 0-3 year old recruits at most locations. The size and robustness of mussels also show significant differences among the sampling sites. Field notes on the Mytilus populations are in Appendix A-1.

5.2.3.2   Tissue Chemistry Data Quality
5.2.3.2.1   <u>Lipid Interference in AHC Analyses</u>

Problems with lipid interference in samples analyzed at GERG were alluded to in the earlier inter-calibration section and have been referred to in numerous KLI/GERG reports, particularly with regard to aliphatic (AHC) analyses in tissues. Lipid interference occurs when naturally occurring fats in living tissues are extracted along with the hydrocarbon components of interest but not adequately separated from the target AHC and PAH components during sample extract fractionation and cleanup (by silica gel (SiO_2) column chromatography and/or HPLC) procedures employed by the laboratory. This flaw results in additional and interfering peaks due to the lipids eluting from the gas chromatographic instrumentation used in the target analyte measurements. Although most of these interfering components can be eliminated by the selected ion monitoring (SIM) GC/MS procedures used for the PAH analyses, there are evidently some lipids that elute at the same time and generate similar ions to those used to identify and quantify specific components. With the AHC analyses, which are done by FID/GC, <u>any</u> lipid or other material that elutes from the GC at the same time or close to the target analytes will interfere or generate a false positive, because the detector does not have the discriminating power to distinguish between hydrocarbons and lipids.

Thus, tissue samples, due to their higher lipid content, are particularly prone to the over-reporting certain analytes. For example, the anomalous fluorene (F1, F2, and F3) pattern observed in GERG's analysis of NIST SRM as part of the laboratory inter-calibration program, is likely due to lipid interference. In the SRM AHC data, lipid interference also led to anomalously high levels of C_{20}, C_{25}, C_{29}, C_{30}, and C_{32} (compared to values reported by ABL). In the inter-laboratory split-tissue samples, the problem manifest itself again in the PAH data as anomalous alkylated fluorene (F, F1, F2, F3) and possibly, alkylated phenanthrenes/anthracenes (P/A1, P/A2, P/A3, P/A4).

In the AHC data for the inter-calibration tissue samples, lipid interference manifest itself as excessively large (two and three order of magnitude greater) contributions of C_{21}, C_{23}, C_{29}, C_{30}, and C_{31} n-alkanes compared to the other components. For example, fairly good agreement was

obtained between GERG and ABL for the lower molecular weight ($C_{12} - C_{16}$) n-alkanes that were measured in the range of 100-500 ng/g dry wt. in both the AMT and GOC tissue split intercalibration samples (just as they were in the NIST SRM samples). But GERG also reported concentrations of heaver-molecular-weight n-alkanes that ranged from 2,000 to 90,000 ng/g dry wt., while these components were essentially not detected by ABL.

These observations prompted us to go back and look at the historical database to see if there were anomalous concentrations of higher molecular weight n-alkanes in the AHC profiles, and whether or not the observed AHC profiles could be correlated with station locations, sampling, dates, percent lipid, or petroleum hydrocarbon contamination when it appeared in PAH profiles. Figures 22-26 present representative AHC histogram plots from several stations (three replicates and the associated procedural blank for each cruise) analyzed during the first few years of the program before AHC analyses were discontinued in the tissue samples.
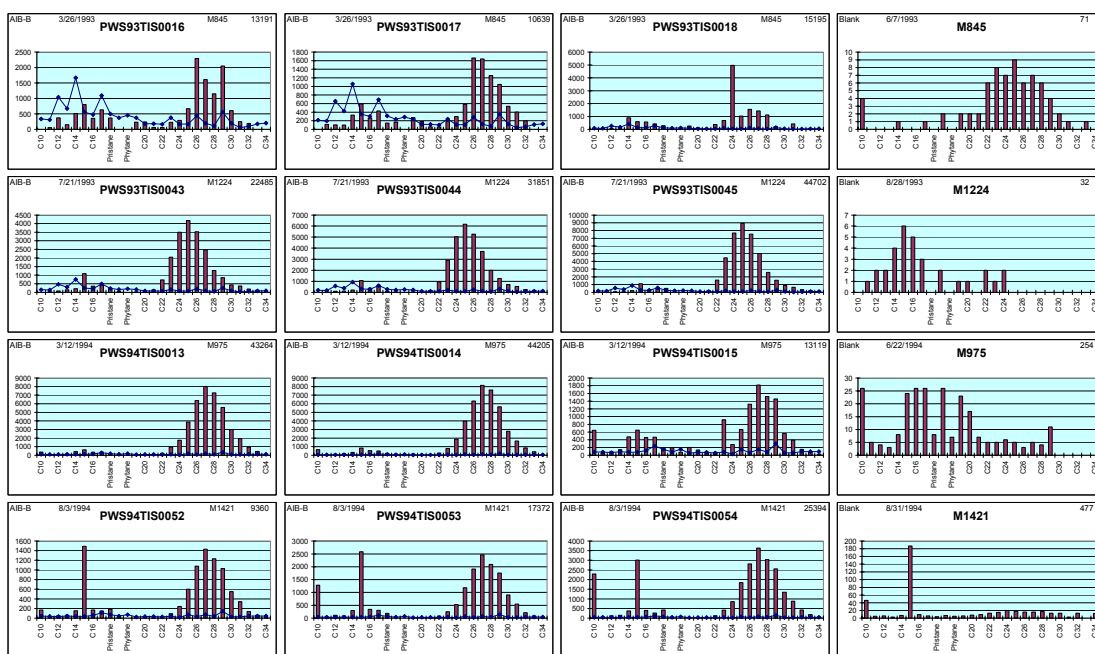
Figure 22 AHC histograms for mussel tissue samples and associated procedural blanks, March and July 1993, and March and August 1994, at Windy Bay.
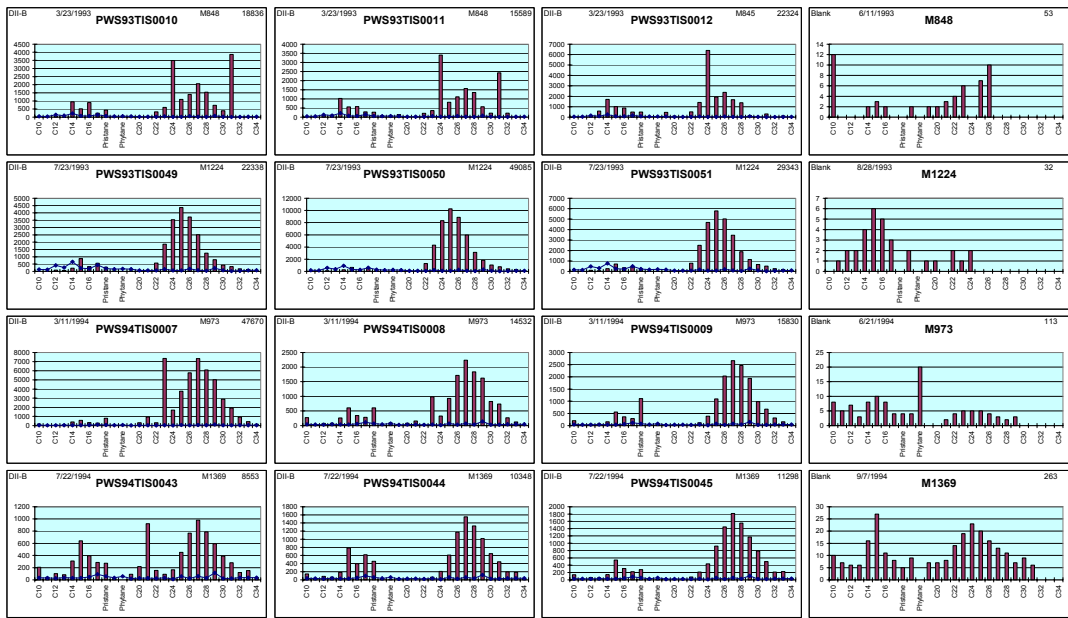
Figure 23 AHC histograms for mussel tissue samples and associated procedural blanks, March and July 1993, and March and August 1994, at Aialik Bay.
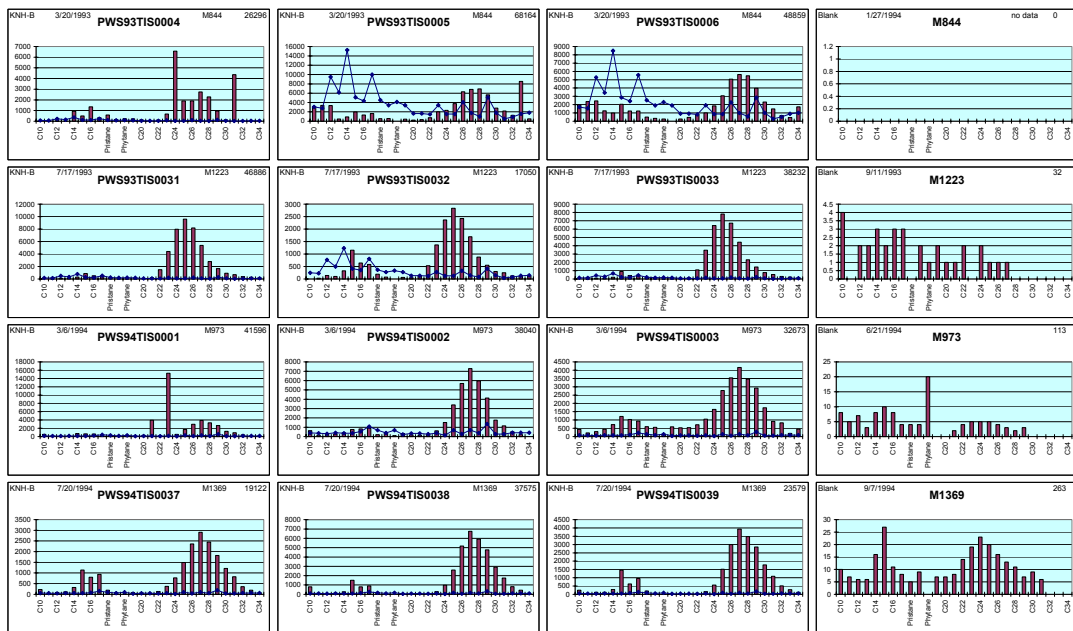
Figure 24 AHC histograms for mussel tissue samples and associated procedural blanks, March and July 1993, and March and August 1994, at Knowles Head.
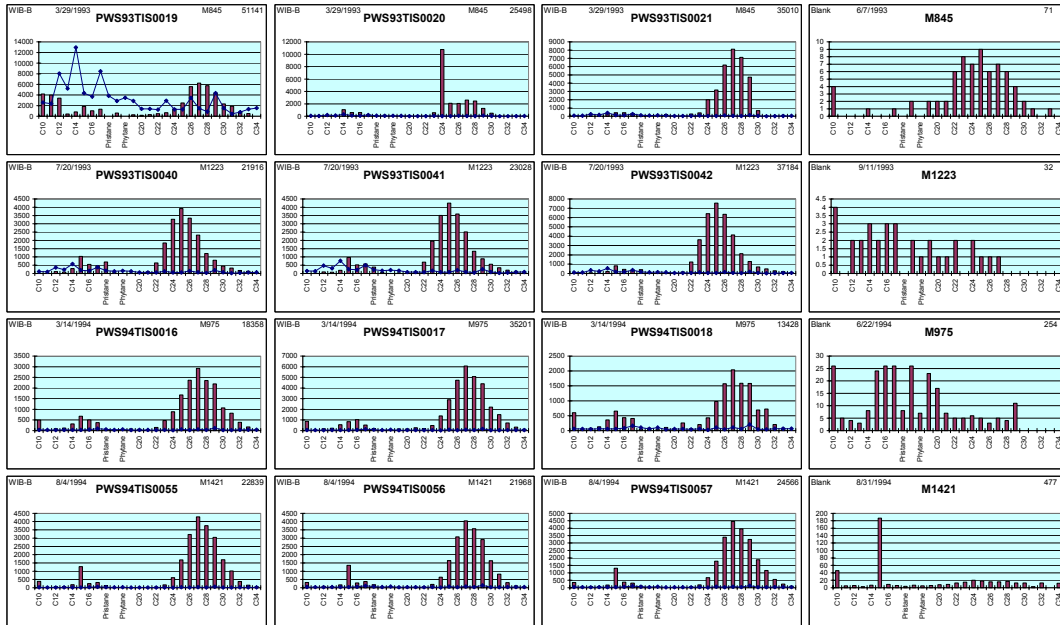
Figure 25 AHC histograms for mussel tissue samples and associated procedural blanks, March and July 1993, and March and August 1994, at Disk Island.
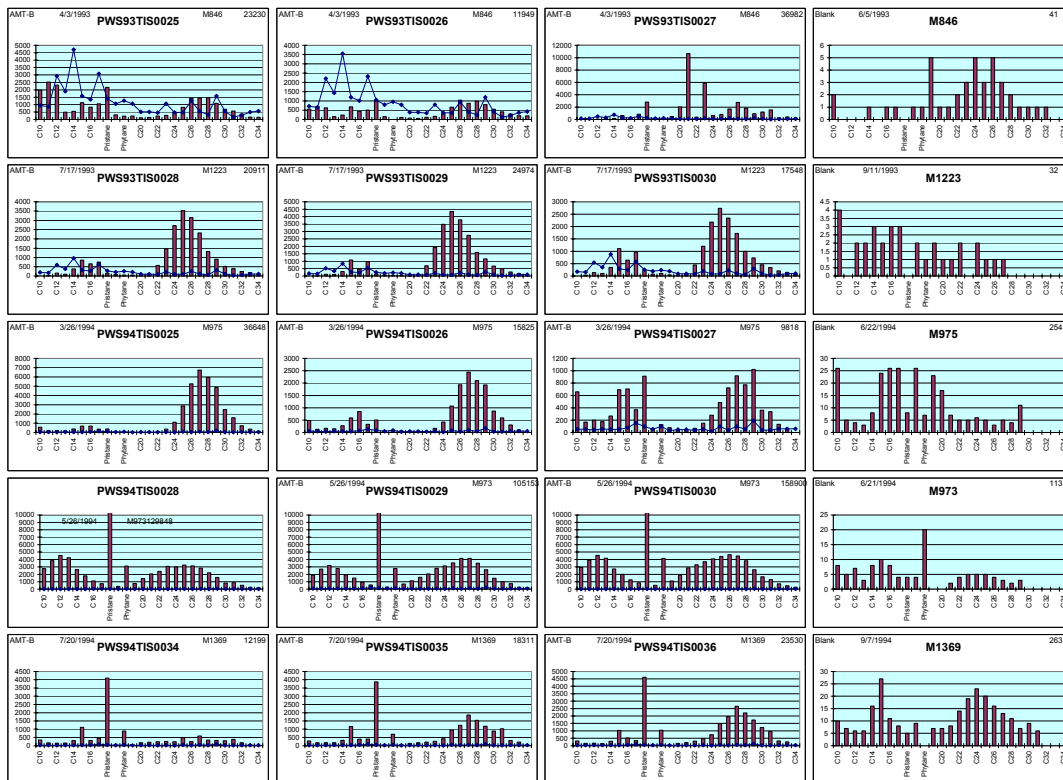
Figure 26 AHC histograms for mussel tissue samples and associated procedural blanks, March 1993- July 1994 at Alyeska Marine Terminal. May 1994 samples were immediately after the T/V Eastern Lion oil spill.

Examination of the early data from Windy Bay, Aialik Bay, Knowles Head, Disk Island, and Alyeska Marine Terminal reveals that there is an anomalous cluster of components that are reported and quantified as n-alkanes from n-C_{22} through n-C_{32} that shows up in over 60% of the samples. This ubiquitous cluster, which we have named the "Upper Aliphatic Hump" or "hump" for short, appears regardless of location, season, and the presence or absence of oil (e.g. Alyeska Marine Terminal) as indicated by the PAH profiles. This same pattern was observed in the majority of the samples for all the other stations (not shown) sampled early in the program, and no doubt prompted KLI and GERG to petition to have tissue AHC analyses discontinued.

During the March 1998 critical review of the LTEMP, Payne et al. (1998) and J. Short (who served as an independent PWS RCAC reviewer of the Payne et al. report) recommended that the AHC analyses be reinstituted, with the proviso that GERG implement a lipid cleanup procedure similar to that utilized at ABL to eliminate this interference in future analyses. As a result of this recommendation, tissue AHC analyses were re-instituted with the July 1998 field collections.

As part of our analysis of the past and present data sets, we have plotted the relative contribution of the upper C_{22}-C_{32} n-alkane hump to the total n-alkanes measured in all the tissue samples completed to date (Figure 27).
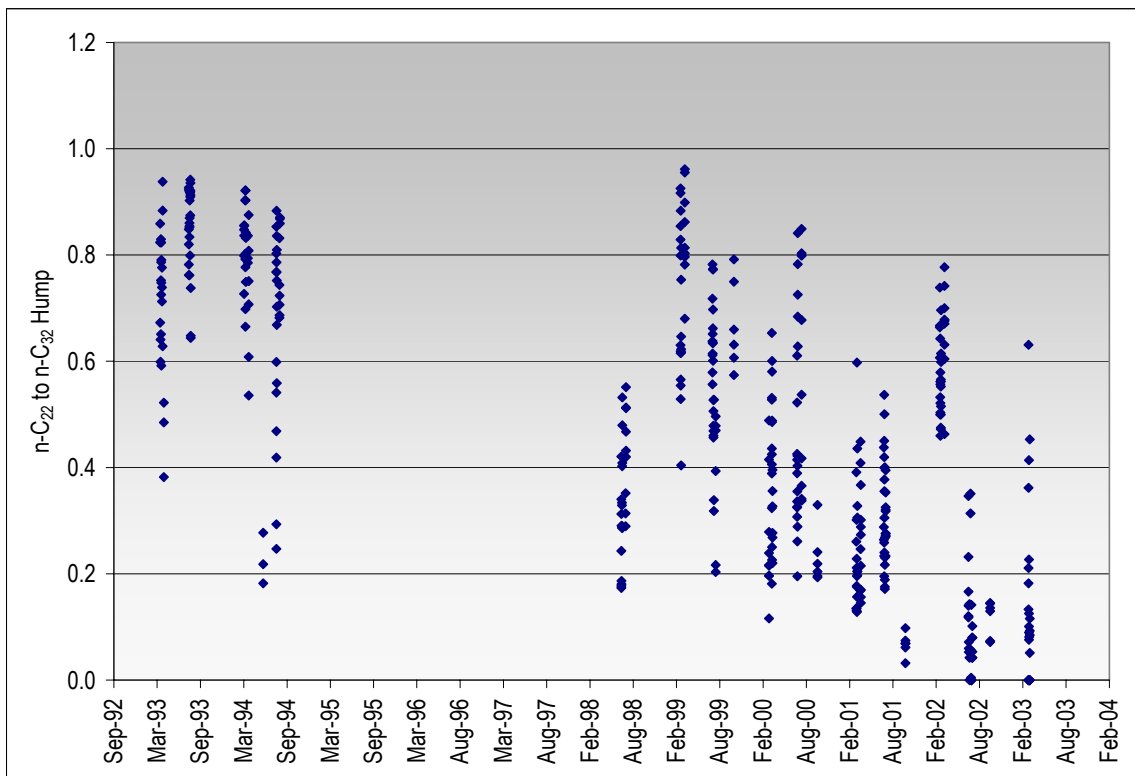
Figure 27 Relative contribution of C22-C32 "hump" to TALK in all mussel tissue samples analyzed in the LTEMP to date.

As shown by the data in the figure, the hump of C_{22}-C_{32} n-alkanes made up between 50-90% of the total n-alkane signal during the first three season's collections and contributed anywhere from 18-88% in July 1994, with most of the samples in the 65-88% range. When tissue AHC analyses were re-instituted in July 1998, the hump contribution was much lower (18-58%), but it then increased again in March 1999. Since then the signal has been somewhat more variable, and it appears to have decreased significantly after July 2002 with the onset of hydrocarbon chemistry analyses at ABL.

Throughout this discussion we want to stress that the hump is not to be confused with the C_{25}, C_{27}, C_{29}, and C_{31} odd-number carbon pattern from terrigenous plant wax hydrocarbons such as those considered earlier in the sediment samples from Gold Creek. Instead, these patterns include even and odd-number hydrocarbons with a CPI close to 1; however, it is clearly not due to petroleum hydrocarbon contamination as demonstrated by the lack of PAH components in the higher-molecular-weight range in the same samples. In addition to the hump, many of the tissue samples also contained anomalous spikes of one or more of the same individual hydrocarbons (C_{20}, C_{25}, C_{29}, C_{30}, and C_{32}) observed in the tissue sample splits and NIST SRM samples analyzed by GERG for the inter-calibration exercise.

5.2.3.2.2 TPAH versus TAHC Correlation Analyses

As indicated earlier in the discussion of the sediment analyses, samples with recent petroleum hydrocarbon contamination should show evidence of characteristic oil-specific compounds in both the aromatic (PAH) and aliphatic (AHC) hydrocarbon fractions (e.g., see Figure 4 (top) and the AHC pattern for the AMT mussels collected after the *T/V Eastern Lion* oil spill in Figure 26).

When there was significant evidence of oil contamination in exposed tissues, there is a strong correlation such as that observed at AMT (Figure 28). In this case, the correlation ($r^2 = 0.71$) is strongly influenced by the elevated particulate/oil-phase TPAH and TAHC levels noted in the three samples (upper right hand corner) collected after the *T/V Eastern Lion* oil spill in 1994. As seen in the figure, however, there are eight samples tracking along the x-axis with TAHC values above 30,000 ng/g dry wt. and TPAH concentrations below 900 ng/g dry weight. Upon closer examination of the AHC histogram plots for these samples, it was discovered that each one contained significant contributions from just one or two individual peaks (e.g., C_{21}, C_{23}, C_{29}, and in one case the "hump" discussed above), which presumably implied lipid interference, and insignificant contributions from the aliphatic components known to be more characteristic of oil contamination. If those eight outliers or data points along the TAHC axis with uniformly low TPAH values are removed from the database, then an even better correlation ($r^2 = 0.93$) between the TPAH and TAHC measurements in the oil-exposed samples is obtained (Figure 29).

This exercise was repeated for all the other stations examined in the LTEMP, and in general, only very low or no correlations between tissue TAHC and TPAH were observed. Table 6 presents the r^2 values generated from linear regression analyses of these other stations when all the data from each site were considered and after selected samples, whose TAHC levels and AHC histogram plots suggested lipid interference, were removed.
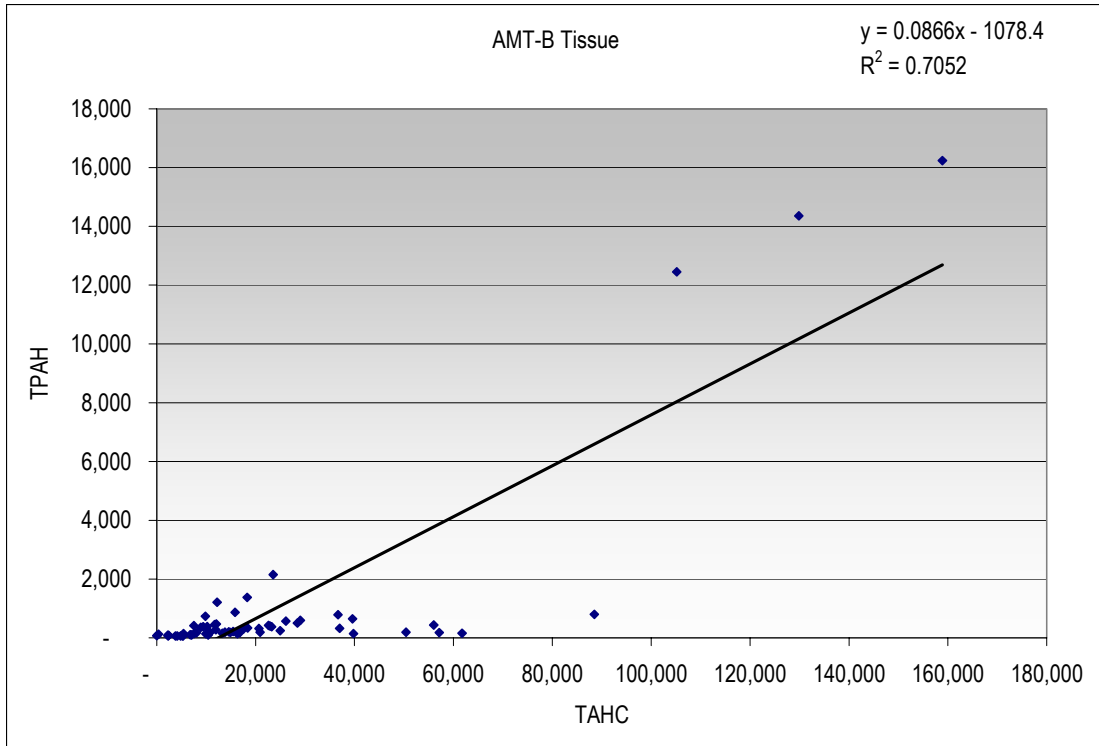
Figure 28 TAHC vs. TPAH for all data from AMT. The three peaks in the upper right hand corner are from the samples collected after the *T/V Eastern Lion* oil spill.
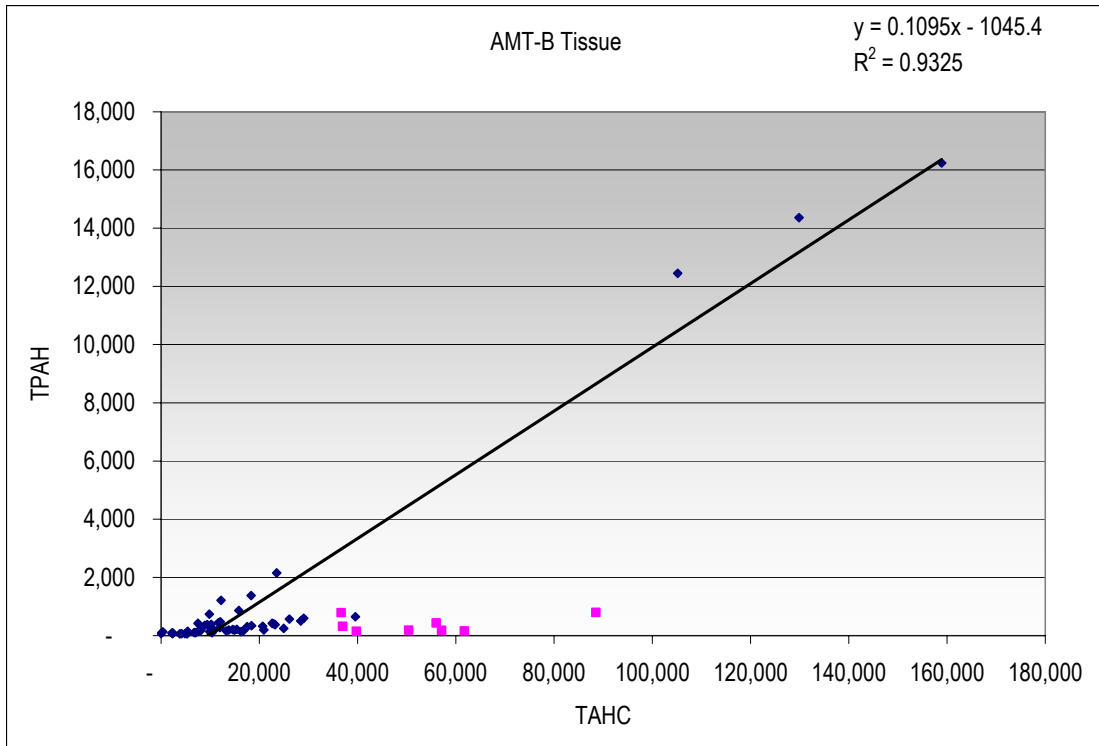
Figure 29 TAHC vs. TPAH for AMT with outliers containing high lipid interference removed (fuschia squares).

Table 6 Station-specific TPAH vs. TAHC correlations for mussel tissue data before and after removal of samples with significant lipid interference.

Station	Initial r^2 Including All Data	Revised r^2 With Lipid-Affected Outliers Removed	Criteria for Selected Sample Removal (ng/g dry wt.)
AIB	0.208	0.415	TAHC > 28,000 + lipid pattern
AMT	0.703	0.931	TAHC > 30,000 + lipid pattern
DII	8×10^{-7}	0.019	TAHC > 28,000 + lipid pattern
GOC	0.397	0.215	TAHC > 25,000 + lipid pattern
KNH	0.154	0.263	TAHC > 30,000 + lipid pattern
SHB	0.162	0.336	TAHC > 30,000 + lipid pattern
SHH	0.002	0.059	TAHC > 20,000 + lipid pattern
SLB	0.263	0.397	TAHC > 25,000 + lipid pattern
WIB	0.540	0.051	TAHC > 30,000 + lipid pattern
ZAB	0.222	0.509	TAHC > 17,000 + lipid pattern

From this analysis, it is apparent that when relatively recent oil contamination is present, there is a strong correlation (AMT, $r^2 > 0.7$) between TPAH and TAHC concentrations in exposed tissues. When there hasn't been recent exposure to oil, the correlation drops off dramatically or was non-existent (e.g., DII, SHH, WIB). This presumably reflects the fact that in the absence of significant oil contamination where the correlation is strong, tissues can still accumulate PAH and AHC from spurious or independent sources. For example, dissolved components (primarily naphthalenes) or combustion products (higher-molecular-weight PAH) are not uncommon contaminants, and neither are strongly associated with n-alkanes. On the other hand, naturally occurring biogenic n-alkanes (primarily n-C_{15}, n-C_{17}, and pristane) will appear in mussels feeding on phytoplankton blooms in the spring. Finally, the correlation between TPAH and TAHC also decreases with the weathering state of the oil, i.e., if transport time allows significant microbial degradation of the oil before it is ingested by the mussels. Hydrocarbon-degrading bacteria will preferentially degrade the n-alkanes first, followed by the isoprenoids, pristane and phytane, and finally the higher molecular weight PAH. This was observed at DII in July 1994, when there was evidence of oil contamination in the PAH signature most likely from local EVOS-related, remedial cleaning activities (see MPI discussion below). The PAH signal in the July 1994 samples spiked as a result of those operations, but the oil was evidently so microbially degraded that a concomitant signal in the AHC histograms from those samples was not observed (see Figure 25).

5.2.3.2.3 Fluorene/Lipid Interference in PAH Analyses

As noted previously in Section 5.1 on the inter-laboratory calibrations and SRM analyses, there appeared to be an interference in the PAH analyses completed at GERG by a series of alkylated fluorenes (F1, F2, and F3). This fluorene cluster was first noted two years ago in our review of the LTEMP samples specific to Port Valdez (Payne et al. 2001). Figure 30 presents representative PAH histogram plots from several stations and times when the "fluorene/lipid" pattern was most apparent in field samples.

We know of no petroleum distillate products or crude oils that would contain just this narrow group of components in the absence of the other alkylated PAH homologues, and yet in the examples shown in Figure 30, these components make up the majority of the TPAH observed in the sample. Figure 31 shows the relative contribution of the fluorenes to the total PAH signal [(F1 + F2 + F3)/TPAH] in all of the tissues samples collected as function of the collection date. As the data in the figure illustrate, the fluorene/lipid interference pattern appeared particularly problematic in July 1994, July 1996, and July/August 1999, where the alkylated fluorenes alone made up 25 to 65 percent of the total measured TPAH.

Interestingly, two of these three sampling times (July 1994 and 1999) correspond to periods when the C_{22}-C_{32} hump in the AHC profiles also contributed a maximum (up to 96%) to the TAHC (see Figure 27). Unfortunately, there are no AHC data for the July 1996 samples; however, we do have data on the lipid measurements completed on the mussels from 1993 through March 2002, and Figure 32 presents the temporal trends noted for this parameter.

From Figure 32, it is possible to see that there were a number of samples in each of these collection periods (July 1994, 1996, and 1999) where the extracted lipids made up 10-15% of the overall sample weight, and while these were not necessarily the highest lipids ever measured, they do coincide with the periods of maximum "fluorene/lipid" pattern interference.

Because of their random appearance in the tissue sample PAH profiles, and the confirmation from GERG that they are likely associated with lipid interference, we have undertaken a series of "fluorene/lipid corrections" to obtain a data set that can be used in various graphing and plotting routines (e.g., MPI and PDR plots) without potentially erroneous contributions from the F1-F3-fluorene artifacts. Initially, we considered simply eliminating the sum of the alkylated fluorenes from the TPAH values used for these plotting routines, but then we realized that the fluorenes are a legitimate but proportional component of the overall PAH profile for crude oils and distillate products, and to simply drop them from the sums would be inappropriate. Therefore, we elected instead to examine each PAH histogram plot individually, and on those plots with obvious F1-F3 anomalies, to proportionally reduce the individual fluorene components to bring them back in line (or at least in the same range) with the other PAH measured in the sample. Table 7 below, lists the samples that were corrected by this procedure and gives the individual correction factors that were applied to the F0, F1, F2, and F3 components.
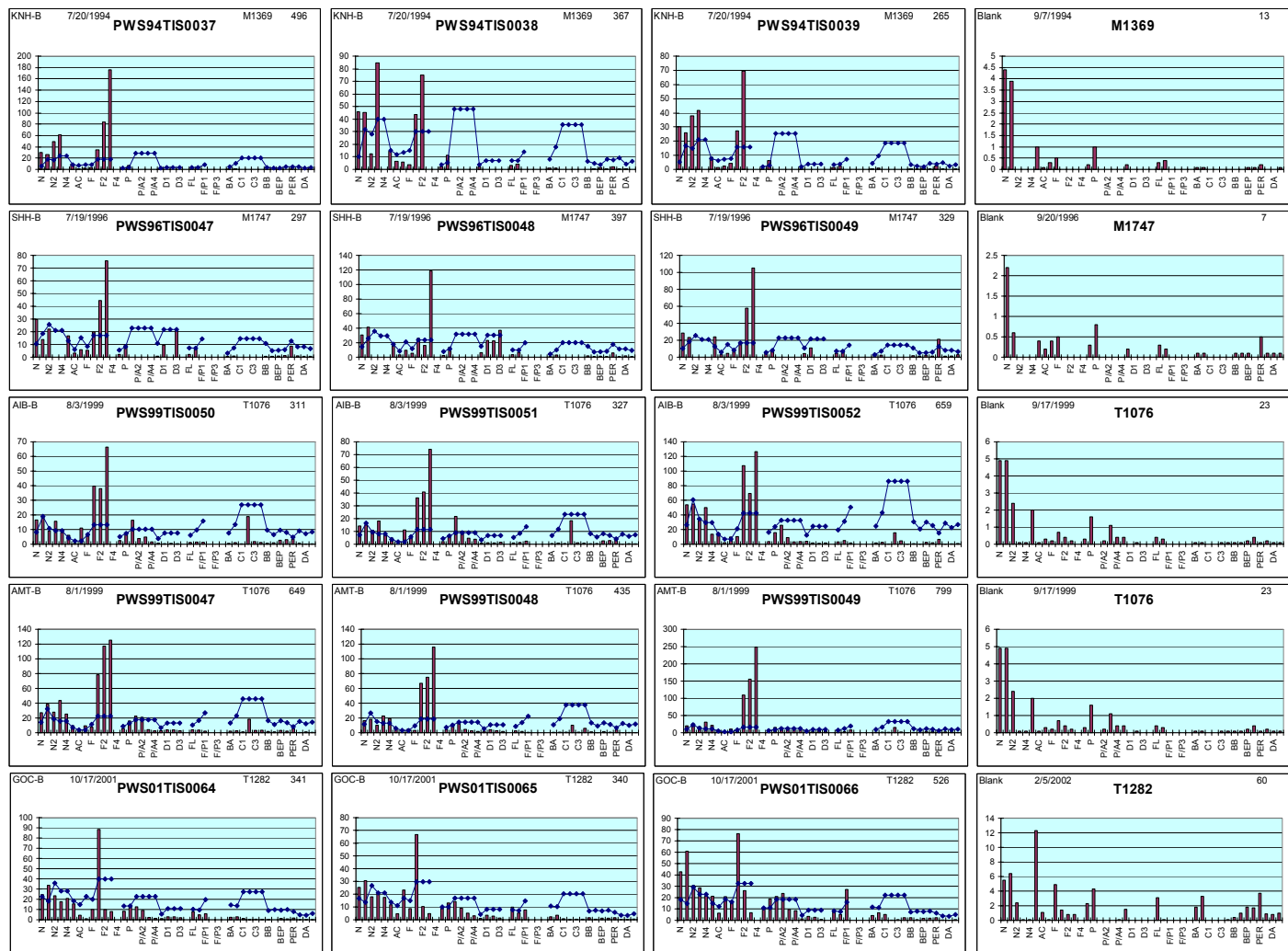
Figure 30 Representative PAH histograms showing fluorene/lipid interference (KNH 7/94, SHH 7/96, AIB 8/99, AMT 8/99, and GOC 10/01).
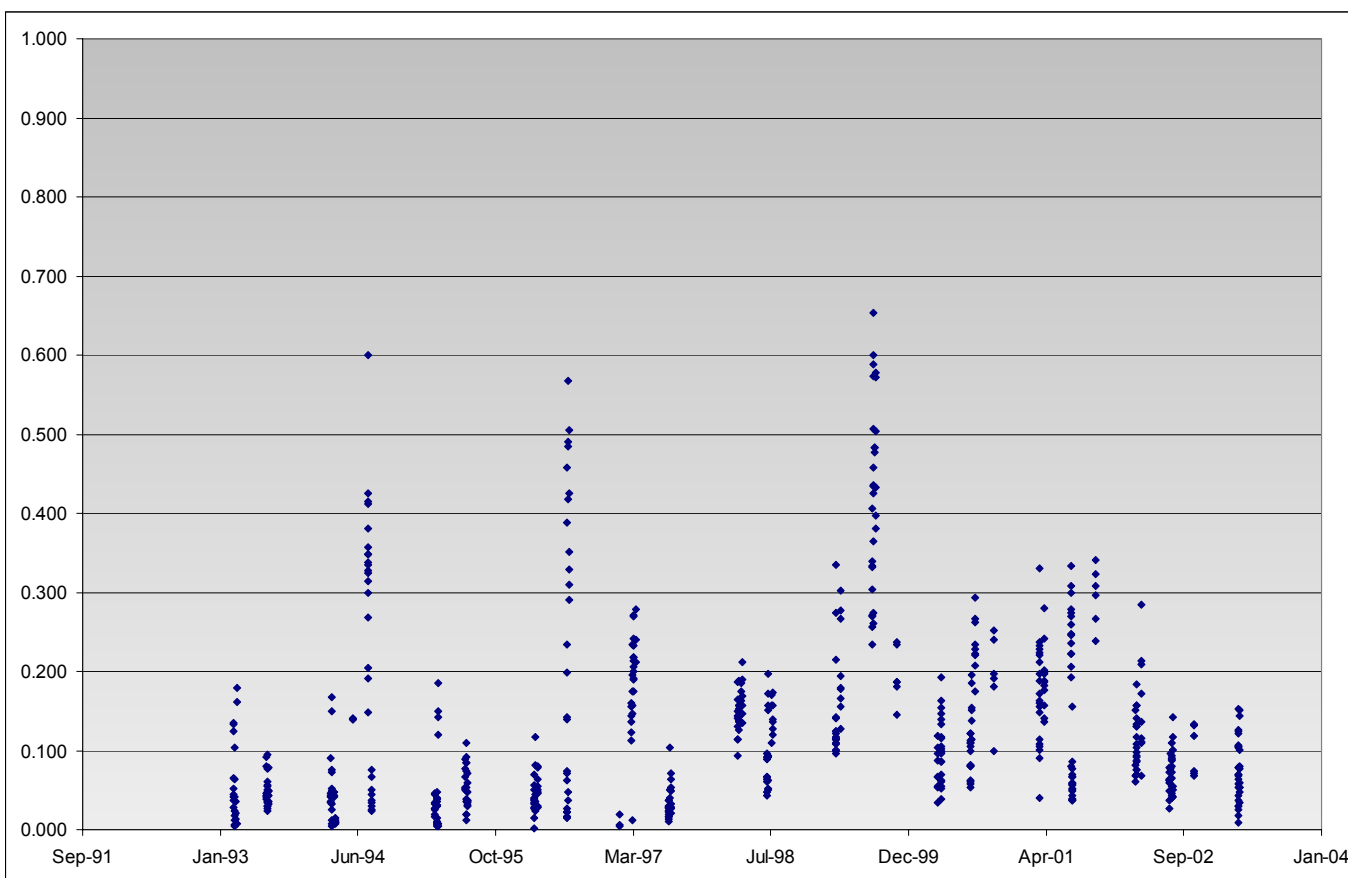
Figure 31 Time series of relative contribution of fluorene (suggesting lipid interference) to TPAH.
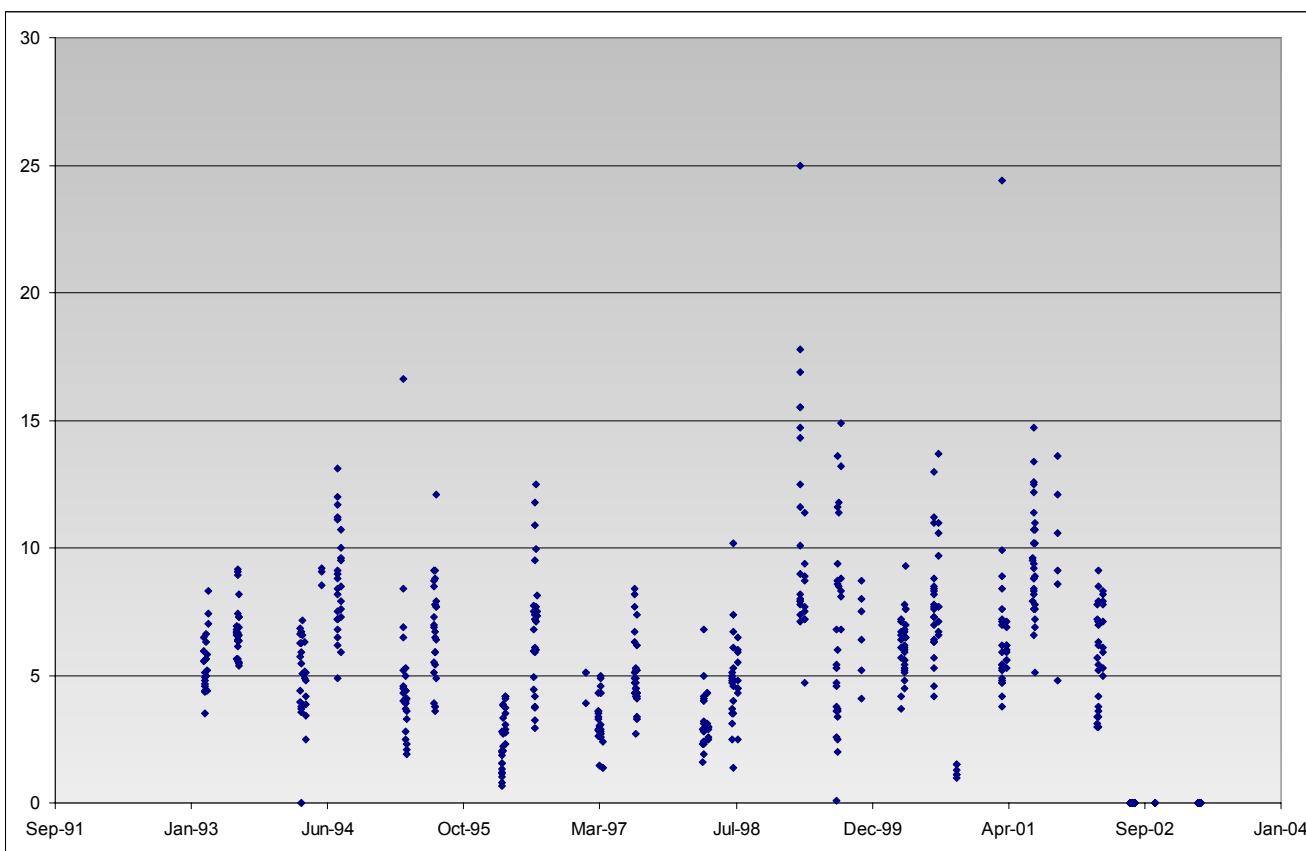
Figure 32 Time series of percent lipids in mussel tissue.

Table 7 Correction factors applied to samples affected by fluorene/lipid interference for F, F1, F2, and F3. Corrected values used to plot MPI and PDR.

	Date	Sample	F	F1	F2	F3
			Fluorene/Lipid Corrections			
AIB	Jul-96	PWS96TIS0042	1	0.33	0.33	0.33
	Jul-96	PWS96TIS0043	1	0.33	0.33	0.33
	Mar-97	PWS97TIS0022	1	1	1	0.33
	Mar-97	PWS97TIS0023	1	1	1	0.33
	Mar-97	PWS97TIS0024	1	1	1	0.33
	Apr-98	PWS98TIS0023	1	1	1	0.5
	Aug-99	PWS99TIS0050	1	0.25	0.25	0.25
	Aug-99	PWS99TIS0051	1	0.25	0.25	0.25
	Aug-99	PWS99TIS0052	1	0.2	0.2	0.2
AMT	Aug-99	PWS99TIS0047	1	0.17	0.17	0.17
	Aug-99	PWS99TIS0048	1	0.17	0.17	0.17
	Aug-99	PWS99TIS0049	1	0.17	0.17	0.17
	Oct-01	PWS01TIS0061	1	0.2	1	1
	Oct-01	PWS01TIS0062	1	0.2	1	1
	Oct-01	PWS01TIS0063	1	0.2	1	1
DII	Jul-99	PWS99TIS0034	1	0.33	0.33	0.33
	Jul-99	PWS99TIS0035	1	0.33	0.33	0.33
	Jul-99	PWS99TIS0036	1	0.33	0.33	0.33
GOC	Aug-99	PWS99TIS0044	1	0.05	0.05	0.05
	Aug-99	PWS99TIS0045	1	0.05	0.05	0.05
	Aug-99	PWS99TIS0046	1	0.05	0.05	0.05
	Oct-99	PWS99TIS0059	1	0.2	0.2	0.2
	Oct-99	PWS99TIS0060	1	0.2	0.2	0.2
	Oct-99	PWS99TIS0061	1	0.2	0.2	0.2
	Oct-01	PWS01TIS0064	1	0.25	1	1
	Oct-01	PWS01TIS0065	1	0.25	1	1
	Oct-01	PWS01TIS0066	1	0.25	1	1
KNH	Jul-94	PWS94TIS0037	1	0.2	0.2	0.2
	Jul-94	PWS94TIS0038	1	0.2	0.2	0.2
	Jul-94	PWS94TIS0039	1	0.2	0.2	0.2
	Jul-96	PWS96TIS0050	1	0.33	0.33	0.33
	Jul-96	PWS96TIS0051	1	0.33	0.33	0.33
	Jul-96	PWS96TIS0052	1	0.33	0.33	0.33
	Mar-98	PWS98TIS0007	1	0.33	0.33	0.33
	Mar-98	PWS98TIS0008	1	0.5	0.5	0.5
	Mar-98	PWS98TIS0009	1	0.5	0.5	0.5

SHB	Jul-94	PWS94TIS0040	1	0.33	0.33	0.33
	Jul-94	PWS94TIS0041	1	0.33	0.33	0.33
	Jul-94	PWS94TIS0042	1	0.33	0.33	0.33
	Jul-96	PWS96TIS0053	1	0.33	0.33	0.33
	Jul-96	PWS96TIS0054	1	0.33	0.33	0.33
	Jul-96	PWS96TIS0055	1	0.33	0.33	0.33
	Mar-97	PWS97TIS0019	1	1	1	0.33
	Mar-97	PWS97TIS0020	1	1	1	0.33
	Mar-97	PWS97TIS0021	1	1	1	0.33
	Mar-98	PWS98TIS0010	1	1	1	0.5
	Mar-98	PWS98TIS0011	1	1	1	0.5
	Mar-98	PWS98TIS0012	1	1	1	0.5
	Mar-99	PWS99TIS0001	1	0.25	1	1
	Mar-99	PWS99TIS0003	1	0.5	0.5	0.5
	Jul-99	PWS99TIS0028	1	0.33	1	0.33
	Jul-99	PWS99TIS0029	1	0.33	1	0.33
	Jul-99	PWS99TIS0030	1	0.2	1	0.2
SHH	Jul-96	PWS96TIS0047	1	0.14	0.14	0.14
	Jul-96	PWS96TIS0048	1	1	1	0.17
	Jul-96	PWS96TIS0049	1	0.10	0.10	0.10
	Mar-97	PWS97TIS0028	1	1	1	0.50
	Mar-97	PWS97TIS0029	1	1	1	0.50
	Mar-97	PWS97TIS0030	0.25	1	1	0.25
	Jul-99	PWS99TIS0025	1	0.33	0.33	0.33
	Jul-99	PWS99TIS0026	1	0.50	0.50	0.50
	Jul-99	PWS99TIS0027	1	0.50	0.50	0.50
	Aug-99	PWS99TIS0053	1	0.17	0.17	0.17
	Aug-99	PWS99TIS0054	1	0.50	0.50	0.50
	Aug-99	PWS99TIS0055	1	0.50	0.50	0.20
SLB	Mar-97	PWS97TIS0013	1	1	1	0.33
	Mar-97	PWS97TIS0014	1	1	0.33	0.33
	Jul-99	PWS99TIS0041	1	1	1	0.5
	Jul-99	PWS99TIS0042	1	0.1	1	1
	Jul-99	PWS99TIS0043	1	0.33	1	0.33
WIB	Jul-96	PWS96TIS0046	1	0.25	0.25	0.25
	Mar-97	PWS97TIS0025	1	1	1	0.5
	Mar-97	PWS97TIS0026	1	1	1	0.5
	Mar-97	PWS97TIS0027	1	1	1	0.5
	Aug-99	PWS99TIS0056	1	0.5	0.5	0.125
	Aug-99	PWS99TIS0057	1	0.5	0.5	0.125
	Aug-99	PWS99TIS0058	1	0.5	0.5	0.125
ZAB	Jul-99	PWS99TIS0038	1	0.2	1	0.2
	Jul-99	PWS99TIS0039	1	0.2	1	0.2
	Jul-99	PWS99TIS0040	1	0.2	1	0.2

Figure 33 shows the PAH histogram plots from mussels collected at AMT in August 1999 before and after this "fluorene/lipid correction" was applied. As shown by the figure, only the alkylated fluorenes were affected, and after the correction they were reduced to at least be closer to what we have historically come to expect in samples not affected by laboratory artifacts. In the context of using correction factors, it is important to point out that TPAH values presented in this report and in the tables in the appendices are the original reported values, not fluorene/lipid corrected values. This correction was used only for MPI and PDR plots where we wanted to eliminate that source of error in the data for our analyses.
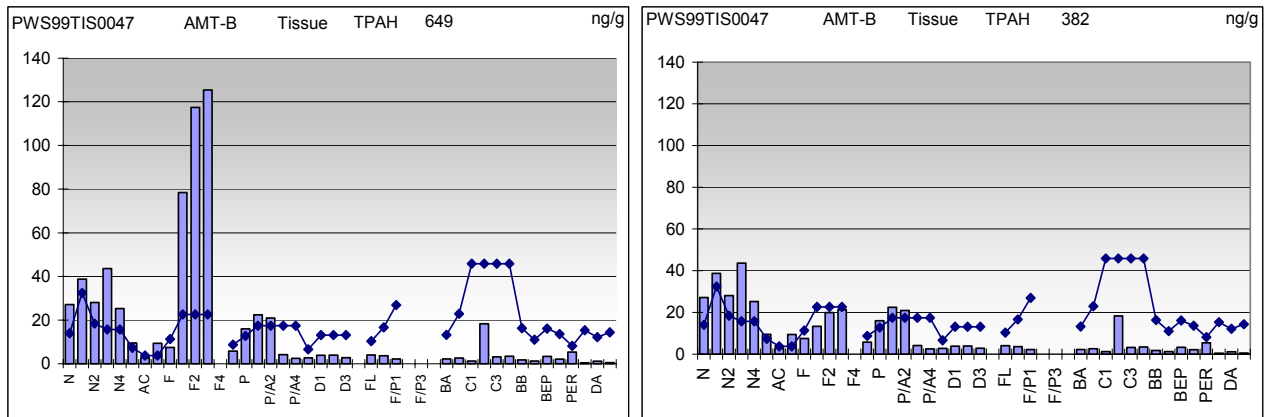
Figure 33 Example of PAH histogram plots before and after fluorene/lipid corrections for Alyeska Marine Terminal mussel sample, July 1999.

5.2.3.3   Total PAH Time Series Plots

Appendix A-7 lists the total PAH and AHC values of individual samples, seasonal averages, and the coefficient variation for all intertidal mussel samples analyzed during the program. The PAH data have NOT been fluorene/lipid corrected, and the AHC data include the spurious contributions from lipids (the C_{22}-C_{32} hump and individual fats and esters occasionally quantified as C_{20}, C_{21}, C_{29}, etc.). Even with these caveats, it is important to point out that, in general, the measured TPAH concentrations are very low, ranging from 18 to 14,350 ng/g dry wt across all stations. Not surprisingly, the concentrations at AMT are the highest, and ranged from 65 to 1,581 ng/g dry wt., excluding the samples collected after the *T/V Eastern Lion* oil spill. The mussel samples collected at AMT following the *T/V Eastern Lion* oil spill exhibited exceptionally TPAH concentrations, with values reaching 14,350 ng/g dry wt.

Figure 34 compares the average TPAH time-series using both original and lipid-corrected values for all ten LTEMP stations. In general, the measured TPAH values are quite low (< 600 ng/g dry weight) for most sample collections. Different concentration scales are used for each station to accentuate the wide ranges observed within a given site over time, so care should be taken to note the individual concentration scales when comparing the TPAH data among sites. From the figures it can be seen that the lipid corrections reduce the within-site variability somewhat, but the qualitative agreement between corrected and non-corrected TPAH values is very close. The

corrections cause some subtle changes in the shapes of the trend lines at two sites (SHB and SHH), while not materially affecting a number of others (AMT, DII, SLB, and ZAB). The most significant differences are noted in the July 1999 values at AIB, SHH, GOC and WIB, where the TPAH values are reduced for those sample collections by as much as a factor of two. With the exception of KNH, however, the overall time-series trends within each site are not affected by the fluorene/lipid corrections. Several sites appear to have a primary or secondary maximum in July 1997 (SHB, SHH, SLB, and KNH), while AIB and DII peak in March 1998, and WIB appears to be high in both March 1997 and March 1998. AMT peaks in July 1994 (as does GOC) and this clearly reflects PAH input from the *T/V Eastern Lion* oil spill in the Port. ZAB has the lowest TPAH values of any site and shows only moderate variability with neither spring nor summer collections showing a consistent trend.

At this time, we can only speculate about the apparent across-the-board TPAH increase in the July1997 to March 1998 time frame. The BWTF spill in January 1997 might be the cause for the increase at GOC and AMT (not readily apparent at the scale plotted in Figure 34, but more visible in additional plots presented in the following section), but the apparent increases at AIB, SHB, SHH, DII, WIB, and KNH are more difficult to explain. The temporal increase may be real, or it may be caused by a systematic change in the laboratory procedures implemented at that time. This point is considered in further detail in the following section where potential contributions from combustion products are factored out by use of the Mytilus Petrogenic Index (MPI).

5.2.3.4   MPI Plots

In our 1998 review of the LTEMP (Payne et al. 1998), we introduced the Mytilus Petrogenic Index (MPI), which is essentially, a total rather than a relative FPPI. It is very similar to the TPAH, except that pyrogenic PAH are excluded, summing instead only the petrogenic PAH components (fluorenes, phenanthrene/anthracenes, dibenzothiophenes and chrysenes). In this application, all of the data have been subject to fluorene/lipid corrections as discussed above. In this way, the contribution from petroleum hydrocarbon contamination in the absence of potential procedural artifacts and combustion byproducts is emphasized.

In Figure 35, all the MPI values have been plotted on the same concentration scale to facilitate comparisons among stations. At this concentration range, the fluorene/lipid corrected MPI values for AMT and SLB are off-scale in July 1994. The spike in the MPI value at AMT and GOC has been attributed to the influence of the *T/V Eastern Lion* oil spill in Port Valdez as is clearly reflected in the PAH histograms for these two sites shown in Figures 36 and 37. The *T/V Eastern Lion* oil spill impact can be readily observed by the relatively fresh and more weathered oil signals in the May and July 1994 samples, respectively. Note the significantly different concentration scales for the oil impacted samples. We previously reported that we believed the DII maximum in July 1994 was the result of mussel bed cleaning operations completed at DII that summer (Payne et al. 1998). The SLB spike in July 1994 may also be related to remediation activities in response to EVOS, but we are not certain at this time.
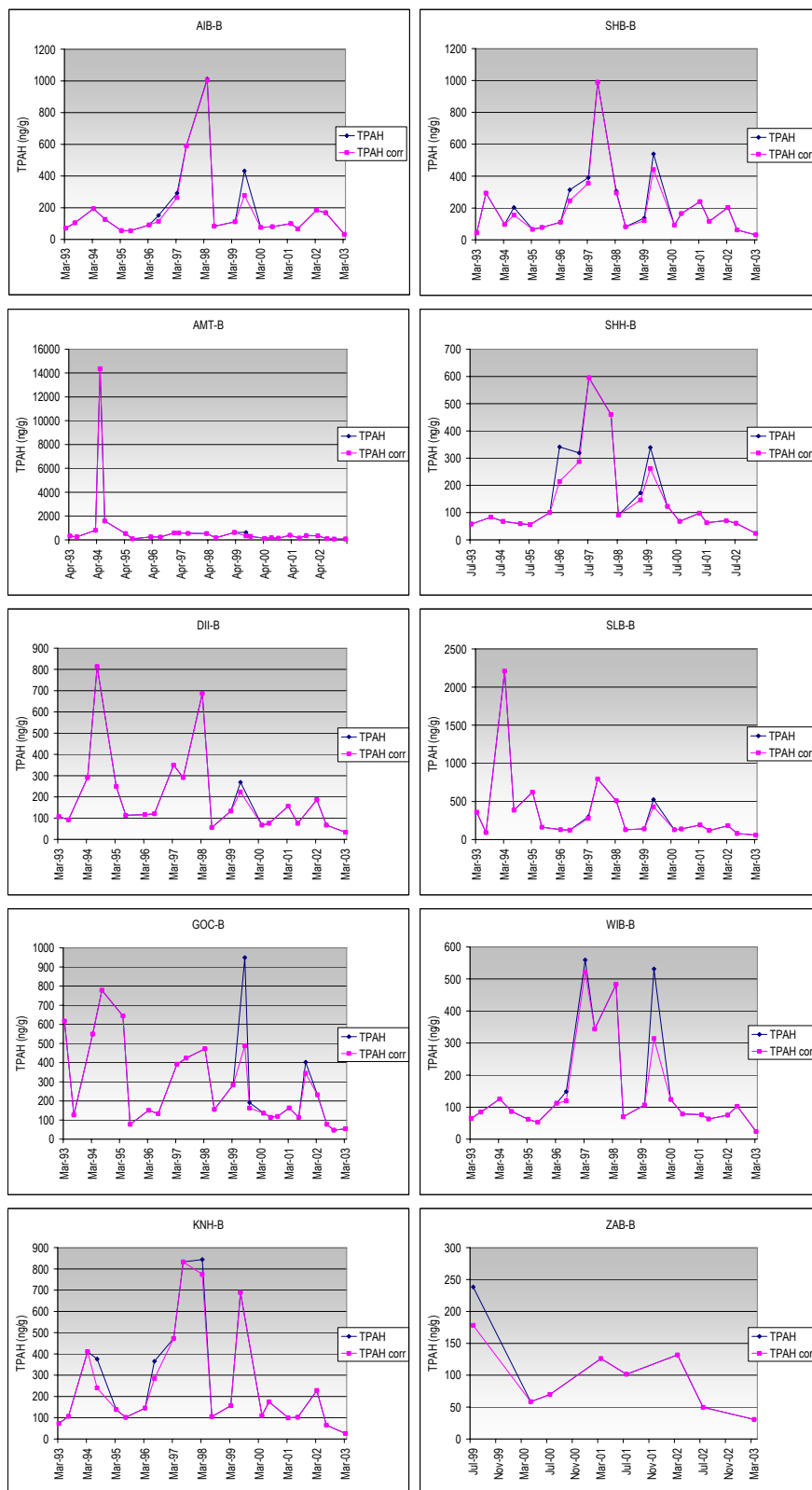
Figure 34 Station-specific mussel TPAH concentrations with and without fluorene/lipid corrections.

The increase in the AMT and GOC MPI values in March 1997 may reflect the BWTF spill that occurred in January 1997; however, the peaking patterns in 1997-98 are difficult to understand. There are synchronous increases at some stations in 1997 while others peak in 1998. Yet it is obvious that an event has occurred during the 1997-98 period before the sites fall into their more predictable behavior of recent years.

In an effort to explain these apparent trends, we re-examined the PAH histogram plots for all of the samples to see if there was an obvious dissolved vs. particulate/oil-droplet phase signature or other commonality that would explain the data. For this effort, we also considered the available AHC data, although there were no AHC data from 1995-1998, and most of the remaining data were compromised because of lipid interference.

In our 2001 report summarizing LTEMP results for Port Valdez (Payne et al. 2001), we presented evidence for a dissolved vs. particulate/oil-droplet signal in the mussels at both AMT and GOC. The seasonal dependence of these signals led us to hypothesize a water-column stratification-controlled transport mechanism to explain the observations (Payne et al. 2001). For this analysis, we have expanded upon that approach and developed the Particulate to Dissolved Ratio (PDR) to quantify the observed qualitative differences in the PAH histograms of particulate/oil-droplet vs. dissolved components. Essentially, the PDR is simply the ratio of the higher molecular weight PAH that have lower water solubilities and are generally associated with finite oil droplets to the sum of the more water soluble alkylated naphthalenes (e.g., see Table 3 and Figure 4 in the Oil Primer at the beginning of this report). Careful correlation of the PDR values with visual examination of the mussel PAH histograms from all stations over all seasons has confirmed that if a sample exhibits a PDR value greater than 2, the PAH pattern will show an accumulation by the mussel of predominately the higher molecular weight alkylated phenanthrene/anthracene (P/A), dibenzothiophene (D), and chrysene (C) components associated with particulate (finite) oil droplets, while a PDR value less than 1 will come from a sample where the naphthalenes (N) predominate. Samples with PDR values between 1 and 2 contain a mixture of components from both the dissolved and particulate phases.
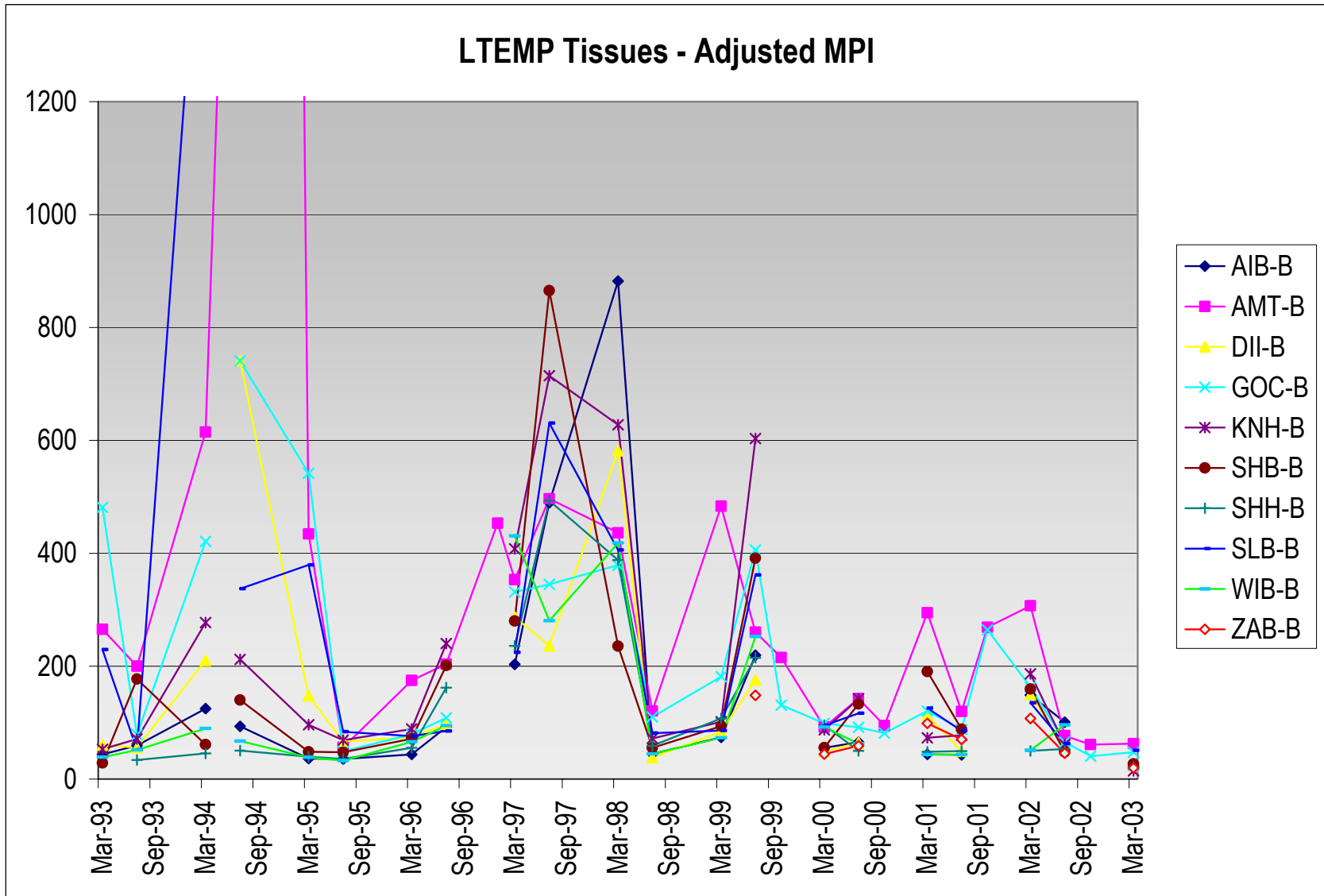
Figure 35 Time series of fluorene/lipid corrected Mytilus Pollution Index plot for all LTEMP stations. The breaks in various time series are artifacts from interim sampling at other stations.
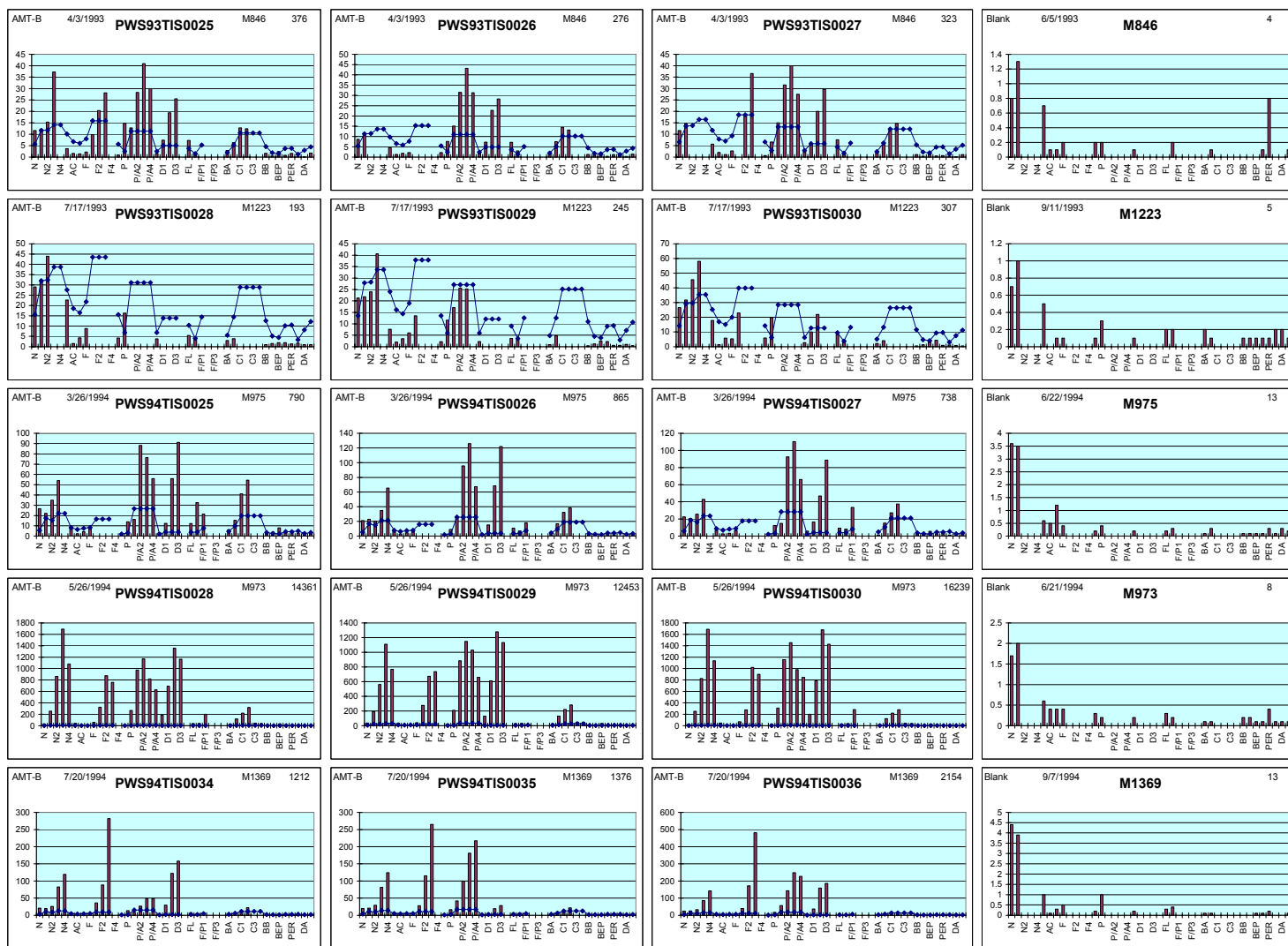
Figure 36 PAH histograms for AMT samples and associated procedural blanks from the April 1993 – July 1994 collections.
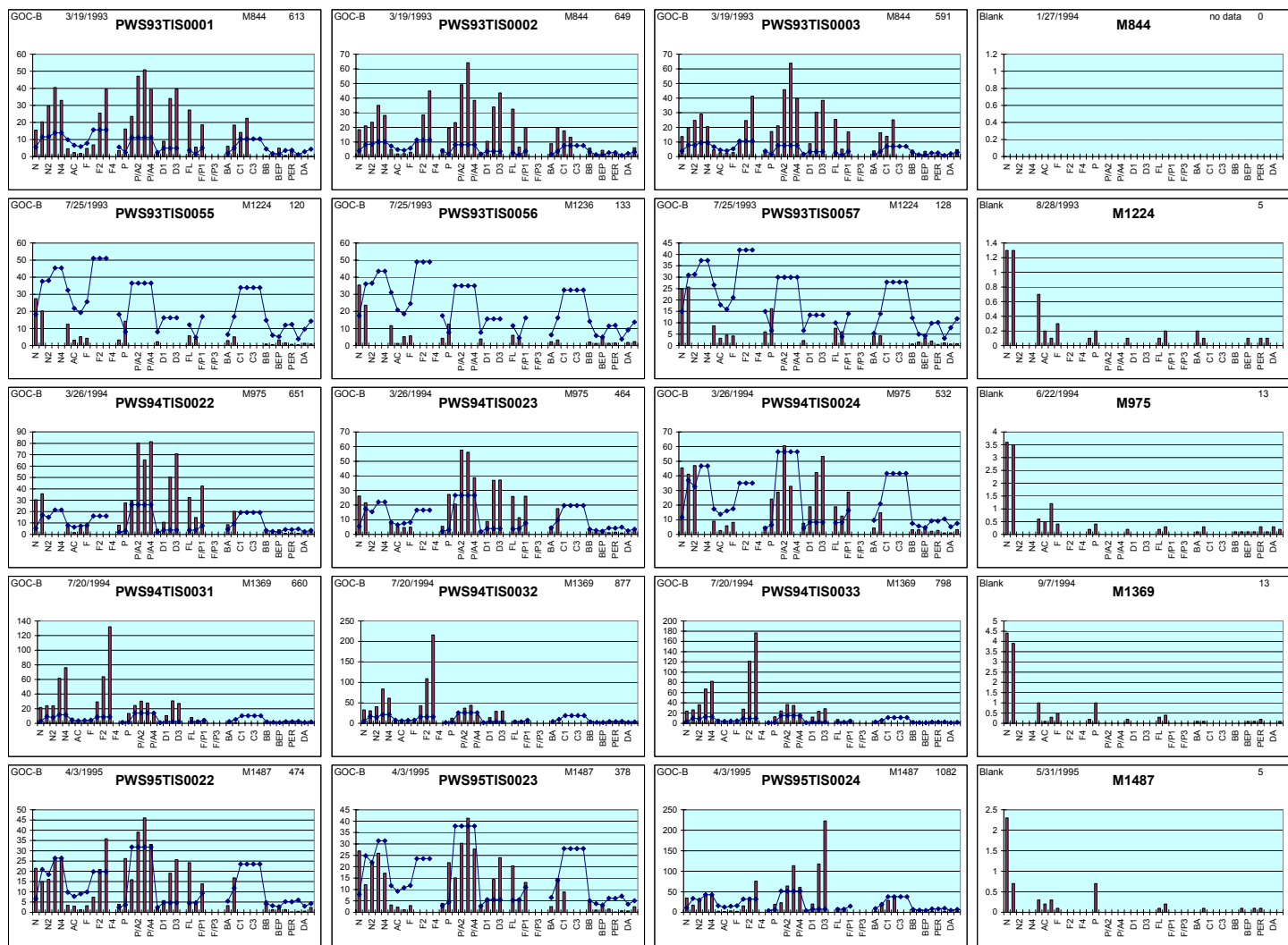
Figure 37 PAH histograms for GOC samples and associated procedural blanks from the April 1993 – July 1994 collections.

Figure 37 presents the individual MPI plots for each station along with the average PDR values generated for each sample set. The data in the figure suggest that the apparent summer-dissolved vs. winter/spring-particulate signal observed at GOC and to a lesser extent at AMT seems to break down after the spring of 2000, when lower overall MPI (and TPAH) values are observed. Also, the other sites do not show the same seasonal pattern as that observed within Port Valdez, and at most of the outer PWS stations, the signal is primarily driven by dissolved components as reflected by the PDR values that are less than one. There are seasonal fluctuations to be sure, but at some of the other stations, the PDR is higher in summer (indicating a mixture of dissolved and particulate/oil-droplet phases) and lower in winter and just the opposite at others. What is common among most stations is the tendency for the apparent MPI maxima in the 1997-1998 time frame to be largely derived from a dissolved-phase signal of primarily naphthalene(s), with an absolute minimum PDR (maximum naphthalene signal) observed at all stations in July 1997.

While it is conceivable that there could be some explanation for an across-the-region increase in a predominantly dissolved-phase signal between March 1997 and March 1998, we found it hard to believe that it could occur in an area as large and diverse as Port Valdez and Prince William Sound (including Kodiak Island). Therefore, we began to look for some other systematic bias or difference in collection or analytical procedures that might explain the observations. For example, we ruled out the possibility that the apparent MPI (and TPAH) increase might have been due to lipid interference, because the maxima occurred during a period when the anomalous fluorene pattern and percent lipids measured in the tissues were at a minimum (see Figures 31 and 32).

During our investigation we learned from Dr. Guy Denoux at GERG (personal communication, 8/7/03), that the laboratory installed new GC/MS instrumentation and integration software in the early 1997 timeframe, and that this resulted in increased sensitivity (lower detection limits) and a greater number of alkylated PAH homologues being routinely integrated with the automated integration software.

Figures 39 and 40 present the PAH histogram plots of field samples and associated procedural blanks from Aialik Bay (AIB) collected and analyzed between March 1993 and November 1997. It should be noted that the PAH patterns were almost identical throughout the early (1993-1996) timeframe, and although the absolute concentrations were usually ten times higher in the field samples, an identical pattern was obtained in the procedural blanks. During the initial years of the LTEMP program, the software with GERG's GC/MS instrumentation did not automatically integrate all the alkylated PAH homologues, and as a result, PAH patterns similar to those observed in Figures 39 and 40 were often obtained on samples from the cleaner areas. Integration of the remaining C_2-, C_3-, and C_4-alkylated homologues had to be done manually by the GC/MS operator, and then only when a recognizable signal was observed. When there was significant oil contamination (such as at the AMT and GOC sites after the *T/V Eastern Lion* oil spill in 1994), the instrumentation was sensitive enough to detect the signal from the remaining alkylated homologues, and they were manually integrated to generated the PAH profiles shown in Figures 36 and 37. The rest of the time, however, profiles closer to those shown in Figure 39 were obtained.
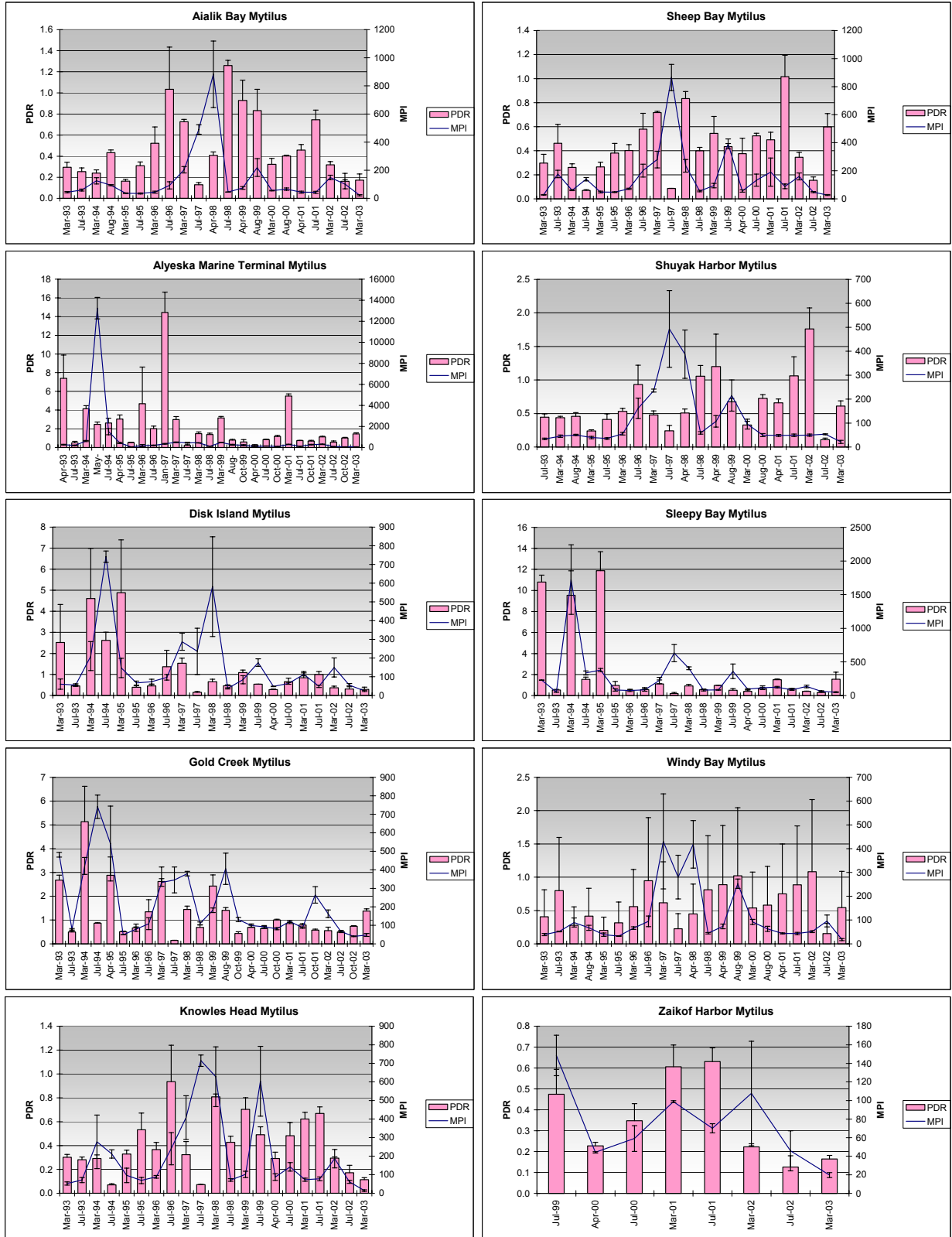
Figure 38 Fluorene/lipid corrected MPI and PDR plots for all LTEMP stations over the March 1993 – March 2003 period.
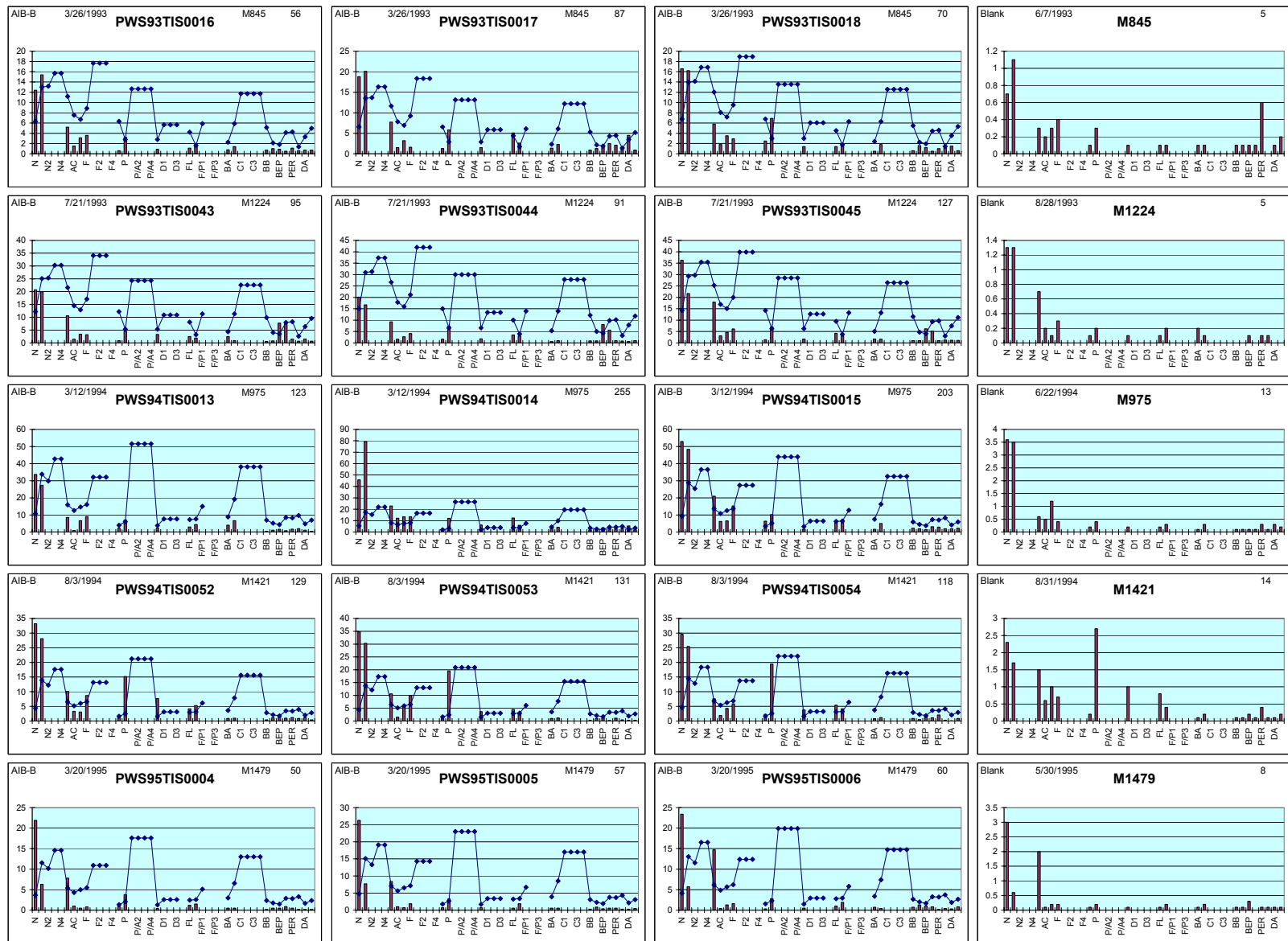
Figure 39 PAH histograms of Aialik Bay mussel samples and associated procedural blanks showing the typical background pattern obtained with the initial GC/MS instrumentation used for the 1993-1995 analyses.
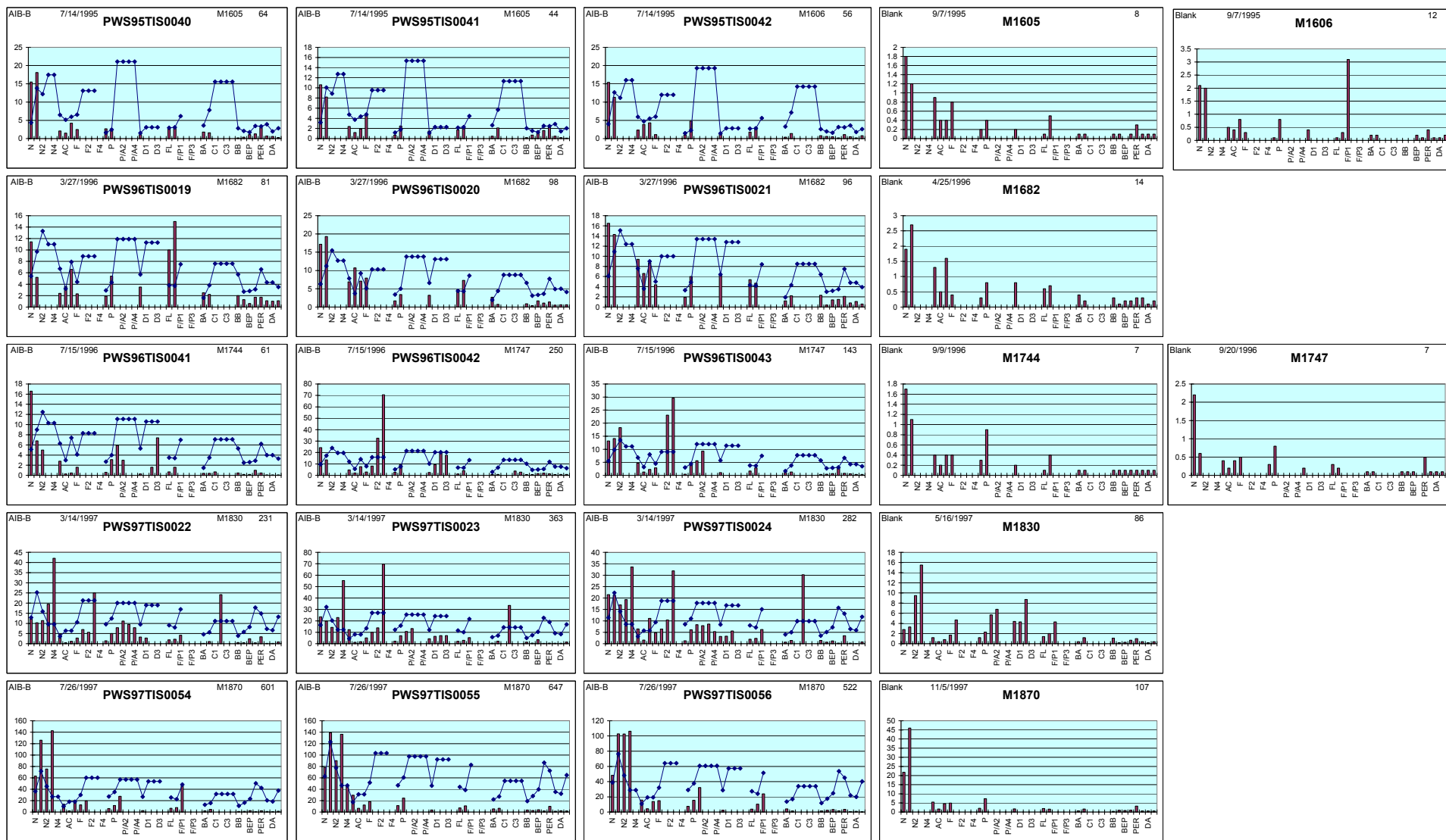
Figure 40 PAH histograms of Aialik Bay mussel samples 1995-1997 and associated procedural blanks showing the increasingly complex background pattern obtained with the change in GC/MS instrumentation beginning with the 1997 analyses.

When a new Mass Selective Detector (MSD) and updated integration software were installed at GERG sometime in 1997, the sensitivity of the GC/MS system used for the LTEMP samples was increased, and automated integration of the previously missing alkylated PAH homologues was initiated. The result was higher TPAH values and much more complex looking PAH profiles, such as those shown from the March and July 1997 AIB samples in Figure 40 (rows four and five) in all the samples examined in the program. Note the appearance in row four of more peaks in homologues of naphthalene, fluorene, dibenzothiophenes, and the first appearance of C_2-chrysenes (C2). In the bottom row, the peaks diminish, reflecting a more dissolved-fraction signature; however, the complexity of the lighter (left end) analytes is still apparent.

With the available data, it is impossible to say if the apparent increase in all the samples across the study region in the 1997-1998 period was just a result of the instrumentation and software changes, or if there really was some event in Port Valdez and PWS that was the cause. Certainly there were some subtle differences among the samples and stations with regard to the MPI and PDR values (see Figure 38), and these signals did not all track together with time   Nevertheless, the possibility of a systematic error or laboratory bias cannot be completely ruled out.

Because of the significant differences in the MPI and PDR signals during the *T/V Eastern Lion* event (before the 1997-1998 period), we believe that the data probably accurately reflect the conditions in the study region at that time. Likewise, the observed MPI and PDR differences noted among the stations since 1998, suggest that if there was a systematic laboratory bias, it has probably been addressed, and the data from 1998 on are representative of the conditions in Port Valdez and PWS. It is just the 1997-1998 period that has us concerned. If the noted region-wide increases are in fact real, then additional research will be required to try and track down the cause.

The use of the MPI and PDR appear to allow real trend and dissolved vs. particulate/oil-droplet source analyses, but as noted before, there is currently no correlation between MPI (and TPAH) and the aliphatic data for the mussel tissues analyzed thus far in the program. This can be corrected with better lipid separation during the sample cleanup, and should be a priority. A tremendous amount of additional information about the state of hydrocarbon contamination can be obtained from this information (e.g., see the examples of paired PAH and AHC histogram plots in the Oil Primer, Section 2).

The mode of hydrocarbon incorporation (particulate or dissolved) into the sentinel organisms is important, because other species and developmental stages are affected differently by dissolved and particulate oil fractions. If the LTEMP is truly going to be used to monitor the impacts of the Alyeska Marine Terminal operations and hydrocarbon transport through Port Valdez and PWS, this mechanism of exposure must also be delineated.

6   Conclusions

Based on the detailed analysis of the historical data set and the results from the July 2002 and March 2003 collections and analyses, the following conclusions have been reached.

- With the exception of identifiable pollution events, most of the LTEMP study sites remain remarkably free of hydrocarbon contaminants from anthropogenic or natural sources, most of the time. The most important hydrocarbon pollution sources evident in samples from these stations may be related to 1) the *T/V Eastern Lion* oil spill in Port Valdez in 1994; 2) a sheen event from the Ballast Water Treatment Facility of the Alyeska Marine Terminal in Port Valdez; and 3) oil from the 1989 *Exxon Valdez* oil spill occasionally evident at two stations that were heavily impacted.   Apart from stations affected by these events, concentrations derived from petrogenic sources are usually near or below the analytical detection limits of the methods used for their analysis, typically in the low parts per billion for individual PAH.

- Field Collection Methods
  - The new streamlined sampling methods appear adequate for LTEMP needs.
  - Standard versus modified Van Veen grab sampler comparisons are pending.
  - Chilled rather than frozen sediment PGS samples are preferred.

- Analytical Chemistry Issues
  The low concentrations of hydrocarbons usually encountered in LTEMP sampling presents substantial challenges to the hydrocarbon analysis laboratories. Despite state of the science methods, outstanding quality assurance programs and exemplary performance track records, the accuracies of some of the hydrocarbon analytes may have been compromised at various times during this program, causing relatively small biases in some of the reported results. The compounds most vulnerable include some of the higher molecular mass alkanes, the alkylated fluorenes and the alkylated phenanthrenes.
  - Perusal of the historic and current results suggest occasional positive interferences from incomplete lipid removal in some samples analyzed at GERG, and possibly a somewhat lowered sensitivity (~ -30%) for alkylated phenanthrenes analyzed at ABL.   Because of these interferences, it remains unclear whether the slight increase in PAH observed at stations remote from identifiable pollution sources during 1997 and 1998 reflect actual changes in the sampled environment, or are the result of artifacts introduced during analysis in the laboratory.
  - Through detailed examination of all PAH and AHC histogram plots for all stations and seasons, it was possible to screen the data and systematically reduce the confounding effects from obvious lipid interference.

- o Removal of the obvious lipid interference did not drastically change the overall conclusions with regard to low-level PAH contamination in mussels across all sites; however, it did affect the apparent temporal maxima previously suggested in July 1999 at GOC and WIB.

- Sediment Chemistry Evaluation
  - o TPAH concentrations at AMT are low (generally below 600 ng/g dry wt.) but highly variable, and the PAH and AHC histogram profiles continue to indicate the accumulation of PAH and AHC components from the BWTF (and presumably other terminal operations). Additional hydrocarbon sources at AMT include combustion products (which may or may not be related to terminal activities) and biogenic marine and terrestrial AHC components.
  - o The PAH components in the sediments at GOC are generally 5-10 times lower than those at AMT, and they do not show the same degree of petrogenic contamination or variability compared to the AMT site. The PAH in GOC sediments are derived primarily from combustion products.
  - o It is not possible to determine if the low but finite petrogenic hydrocarbons in the GOC sediments are from the BWTF and/or other activities at the Alyeska Marine Terminal, or if they represent input from other sources, including boat traffic; sewage and wastewater effluent; and surface/stormwater runoff from the city of Valdez.
  - o The AHC pattern in the GOC sediments clearly suggests marine biogenic input and terrestrial-sourced plant wax components.

- Tissue Chemistry Evaluation
  - o The historic data demonstrate that mussels do accumulate and show PAH patterns that can be clearly associated with known spill events such as the *T/V Eastern Lion* oil spill in 1994 and the BWTF sheening incident in 1997. In addition, they can pick up petrogenic hydrocarbons from other activities such as the beach cleaning operations at Disk Island (and possibly Sleepy Bay) in the summer of 1994.
  - o PAH concentrations as reflected in TPAH and MPI plots appear to have declined at both AMT and GOC since October 2001 and March 2002.
  - o Although the concentrations are low, the data from AMT continue to indicate the accumulation of dissolved and particulate/oil-phase PAH components from the BWTF (and presumably other terminal operations).
  - o While GOC mussels have historically indicated low concentrations of PAH contamination that appears to be introduced from seasonal, water-column stratification-controlled transport of dissolved PAH and particulate/oil-droplets, the winter vs. summer pattern appears to have abated (with a primarily dissolved-phase pattern observed) after March 2000 with the overall decline in TPAH and MPI levels at the site.

o The TPAH and MPI plots for the regional PWS stations (including Kodiak Island) are generally very low (< 200 ng/g wt.) and appear to have declined at most stations since March 2002 reflecting an almost exclusively dissolved-phase signal (PDR < 1).

o The apparent increase across the region (Port Valdez and PWS, including Kodiak Island) in TPAH and MPI in mussels during the 1997-1998 timeframe might be related to a systematic change in laboratory procedures implemented at that time. However, it is impossible to definitively state whether or not the trend was real (reflecting a region-wide input of primarily dissolved PAH components) or a laboratory artifact without additional laboratory data (Total Ion Current (TIC) profiles and hardcopy FID gas chromatographic profiles for all tissue samples).

7   Recommendations

- To facilitate evaluation of lipid interferences we recommend in the future that analytical laboratories supply hard and electronic copies of total ion current chromatograms for the GC/MS analyses and the detector response for GC/FID analyses, to facilitate evaluation of lipid interferences. These products would provide conclusive evidence for the presence of positive interferences in these analyses.

- Maybe the elimination of the lipid measurements beginning with the 2002 mussel collections was a mistake. The lipid measurements were very helpful in investigating the problems with laboratory artifacts during this data analysis, and it may be prudent to re-introduce this measurement back into the program.

- It is not possible to tell if the low-level petroleum source in the subtidal sediments at GOC is from the BWTF and other activities at AMT or other sources (boat traffic, sewage and wastewater discharges from the City of Valdez). This source may be identified through a limited set of sterane/triterpane analyses of AMT and GOC sediments for comparison to Alyeska BWTF discharges as part of future LTEMP or other PWS RCAC research activities.

- For data quality purposes, if either the NIST Standard Reference Materials (SRMs) or analytical laboratories are changed, parallel analyses of the old and new SRMs should be run by each participating laboratory. For instance, when a NIST SRM has to be changed (due to limited or diminishing supplies), a minimum of six old and six new SRM samples should be run within the same group of analytical samples (i.e. analytical "batch" or "string") to generate intra-laboratory comparability data. Likewise, when changing laboratories, the same NIST SRM should be analyzed by both analytical laboratories, again with a minimum of six SRM replicates completed at each laboratory. If the SRM and laboratory are to be changed simultaneously, then six old and six new SRM samples should be run within the same analytical string at each laboratory.

8 References

Kinnetic Laboratories, Inc. (KLI), 2002. 2000-2002 LTEMP Monitoring Report. Prepared for the Prince William Sound Regional Citizens' Advisory Council Long-Term Environmental Monitoring Program. 94pp. and appendices.

Payne, J.R., J.R. Clayton, Jr., G.D. McNabb, Jr., B.E. Kirstein, C.L. Clary, R.T. Redding, J.S. Evans, E. Reimnitz, and E. Kempema. 1989. Oil-ice sediment interactions during freezeup and breakup. Final Reports of Principal Investigators, U.S. Dept. Commer., NOAA, OCEAP Final Rep. 64, 1-382 (1989). NTIS Accession Number PB-90-156217.

Payne, J.R., W.B. Driskell, and D.C. Lees. 1998. Long Term Environmental Monitoring Program Data Analysis of Hydrocarbons in Intertidal Mussels and Marine Sediments, 1993-1996. Final Report prepared for the Prince William Sound Regional Citizens Advisory Council, Anchorage, Alaska 99501. (PWS RCAC Contract No. 611.98.1). March 16, 1998. 97 pp plus appendices.

Payne, J.R., W.B. Driskell, M.G. Barron, D.C. Lees. 2001. Assessing transport and exposure pathways and potential petroleum toxicity to marine resources in Port Valdez, Alaska. Final Report Prepared for Prince William Sound Regional Citizens' Advisory Council Contract No. 956.02.1. Prepared by Payne Environmental Consultants, Inc., Encinitas, CA. December 21, 2001. 64 pp plus appendices.

Payne, J.R., J.R. Clayton, Jr., and B.E. Kirstein. 2003. Oil/suspended particulate material interactions and sedimentation. Spill Science & Technology Bulletin, Vol. 8(2), pp 201-221.

Salazar, M., J.W. Short, S.M. Salazar, and J.R. Payne. 2002. Port Valdez Monitoring Report. Prince William Sound Regional Citizens' Advisory Council Contract No. 633.01.1. February 7, 2002. 109 pp plus appendices.

9   APPENDICES

Appendix A- 1 Field notes on Mytilus populations

Station	Field notes
Aialik Bay	Very good population. Dense, 5-6 yr old, plump and healthy crop of recruits. Few predators visible.
Alyeska Marine Terminal	Denser population and not as patchy as GOC
Disk Island	Healthy, plump, vivid blue shells. No mussels in mid-transect swale.
Gold Creek	Colony in patchy strips, slippery, silt-covered with reduced shell volume.
Knowles Head	Mussels dense but small. Good crop of 3 yr old recruits.
Sheep Bay	Harvestable mussels discontinuous in mid transect. Shells small (<2 cm) but still 6-7 yr old. Distinct zone in KLI photos no longer visible. 3 yr old recruits appearing on upper surfaces.
Shuyak Harbor	Mytilus patchy near right end. But healthy and aged 5-6 yr old. Less patchy near left end but slightly smaller. Good recruitment.
Sleepy Bay	Mussels are only in broken shale above the marker. Mostly small 3-5 yr olds. No mussels in mid-section. Large *Nucella* present at right end but not in high numbers. Higher numbers of smaller *Nucella* at left end. KLI notes earlier predator infestation.
Windy Bay	Good site. Beds dense and continuous. Mytilus healthy, plump and aged. Good recruitment.
Zaikof Bay	Very dense, medium-sized population.

Appendix A- 2 Comparison of split-sample analysis for sediment grain size, total carbon, total organic and inorganic carbon for inter-laboratory calibration.

	GERG	ABL	Difference
AMT-S-2-02-1			
Gravel %	0.0	0.00	0.00
Sand	6.7	3.24	3.46
Silt	51.8	46.99	4.85
Clay	41.5	49.77	-8.30
TOC %	0.55	0.64	-0.09
TC%	0.59	0.65	-0.06
TIC%	0.04	0.01	0.03
GOC-S-2-02-1			
Gravel	0.0	0.00	0.00
Sand	7.7	5.48	2.26
Silt	50.1	48.36	1.78
Clay	42.1	46.16	-4.04
TOC %	0.51	0.60	-0.09
TC%	0.60	0.61	-0.01
TIC%	0.09	0.01	0.08

Appendix A- 3 Inter-laboratory comparison of split tissue samples.

Laboratory		ABL	GERG	ABL	GERG	ABL	GERG
Sample Field Number		AMT-B 1A		AMT-B 2A		GOC-B 1A	
Sample ID		1303901		1303903		1303915	
Matrix		TISSUE		TISSUE		TISSUE	
Dry Weight (g)		0.61	0.30	0.57	0.28	0.72	0.37
Wet Weight (g)		10.03	5.63	10.09	5.14	9.95	5.12
PAH Data							
Surrogate Recoveries (%)							
Naphthalene D-8		64.8	62.9	26.3	60.8	51.9	56.3
Acenaphthene D-10		79.4	73.0	30.4	64.4	68.6	61.7
Phenanthrene D-10		99.8	88.3	43.9	78.7	95.9	78.7
Chrysene D-12		88.4	73.2	36.1	57.9	95.2	63.7
Benzo-a-Pyrene D-12		39.8		11.4		42.3	
Perylene D-12		31.9	61.0	8.0	50.4	31.5	58.1
Analyte concentrations (ng/g)							
Naphthalene	N	15.99 b	17.5 J	30.16 b	22.3 J	28.29 b	23.0 J
C-1 Naphthalenes	N1	10.74 b	18.3 J	11.65 b	17.4 J	15.07 b	11.6 J
C-2 Naphthalenes	N2	5.51 b	21.3 J	6.31 b	17.7 J	2.34 b	11.0 J
C-3 Naphthalenes	N3	4.62 b	16.0 J	2.29 b	14.3 J	1.62 b	16.6 J
C-4 Naphthalenes	N4	0.84 b	29.7 J	3.07 b	0.0 ND	0.00 b	25.3 J
Biphenyl	BI	0.00 b	8.4 J	5.49 b	10.1 J	19.04 b	8.4 J
Acenaphthylene	AC	0.00 a	1.4 J	0.00 a	1.7 J	0.00 a	1.1 J
Acenaphthene	AE	1.19 b	12.3 J	1.51 b	12.2 J	1.28 b	14.5 J
Fluorene	F	1.50 b	6.3 J	2.19 b	6.0 J	2.54 b	3.6 J
C-1 Fluorenes	F1	2.86 b	34.0 J	3.28 b	70.7 J	3.51 b	137.7
C-2 Fluorenes	F2	3.19 b	219.4	0.00 a	3.2 J	0.00 a	386.8
C-3 Fluorenes	F3	0.00 a	470.8	0.00 a	35.2 J	0.00 a	705.0
C-4 Fluorenes	F4	0.00 a		0.00 a		0.00 a	
Dibenzothiophene	D	2.30 b	1.1 J	0.00 a	1.3 J	1.35 b	1.7 J
C-1 Dibenzothiophenes	D1	1.46 b	7.1 J	1.67 b	3.6 J	0.91 b	10.6 J

C-2 Dibenzothiophenes	D2	2.56	b	27.3	J	2.00	b	9.3	J	1.37	b	11.2	J
C-3 Dibenzothiophenes	D3	1.23	b	14.0	J	0.00	a	4.6	J	0.00	a	23.8	
C-4 Dibenzothiophenes	D4	0.46	b			0.00	a			0.00	a		
Phenanthrene	P	7.29	b	10.4	J	5.91	b	9.7	J	9.22	b	10.0	J
C-1 Phenanthrenes/Anthracenes	P/A1	4.39	b	11.2	J	3.06	b	106.8		3.39	b	44.5	J
C-2 Phenanthrenes/Anthracenes	P/A2	5.69	b	55.6	J	4.23	b	31.3	J	3.20	b	53.7	
C-3 Phenanthrenes/Anthracenes	P/A3	0.00	a	115.7		0.00	a	78.2		0.00	a	289.6	
C-4 Phenanthrenes/Anthracenes	P/A4	0.00	a	35.9	J	0.00	a	27.3	J	0.00	a	80.4	
Anthracene	A	1.19	b	8.6	J	0.00	a	5.4	J	0.00	a	18.2	J
Fluoranthene	FL	2.85	b	5.7	J	2.41	b	3.6	J	2.79	b	4.1	J
Pyrene	PY	0.76	b	4.8	J	0.67	b	4.7	J	0.76	b	0.7	J
C-1 Fluoranthenes/Pyrenes	F/P1	0.00	a	33.3	J	0.00	a	16.4	J	1.03	b	82.7	
C-2 Fluoranthenes/Pyrenes	F/P2	0.00	a			0.00	a			0.00	a		
C-3 Fluoranthenes/Pyrenes	F/P3	0.00	a			0.00	a			0.00	a		
C-4 Fluoranthenes/Pyrenes	F/P4	0.00	a			0.00	a			0.00	a		
Benz-a-Anthracene	BA	0.00	a	2.0	J	0.00	a	2.1	J	0.00	a	1.1	J
Chrysene	C	0.00	a	4.0	J	0.00	a	3.5	J	0.00	b	1.5	J
C-1 Chrysenes	C1	0.00	a	0.0	J	0.00	a	1.2	J	0.00	a	2.7	J
C-2 Chrysenes	C2	0.00	a	22.4	J	0.00	a	24.5	J	0.00	a	20.5	J
C-3 Chrysenes	C3	0.00	a	1.1	J	0.00	a	6.6	J	0.00	a	6.1	J
C-4 Chrysenes	C4	0.00	a	9.9	J	0.00	a	4.8	J	0.00	a	17.2	J
Benzo-b-Fluoranthene	BB	5.17	b	2.1	J	0.00	a	2.0	J	0.00	a	1.7	J
Benzo-k-Fluoranthene	BK	2.03	b	0.9	J	0.00	a	0.3	J	0.00	a	0.5	J
Benzo-e-Pyrene	BEP	2.17	b	2.9	J	0.00	a	3.3	J	0.00	a	1.9	J
Benzo-a-Pyrene	BAP	4.61	b	1.9	J	0.00	a	5.0	J	0.00	a	1.2	J
Perylene	PER	4.94	b	4.2	J	0.00	a	5.7	J	0.00	a	0.3	J
Indeno-123-cd-Pyrene	IP	12.13	b	1.0	J	0.00	a	1.6	J	0.00	a	0.1	J
Dibenzo-a,h-Anthracene	DA	13.81	b	0.2	J	0.00	a	0.6	J	0.00	a	0.5	J
Benzo-g,h,i-Perylene	BP	5.48	b	1.2	J	0.00	a	1.9	J	0.00	a	1.2	J
Total PAH		126.93		1239.61		85.91		575.82		97.72		2032.14	

4

Laboratory		ABL	GERG	ABL	GERG	ABL	GERG	
Sample Field Number		GOC-B 2A		AMT-S 1		GOC-S 1		
Sample ID		1303917		1303910		1303912		
Matrix		TISSUE		SEDIMENT		SEDIMENT		
Dry Weight (g)		1.00	0.46	24.96	2.53	27.12	0.64	
Wet Weight (g)		10.13	5.08	50.46	5.06	52.44	1.23	
PAH Data								
Surrogate Recoveries (%)								
Naphthalene D-8		56.7	59.4	57.6	47.8	50.8	72.4	
Acenaphthene D-10		73.3	64.3	79.4	83.0	73.2	86.9	
Phenanthrene D-10		95.5	73.9	93.1	90.3	80.1	91.1	
Chrysene D-12		93.1	49.9	94.0	103.5	72.7	82.2	
Benzo-a-Pyrene D-12		40.9		97.9		52.0		
Perylene D-12		31.6	47.7	93.0	77.8	49.7	50.6	
Analyte concentrations (ng/g)								
Naphthalene	N	22.02 b	11.7 J	1.90 b	36.7	1.90 b	10.1 J	
C-1 Naphthalenes	N1	12.37 b	9.2 J	4.97 b	34.9	4.43 b	11.5 J	
C-2 Naphthalenes	N2	3.91 b	8.7 J	4.76 -	11.0	3.44 -	6.9 J	
C-3 Naphthalenes	N3	3.12 b	12.4 J	4.51 -	9.5	3.46 -	10.4 J	
C-4 Naphthalenes	N4	0.71 b	21.8 J	2.48 b	7.2	1.31 b	10.9 J	
Biphenyl	BI	2.10 b	5.0 J	1.62 b	3.9	1.10 b	3.1 J	
Acenaphthylene	AC	0.00 a	0.9 J	0.35 b	0.8 J	0.21 b	1.3 J	
Acenaphthene	AE	1.45 b	8.3 J	0.64 b	9.5	0.70 b	2.4 J	
Fluorene	F	2.10 b	3.4 J	2.57 b	8.4	1.96 b	5.5 J	
C-1 Fluorenes	F1	3.37 b	93.6	1.79 b	5.2 J	1.33 b	10.0 J	
C-2 Fluorenes	F2	0.00 a	179.6	2.52 b	8.2 J	0.76 b	10.8 J	
C-3 Fluorenes	F3	0.00 a	405.3	3.22 b	17.7	0.65 b	26.7 J	
C-4 Fluorenes	F4	0.00 a		0.00 a		0.04 b		
Dibenzothiophene	D	1.30 b	0.8 J	1.41 b	2.7	1.07 b	2.3 J	
C-1 Dibenzothiophenes	D1	1.02 b	6.9 J	2.15 b	3.4	0.82 b	3.6 J	

Compound	Code												
C-2 Dibenzothiophenes	D2	1.13	b	9.4	J	6.57	-	10.7		0.70	b	6.5	J
C-3 Dibenzothiophenes	D3	0.72	b	17.2	J	7.22	-	16.8		0.36	b	6.1	J
C-4 Dibenzothiophenes	D4	0.00	a			3.62	b			0.03	b		
Phenanthrene	P	8.58	b	7.4	J	10.94	-	30.2		5.29	-	15.8	J
C-1 Phenanthrenes/Anthracenes	P/A1	3.73	b	7.6	J	7.95	-	12.4		2.36	b	9.9	J
C-2 Phenanthrenes/Anthracenes	P/A2	3.10	b	23.3	J	11.23	-	18.0		1.30	b	13.6	J
C-3 Phenanthrenes/Anthracenes	P/A3	0.00	a	98.4		9.73	-	20.3		0.45	b	8.0	J
C-4 Phenanthrenes/Anthracenes	P/A4	0.00	a	55.9		2.19	b	22.6		0.07	b	6.1	J
Anthracene	A	0.00	a	3.1	J	1.69	b	12.6		0.20	b	3.4	J
Fluoranthene	FL	2.86	b	2.7	J	10.76	-	40.8		2.87	-	21.7	J
Pyrene	PY	0.00	a	3.1	J	7.11	-	35.4		1.45	b	15.1	J
C-1 Fluoranthenes/Pyrenes	F/P1	1.09	b	32.0	J	10.01	-	20.6	J	0.60	b	8.8	J
C-2 Fluoranthenes/Pyrenes	F/P2	0.00	a			3.86	-			0.18	b		
C-3 Fluoranthenes/Pyrenes	F/P3	0.00	a			3.72	-			0.00	a		
C-4 Fluoranthenes/Pyrenes	F/P4	0.00	a			1.35	b			0.00	a		
Benz-a-Anthracene	BA	0.00	a	0.9	J	7.97	-	21.9		0.10	b	5.1	J
Chrysene	C	0.00	b	1.2	J	11.04	-	21.4		1.02	b	6.9	J
C-1 Chrysenes	C1	0.00	a	7.8	J	6.53	-	16.9		0.20	b	4.2	J
C-2 Chrysenes	C2	0.00	a	15.3	J	3.46	b	17.3		0.08	b	5.3	J
C-3 Chrysenes	C3	0.00	a	7.3	J	0.87	b	4.5	J	0.00	a	0.9	J
C-4 Chrysenes	C4	0.00	a	9.6	J	0.00	a	0.2	J	0.00	a	0.2	J
Benzo-b-Fluoranthene	BB	0.00	a	1.4	J	5.87	-	26.3		0.37	b	6.6	J
Benzo-k-Fluoranthene	BK	0.00	a	0.6	J	5.97	-	8.1		0.43	b	2.5	J
Benzo-e-Pyrene	BEP	0.00	a	1.5	J	5.35	-	18.0		0.40	b	4.5	J
Benzo-a-Pyrene	BAP	0.00	a	1.6	J	5.36	-	27.0		0.38	b	3.8	J
Perylene	PER	0.00	a	0.6	J	1.02	b	8.0		0.21	b	5.0	J
Indeno-123-cd-Pyrene	IP	0.00	a	0.2	J	2.61	-	17.6		0.11	b	2.0	J
Dibenzo-a,h-Anthracene	DA	0.00	a	0.2	J	0.71	b	3.7		0.00	a	0.7	J
Benzo-g,h,i-Perylene	BP	0.00	a	0.3	J	2.94	-	17.0		0.11	b	3.0	J
Total PAH		74.69		1076.25		192.54		607.37		42.45		281.00	

Laboratory		ABL	GERG	ABL	GERG	ABL	GERG
Sample Field Number		AMT-B 1A		AMT-B 2A		GOC-B 1A	
Sample ID		1303901		1303903		1303915	
Matrix		TISSUE		TISSUE		TISSUE	
Dry Weight (g)		0.61	0.30	0.57	0.28	0.72	0.37
Wet Weight (g)		10.03	5.63	10.09	5.14	9.95	5.12

ALIPHATIC Data
Surrogate Recoveries (%):

		ABL	GERG	ABL	GERG	ABL	GERG
C12 - d26		63.18	76.0	62.90	74.0	65.38	76.0
C16 - d34		69.25		69.25		70.27	
C20 - d42		79.36	104.0	81.42	96.0	78.69	104.0
C24 - d50		73.26	92.0	78.71	96.0	70.74	68.0
C30 - d64		69.45	78.0	80.02	100.0	66.70	102.0

Analyte concentrations (ng/g):

		ABL		GERG		ABL		GERG		ABL		GERG	
C10- (n-Decane)	C10	0.00	a	0.0	ND	279.33	b	0.0	ND	280.67	b	773.9	
C11- (n-Undecane)	C11	0.00	a	0.0	ND	73.99	b	0.0	ND	148.56	b	0.0	ND
C12- (n-Dodecane)	C12	0.00	a	82.2	J	42.48	b	230.3	J	50.30	b	66.2	J
C13- (n-Tridecane)	C13	104.25	b	133.3	J	195.43	b	164.5	J	187.67	b	163.4	J
C14- (n-Tetradecane)	C14	93.72	b	288.2		120.19	b	377.4		111.80	b	264.4	
C15- (n-Pentadecane)	C15	459.24	b	841.9		542.74	b	759.4		413.20	b	520.0	
C16- (n-Hexadecane)	C16	222.47	b	527.2		238.27	b	534.8		220.97	b	222.7	J
C17- (n-Heptadecane)	C17	274.43	b	1759.7		320.58	b	2781.2		354.75	b	1298.5	
Pristane	Pristane	154.89	b	702.7		184.63	b	549.8		140.41	b	261.2	
C18- (n-Octadecane)	C18	0.00	a	182.1	J	0.00	a	315.5	J	0.00	a	219.4	J
Phytane	Phytane	53.44	b	0.0	ND	61.60	b	72.4	J	0.00	a	71.9	J
C19- (n-Nonadecane)	C19	0.00	a	0.0	ND	0.00	a	668.5		0.00	a	684.8	
C20- (n-Eicosane)	C20	0.00	a	0.0	ND	0.00	a	1903.4	J	0.00	a	2020.1	

C21- (n-Heneicosane)	C21	0.00	a	8014.7		0.00	a	5270.5		0.00	a	6927.6	
C22- (n-Docosasne)	C22	0.00	a	131.0	J	0.00	a	168.2	J	0.00	a	103.0	J
C23- (n-Tricosane)	C23	0.00	a	2118.6	J	0.00	a	1115.3	J	0.00	a	2134.2	J
C24- (n-Tetracosine)	C24	0.00	a	91.4	J	0.00	a	0.0	ND	0.00	a	92.3	J
C25- (n-Pentacosane)	C25	84.68	b	0.0	ND	116.83	b	122.7	J	0.00	a	75.4	J
C26- (n-Hexacosane)	C26	0.00	a	182.9	J	0.00	a	248.0	J	0.00	a	218.5	J
C27- (n-Heptacosane)	C27	109.18	b	262.1	J	95.59	b	686.2		103.92	b	0.0	ND
C28- (n-Octacosane)	C28	95.20	b	550.4		0.00	a	665.2		0.00	a	212.6	J
C29- (n-Nonacosane)	C29	100.96	b	88760.4		91.70	b	90444.2		43.67	b	12254.1	
C30- (n-Triacontane)	C30	92.90	b	23714.5		0.00	a	24160.9		0.00	a	4544.9	
C-31	C31			3548.1				4277.1				730.8	J
C32- (n-Dotriacontane)	C32	0.00	a	241.8	J	0.00	a	0.0	ND	0.00	a	532.5	J
C33	C33			0.0	ND			0.0	ND			0.0	ND
C34- (n-Tetratriacontane)	C34	0.00	a	0.0	ND	0.00	a	0.0	ND	0.00	a	0.0	ND
Tot. Alkanes		363.38		132133.2		2405.67		135515.7		50522.98		34392.5	
UCM (ng/g)		29877.07				23723.36				11594.22		ug/g	
Total UCM (ug/g)				96.7				109.3				430.4	
Total Resolved (ug/g)				762.7				731.4				643.6	
TRAHC (ug/g)				859.4				840.7					

Laboratory		ABL	GERG		ABL	GERG		ABL	GERG	
Sample Field Number		GOC-B 2A			AMT-S 1			GOC-S 1		
Sample ID		1303917			1303910			1303912		
Matrix		TISSUE			SEDIMENT			SEDIMENT		
Dry Weight (g)		1.00	0.46		24.96	2.53		27.12	0.64	
Wet Weight (g)		10.13	5.08		50.46	5.06		52.44	1.23	
ALIPHATIC Data										
Surrogate Recoveries (%):										
C12 - d26		65.87	76.0		73.75	57.9		68.08	59.0	
C16 - d34		69.82			74.08			71.25		
C20 - d42		82.32	112.0		82.26	94.0		77.40	84.0	
C24 - d50		80.02	90.0		78.55	100.0		69.12	89.0	
C30 - d64		81.67	126.0	M	99.86	99.0		68.82	100.0	
Analyte concentrations (ng/g):										
C10- (n-Decane)	C10	281.51 b	787.1		0.00 a	22.6		0.00 a	0.0	ND
C11- (n-Undecane)	C11	387.57 b	0.0	ND	0.12 b	0.0	ND	2.32 b	0.0	ND
C12- (n-Dodecane)	C12	60.68 b	51.6	J	0.00 a	6.7	J	0.00 a	56.2	J
C13- (n-Tridecane)	C13	154.38 b	72.2	J	0.00 a	7.0	J	0.00 a	0.0	ND
C14- (n-Tetradecane)	C14	126.42 b	239.3		1.96 b	22.8		2.11 b	96.8	
C15- (n-Pentadecane)	C15	313.83 b	633.9		2.91 b	47.3	J	3.93 b	56.9	J
C16- (n-Hexadecane)	C16	212.22 b	298.6		5.13 b	16.0	J	3.89 b	50.2	J
C17- (n-Heptadecane)	C17	440.05 b	1388.9		8.31 b	31.3	J	5.05 b	50.3	J
Pristane	Pristane	160.56 b	218.4		10.07 b	24.5	J	14.89 b	53.9	J
C18- (n-Octadecane)	C18	0.00 a	221.2		3.86 b	11.8	J	2.11 b	25.5	J
Phytane	Phytane	23.91 b	346.1		7.52 b	18.5	J	2.24 b	0.0	ND
C19- (n-Nonadecane)	C19	0.00 a	147.4	J	2.41 b	15.2	J	2.17 b	34.3	J

Compound	Code												
C20- (n-Eicosane)	C20	0.00	a	1893.4		3.54	b	11.6	J	1.30	b	29.9	J
C21- (n-Heneicosane)	C21	0.00	a	4959.9		3.82	b	18.7	J	2.07	b	48.7	J
C22- (n-Docosasne)	C22	0.00	a	52.2	J	2.79	b	16.4	J	2.13	b	55.0	J
C23- (n-Tricosane)	C23	0.00	a	1628.8	J	11.38	b	27.7	J	4.43	b	85.5	J
C24- (n-Tetracosine)	C24	0.00	a	35.3	J	6.71	b	19.5	J	1.30	b	60.4	J
C25- (n-Pentacosane)	C25	0.00	a	61.5	J	8.94	b	36.7		12.97	b	131.0	
C26- (n-Hexacosane)	C26	0.00	a	207.1	J	19.00	b	21.2	J	0.77	b	83.9	J
C27- (n-Heptacosane)	C27	55.72	b	128.2	J	38.25	b	153.7		60.52	-	523.1	
C28- (n-Octacosane)	C28	0.00	a	215.2	J	19.57	b	43.0	J	3.07	b	78.3	J
C29- (n-Nonacosane)	C29	41.33	b	47980.3		38.49	b	96.8		28.08	b	242.4	
C30- (n-Triacontane)	C30	0.00	a	20130.5		24.89	b	107.5		0.00	a	48.0	J
	C31			2931.4				183.6				671.9	
C32- (n-Dotriacontane)	C32	0.00	a	0.0	ND	69.42	-	134.3		5.99	b	133.6	J
	C33			0.0	ND			0.0	ND			0.0	ND
C34- (n-Tetratriacontane)	C34	0.00	a	0.0	ND	64.47	-	196.6		0.00	a	44.9	J
Tot. Alkanes		42278.16		84628.2				1290.8		325.78		2660.8	
UCM (ng/g)		73327.98		ug/g		1235.52		ug/g		617.54		ug/g	
Total UCM (ug/g)				565.2				5.0				13.9	
Total Resolved (ug/g)				640.9				85.5				96.8	
TRAHC (ug/g)													

Appendix A- 4 Inter-laboratory comparison of mussel tissue NIST SRM 1947a

		Mussel Tissue Organics Standard - NIST SRM 1974a			
		NIST	ABL average	GERG	Seattle NMFS avg
Dry Weight			0.85	1.53	na
Wet Weight			7.49	13.38	na
% Solid			na	11.4	na
% Lipid			na	5.6	na
Surrogate Compounds					
Naphthalene D-8			60.2	63.7	na
Acenaphthene D-10			74.3	76.9	na
Phenanthrene D-10			96.7	107.9	na
Chrysene D-12			88.0	78.8	na
Benzo-a-Pyrene D-12			45.9		na
Perylene D-12			36.8	63.6	na
PAH Compounds					
Naphthalene	N	23.5	15.7	5.8 J	21.38
2-Methylnaphthalene	2N1	10.2	9.6	5.5	
1-Methylnaphthalene	1N1	5.3	5.3	2.9 J	24.55
C2-Naphthalenes	N2		13.2	9.1 J	20.68
C3-Naphthalenes	N3		30.7	23.6	34.66
C4-Naphthalenes	N4		54.1	71.2	58.55
Biphenyl	BI	5.11	5.2	2.9 J	
Acenaphthylene	AC	5.25	4.1	8.2	7.32
Acenaphthene	AE	3.15	3.3	5.4 J	4.48
Fluorene	F	5.72	6.4	7.3 J	5.39
C1-Fluorenes	F1		18.1	48.6	19.85
C2-Fluorenes	F2		52.5	122.4	60.03
C3-Fluorenes	F3		40.5	288.4	103.15
C4-Fluorenes	F4		0.0		
Dibenzothiophene	D		3.1	2.0 J	4.72

C1-Dibenzothiophenes	D1		13.3	14.7		14.80	
C2-Dibenzothiophenes	D2		77.5	60.6		69.78	
C4-Dibenzothiophenes	D3		86.9	67.3		103.74	
C3-Dibenzothiophenes	D4		38.5				
Phenanthrene	P	22.2	23.3	14.2		23.73	
C1-Phenanthrenes/Anthracenes	P/A1		58.8	45.8		198.54	
C2-Phenanthrenes/Anthracenes	P/A2		158.2	98.6		293.70	
C3-Phenanthrenes/Anthracenes	P/A3		155.7	208.5		196.19	
C4-Phenanthrenes/Anthracenes	P/A4		25.0	111.5			
Anthracene	A	6.1	5.7	17.5			
Fluoranthene	FL	163.7	180.8	151.1		230.26	
Pyrene	PY	151.6	166.3	143.4		212.64	
C1-Fluoranthenes/Pyrenes	F/P1		115.4	148.4		140.98	
C2-Fluoranthenes/Pyrenes	F/P2		52.1				
C3-Fluoranthenes/Pyrenes	F/P3		11.0				
C4-Fluoranthenes/Pyrenes	F/P4		1.6				
Benzo(a)anthracene	BA	32.5	31.2	28.5		45.94	
Chrysene	C	44.2	88.7	87.3		110.43	
C1-Chrysenes	C1		42.0	53.0		57.21	
C2-Chrysenes	C2		14.6	31.4		30.66	
C3-Chrysenes	C3		1.8	4.8	J	14.57	
C4-Chrysenes	C4		0.0	3.1	J	10.25	
Benzo(b)fluoranthene	BB	46.4	48.9	45.5		47.70	
Benzo(k)fluoranthene	BK	20.18	19.7	14.5		44.53	

Benzo(e)pyrene	BEP	84	89.2	66.5		
Benzo(a)pyrene	BAP	15.63	16.2	17.2		18.56
Perylene	PER	7.68	7.7	8.1		
Indeno(1,2,3-c,d)pyrene	IP	14.2	13.7	7.9		17.27
Dibenzo(a,h)anthracene	DA	3	2.9	2.0	J	7.15
Benzo(g,h,i)perylene	BP	22	20.6	15.5		29.84
Total PAHs with Perylene			1829	2070		2262
Total PAHs without Perylene			1821	2062		2245

	Tissue SRM 1974a	
	GERG	ABL
Dry Weight (g)	1.53	0.85
Wet Weight (g)	13.38	7.49
Matrix	Tissue	Tissue
% solid	11.4	
% Lipid	5.6	
Surrogate Compounds		
C12 - d26	84.0	62.4
C16 - d34		70.2
C20 - d42	108.3 Q	79.6
C24 - d50	92.0	75.7
C30 - d64	126.0 Q	79.9
Alkanes (ng/g)		
n-C10	0 ND	47.5
n-C11	0 ND	55.4
n-C12	0 ND	179.9
n-C13	0 ND	145.1
n-C14	202.5	402.7
n-C15	258.8	186.5
n-C16	179.3	205.1
n-C17	259.7	247.6
Pristane	23.5 J	77.5
n-C18	0 ND	48.0
Phytane	0 ND	80.4
n-C19	121.5	11.1
n-C20	544.7	46.7
n-C21	0 ND	55.3
n-C22	30.8 J	0.7
n-C23	0.0 ND	55.4
n-C24	44.0 J	20.2
n-C25	459.8	64.0
n-C26	244.9 J	102.5
n-C27	0 ND	87.0
n-C28	210.5	63.4
n-C29	37589.8	156.0
n-C30	12799.5	67.3
n-C31	3293.9	
n-C32	68.5 J	94.6
n-C33	0 ND	
n-C34	0 ND	0
Total Alkanes	56332	2500
Reporting Units	ug/g	ng/g
Total UCM	1844.57	1712.02
Total Resolved	2078.53	23699.07
TRAHC	233.96	

Appendix A- 5 Laboratory results for sediment NIST SRMs 1941b and SRM1944

		SRM1941b		SRM 1944		
		Certificate Values	GERG	Certificate Values	ABL	
Sample Descriptor			NIST 1941b		NIST 1944	NIST 1944
Dry Weight (g)			1.07		0.51	0.51
Matrix		Sediment	Sediment		Sediment	Sediment
Surrogate Compounds					AREF	BREF
Naphthalene D-8			81.3		44.52	49.52
Acenaphthene D-10			91.2		69.89	75.87
Phenanthrene D-10			90.1		98.16	95.37
Chrysene D-12			98.1		107.53	101.67
Benzo-A-Pyrene D-12					125.45	138.63
Perylene D-12			77.4		97.85	97.29
PAH Compounds (ng/g)						
Naphthalene	N	848.0	789.5	1650	1256	1307
2-Methylnaphthalene	N1		247.3	950	932	1041
1-Methylnaphthalene	N1		117.3	520	552	621
C2-Naphthalenes	N2		192.8		2540	3064
C3-Naphthalenes	N3		133.3		3683	4457
C4-Naphthalenes	N4		79.3		2894	3993
Biphenyl	BI	74.0	63.6	320	349	375
Acenaphthylene	AC	53.3	76.1		327	385
Acenaphthene	AE	38.4	47.9	570	524	602
Fluorene	F	85.0	104.0	850	969	989
C1-Fluorenes	F1		88.7		1211	1328
C2-Fluorenes	F2		160.7		1852	2153
C3-Fluorenes	F3		201.3		982	1301
C4-Fluorenes	F4				135	219
Dibenzothiophene	D		51.2	620	887	1014
C1-Dibenzothiophenes	D1		63.0		1901	2202
C2-Dibenzothiophenes	D2		123.0		4125	4644
C3-Dibenzothiophenes	D3		114.7		2974	3409

Compound	Code						
C4-Dibenzothiophenes	D4					1027	745
Phenanthrene	P	406.0	387.8		5270	5342	5529
C1-Phenanthrenes/Anthracenes	P/A1		272.1			8584	9429
C2-Phenanthrenes/Anthracenes	P/A2		249.5			10711	11869
C3-Phenanthrenes/Anthracenes	P/A3		201.6			6903	7854
C4-Phenanthrenes/Anthracenes	P/A4		242.1			1071	1404
Anthracene	A	184.0	260.8		1770	1549	1742
Fluoranthene	FL	651.0	640.1		8920	7626	7815
Pyrene	PY	581.0	550.6		9700	8374	8558
C1-Fluoranthenes/Pyrenes	F/P1		371.8			8951	9605
C2-Fluoranthenes/Pyrenes	F/P2					3149	3948
C3-Fluoranthenes/Pyrenes	F/P3					523	586
C4-Fluoranthenes/Pyrenes	F/P4					0	0
Benzo(a)anthracene	BA	335.0	355.7		4720	3984	4512
Chrysene	C	291.0	326.5		4860	5097	5631
C1-Chrysenes	C1		256.5			4967	5979
C2-Chrysenes	C2		135.7			1776	2490
C3-Chrysenes	C3		19.5	J		110	260
C4-Chrysenes	C4		0.3	J		0	0
Benzo(b)fluoranthene	BB	453.0	630.3		3870	4155	2957
Benzo(k)fluoranthene	BK	225.0	217.7		2300	2480	2396
Benzo(e)pyrene	BEP	325.0	312.7		3280	2979	2853
Benzo(a)pyrene	BAP	358.0	447.8		4300	3792	3694
Perylene	PER	397.0	418.6		1170	1173	1436
Indeno(1,2,3-c,d)pyrene	IP	341.0	437.2		2780	2765	2973
Dibenzo(a,h)anthracene	DA	53.0	77.1		424	421	551
Benzo(g,h,i)perylene	BP	307.0	317.9		2840	2850	3142
Total PAHs							
Total PAHs with Perylene			9783			128453	141060
Total PAHs without Perylene			9365			127280	139624

Appendix A- 6 TPAH and TAHC summary table for all AMT and GOC sediment samples, all years

Date	Sample ID	Total AHC	Mean	Std Dev	CV	Total PAH	Mean	Std Dev	CV
Alyeska Marine Terminal Subtidal Sediments (AMT-S)									
3-Apr-93	PWS93PAT0040	1868				196			
3-Apr-93	PWS93PAT0041	2533				341			
3-Apr-93	PWS93PAT0042	1873	2091	383	18.3	191	243	85	35.1
16-Jul-93	PWS93PAT0043	1164				146			
16-Jul-93	PWS93PAT0044	3183				198			
16-Jul-93	PWS93PAT0045	1707	2018	1045	51.8	394	246	131	53.2
26-Mar-94	PWS94PAT0025	1047				202			
26-Mar-94	PWS94PAT0026	1698				167			
26-Mar-94	PWS94PAT0027	1675	1473	369	25.1	239	203	36	17.8
20-Jul-94	PWS94PAT0031	1425				174			
20-Jul-94	PWS94PAT0032	1242				230			
20-Jul-94	PWS94PAT0033	1922	1530	352	23.0	389	264	112	42.2
3-Apr-95	PWS95PAT0022	1291				206			
3-Apr-95	PWS95PAT0023	1093				244			
3-Apr-95	PWS95PAT0024	1785	1390	356	25.6	186	212	29	13.9
11-Jul-95	PWS95PAT0028	2189				1650			
11-Jul-95	PWS95PAT0029	1872				362			
11-Jul-95	PWS95PAT0030	2763	2275	452	19.9	629	880	680	77.2
16-Mar-96	PWS96PAT0004	1109				160			
16-Mar-96	PWS96PAT0005	1578				311			
16-Mar-96	PWS96PAT0006	1100	1262	273	21.7	135	202	95	47.1
12-Jul-96	PWS96PAT0025	2265				326			
12-Jul-96	PWS96PAT0026	1782				201			
12-Jul-96	PWS96PAT0027	1602	1883	343	18.2	381	303	92	30.5
6-Mar-97	PWS97PAT0001	2203				417			
6-Mar-97	PWS97PAT0002	1980				449			
6-Mar-97	PWS97PAT0003	2929	2371	496	20.9	388	418	31	7.3
17-Jul-97	PWS97PAT0029	1124				246			
17-Jul-97	PWS97PAT0030	1477				377			
17-Jul-97	PWS97PAT0031	1892	1498	384	25.7	288	303	67	22.0
29-Mar-98	PWS98PAT0016	1112				120			
29-Mar-98	PWS98PAT0017	1668				451			
29-Mar-98	PWS98PAT0018	972	1251	368	29.4	144	238	185	77.6
5-Apr-00	PWS00PAT0004	1465				313			
5-Apr-00	PWS00PAT0005	1575				335			
5-Apr-00	PWS00PAT0006	1568	1536	62	4.0	412	353	52	14.7
21-Jul-00	PWS00PAT0010	2080				392			
21-Jul-00	PWS00PAT0011	3016				452			
21-Jul-00	PWS00PAT0012	2107	2401	533	22.2	571	472	91	19.4
28-Mar-01	PWS01PAT0001	2987				814			
28-Mar-01	PWS01PAT0002	1803				465			
28-Mar-01	PWS01PAT0003	2659	2483	611	24.6	564	614	180	29.3

17

Date	Sample								
22-Jul-01	PWS01PAT0010	1044				160			
22-Jul-01	PWS01PAT0011	1276				536			
22-Jul-01	PWS01PAT0012	1969	1429	481	33.7	311	335	189	56.4
15-Mar-02	PWS02PAT0004	2508				10			
15-Mar-02	PWS02PAT0005	2452				68			
15-Mar-02	PWS02PAT0006	3514	2825	598	21.2	149	76	70	92.2
10-Jul-02	AMT-S-2-02-1	473				192			
10-Jul-02	AMT-S-2-02-2	504				158			
10-Jul-02	AMT-S-2-02-3	551	509	39	7.7	1089	480	528	110.2
18-Mar-03	AMT-S-1-03-1	654				134			
18-Mar-03	AMT-S-1-03-2	694				271			
18-Mar-03	AMT-S-1-03-3	594	648	51	7.8	131	179	80	44.7
Alyeska Marine Terminal Intertidal Sediments (AMT-L)									
14-Jul-98	PWS98PAT0043	254				26			
14-Jul-98	PWS98PAT0044	131				38			
14-Jul-98	PWS98PAT0045	2492	959	1329	138.6	123	62	53	84.8
Gold Coast Subtidal Sediments (GOC-S)									
19-Mar-93	PWS93PAT0001	941				47			
19-Mar-93	PWS93PAT0002	436				36			
19-Mar-93	PWS93PAT0003	1460	946	512	54.1	58	47	11	23.4
25-Jul-93	PWS93PAT0071	1036				57			
25-Jul-93	PWS93PAT0072	408				31			
25-Jul-93	PWS93PAT0073	256	567	413	73.0	25	38	17	45.2
26-Mar-94	PWS94PAT0022	1429				60			
26-Mar-94	PWS94PAT0023	571				45			
26-Mar-94	PWS94PAT0024	638	879	477	54.3	106	70	32	45.2
19-Jul-94	PWS94PAT0028	385				47			
19-Jul-94	PWS94PAT0029	378				18			
19-Jul-94	PWS94PAT0030	737	500	205	41.1	68	44	25	56.6
3-Apr-95	PWS95PAT0019	463				57			
3-Apr-95	PWS95PAT0020	322				34			
3-Apr-95	PWS95PAT0021	528	438	105	24.1	31	41	14	35.0
11-Jul-95	PWS95PAT0025	750				67			
11-Jul-95	PWS95PAT0026	598				59			
11-Jul-95	PWS95PAT0027	444	597	153	25.6	31	52	19	36.1
16-Mar-96	PWS96PAT0001	588				78			
16-Mar-96	PWS96PAT0002	470				156			
16-Mar-96	PWS96PAT0003	523	527	59	11.2	33	89	62	69.9
12-Jul-96	PWS96PAT0028	541				56			
12-Jul-96	PWS96PAT0029	440				45			
12-Jul-96	PWS96PAT0030	629	537	95	17.6	52	51	6	10.9
6-Mar-97	PWS97PAT0004	624				54			
6-Mar-97	PWS97PAT0005	431				39			
6-Mar-97	PWS97PAT0006	441	499	109	21.8	40	44	8	18.9
17-Jul-97	PWS97PAT0026	514				53			
17-Jul-97	PWS97PAT0027	788				55			
17-Jul-97	PWS97PAT0028	552	618	148	24.0	60	56	3	5.7

Date	Sample ID								
29-Mar-98	PWS98PAT0013	341				42			
29-Mar-98	PWS98PAT0014	301				48			
29-Mar-98	PWS98PAT0015	352	331	27	8.1	38	43	5	11.6
5-Apr-00	PWS00PAT0001	590				126			
5-Apr-00	PWS00PAT0002	668				81			
5-Apr-00	PWS00PAT0003	918	725	171	23.6	126	111	26	23.4
20-Jul-00	PWS00PAT0007	966				105			
20-Jul-00	PWS00PAT0008	753				111			
21-Jul-00	PWS00PAT0009	912	877	111	12.7	92	103	10	9.3
28-Mar-01	PWS01PAT0004	904				125			
28-Mar-01	PWS01PAT0005	833				131			
28-Mar-01	PWS01PAT0006	901	879	40	4.6	120	126	5	4.2
21-Jul-01	PWS01PAT0007	311				40			
21-Jul-01	PWS01PAT0008	506				59			
21-Jul-01	PWS01PAT0009	2993	1270	1495	117.8	108	69	35	50.8
15-Mar-02	PWS02PAT0002	1568				91			
15-Mar-02	PWS02PAT0003	1165				33			
15-Mar-02	PWS02PAT0007	1407	1380	203	14.7	134	86	51	59.1
10-Jul-02	GOC-S-2-02-1	188				42			
10-Jul-02	GOC-S-2-02-2	147				46			
10-Jul-02	GOC-S-2-02-3	117	151	36	23.9	29	39	9	22.4
18-Mar-03	GOC-S-1-03-1	291				31			
18-Mar-03	GOC-S-1-03-2	368				52			
18-Mar-03	GOC-S-1-03-3	280	313	48	15.4	45	43	11	24.7
Gold Coast Intertidal Sediments (GOC-L)									
13-Jul-98	PWS98PAT0040	52				12			
13-Jul-98	PWS98PAT0041	14				5			
13-Jul-98	PWS98PAT0042	26	31	19	63.3	12	10	4	41.8

Appendix A- 7 Summary of tissue TPAH and TAHC for 2002-2003 program.

Sample ID	Sample Date	TPAH	Mean	Std Dev	CV	TSHC	Mean	Std Dev	CV
AIB-B-2-02-1	13-Jul-02	339				4,015			
AIB-B-2-02-2	13-Jul-02	114				2,268			
AIB-B-2-02-3	13-Jul-02	51	168	152	90.18	1,775	2686	1177	43.81
AMT-B-2-02-1	9-Jul-02	122				2,085			
AMT-B-2-02-2	9-Jul-02	86				2,471			
AMT-B-2-02-3	9-Jul-02	92	100	19	19.36	1,825	2127	325	15.27
DII-B-2-02-1	20-Jul-02	91				2,134			
DII-B-2-02-2	20-Jul-02	50				2,059			
DII-B-2-02-3	20-Jul-02	61	67	21	31.38	1,622	1938	277	14.27
GOC-B-2-02-1	10-Jul-02	98				2,056			
GOC-B-2-02-2	10-Jul-02	75				2,298			
GOC-B-2-02-3	10-Jul-02	61	78	19	23.79	2,134	2163	123	5.71
KNH-B-2-02-1	20-Jul-02	80				1,385			
KNH-B-2-02-2	20-Jul-02	70				1,570			
KNH-B-2-02-3	20-Jul-02	46	65	17	26.62	617	1191	505	42.43
SHB-B-2-02-1	21-Jul-02	65				1,494			
SHB-B-2-02-2	21-Jul-02	63				1,136			
SHB-B-2-02-3	21-Jul-02	45	58	11	19.25	1,804	1478	334	22.60
SHH-B-2-02-1	17-Jul-02	67				779			
SHH-B-2-02-2	17-Jul-02	61				1,083			
SHH-B-2-02-3	17-Jul-02	54	61	7	11.09	1,066	976	171	17.52
SLB-B-2-02-1	25-Jul-02	81				1,843			
SLB-B-2-02-2	25-Jul-02	78				2,093			
SLB-B-2-02-3	25-Jul-02	81	80	2	2.13	958	1632	596	36.55
WIB-B-2-02-1	9-Jul-02	142				1,774			
WIB-B-2-02-2	9-Jul-02	91				1,305			
WIB-B-2-02-3	9-Jul-02	68	100	38	38.01	1,591	1557	237	15.21
ZAB-B-2-02-1	25-Jul-02	29				2,155			
ZAB-B-2-02-2	25-Jul-02	21				1,940			
ZAB-B-2-02-3	25-Jul-02	91	47	38	80.91	1,911	2002	133	6.64
AMT-B-3-02-1	8-Oct-02	67				1,442			
AMT-B-3-02-2	8-Oct-02	70				2,202			
AMT-B-3-02-3	8-Oct-02	58	65	6	9.71	1,776	1807	381	21.09
GOC-B-3-02-1	8-Oct-02	39				1,525			
GOC-B-3-02-2	8-Oct-02	50				5,544			
GOC-B-3-02-3	8-Oct-02	50	46	6	13.73	2,421	3163	2110	66.70
AIB-B-1-03-1	21-Mar-03	35				294			
AIB-B-1-03-2	21-Mar-03	27				400			
AIB-B-1-03-3	21-Mar-03	36	33	5	14.96	285	326	64	19.69
AMT-B-1-03-1	18-Mar-03	63				485			
AMT-B-1-03-2	18-Mar-03	67				381			
AMT-B-1-03-3	18-Mar-03	75	68	6	8.83	783	549	209	38.00
DII-B-1-03-1	20-Mar-03	20				379			
DII-B-1-03-2	20-Mar-03	36				583			
DII-B-1-03-2D	20-Mar-03	30				583			
DII-B-1-03-3	20-Mar-03	31	29	7	22.57	541	522	97	18.66

Sample ID	Date								
GOC-B-1-03-1	18-Mar-03	65				860			
GOC-B-1-03-2	18-Mar-03	48				348			
GOC-B-1-03-3	18-Mar-03	41	51	12	23.62	584	597	256	42.89
KNH-B-1-03-1	20-Mar-03	36				181			
KNH-B-1-03-2	20-Mar-03	21				146			
KNH-B-1-03-3	20-Mar-03	20	26	9	35.21	214	181	34	18.90
SHB-B-1-03-1	20-Mar-03	30				410			
SHB-B-1-03-1D	20-Mar-03	39				410			
SHB-B-1-03-2	20-Mar-03	20				704			
SHB-B-1-03-3	20-Mar-03	28	29	8	27.54	311	459	170	37.02
SHH-B-1-03-1	23-Mar-03	13				642			
SHH-B-1-03-2	23-Mar-03	17				435			
SHH-B-1-03-3	23-Mar-03	23	18	5	28.35	752	610	161	26.35
SLB-B-1-03-1	20-Mar-03	58				831			
SLB-B-1-03-2	20-Mar-03	46				1,127			
SLB-B-1-03-3	20-Mar-03	50	51	6	11.92	636	864	247	28.59
WIB-B-1-03-1	23-Mar-03	32				791			
WIB-B-1-03-2	23-Mar-03	9				109			
WIB-B-1-03-2D	23-Mar-03	39				109			
WIB-B-1-03-3	23-Mar-03	12	23	15	62.86	370	345	322	93.47
ZAB-B-1-03-1	20-Mar-03	45				451			
ZAB-B-1-03-2	20-Mar-03	27				657			
ZAB-B-1-03-3	20-Mar-03	19	30	13	44.04	810	640	180	28.17